GEOTHERMAL GRADIENTS AND BURIAL HISTORY MODELLING IN PARTS OF THE EASTERN NIGER DELTA, NIGERIA

BY

ODUMODU, CHUKWUEMEKA FRANK RALUCHUKWU

B.Sc. (*Nig.*), M.Sc. *(Unical)*

(PG/Ph.D/06/42148)

Thesis Submitted to the
UNIVERSITY OF NIGERIA, NSUKKA, for the award of PhD degree
(Petroleum Geology)

Department of Geology
University of Nigeria, Nsukka
Nigeria

June, 2011

CERTIFICATION

ODUMODU, CHUKWUEMEKA FRANK, a Postgraduate student in the Department of Geology and with the Reg. No. PG/Ph.D/06/42148 has satisfactorily completed the requirements for course and research work for the degree of Ph.D in PETROLEUM GEOLOGY. The work embodied in this thesis is original and has not been submitted in part or in full for any diploma or degree of this or any other University.

Dr. A. W. Mode	Date	Dr A. W. Mode	Date
SUPERVISOR		Head of Department	

DEDICATION

This work is specially dedicated to my dear wife Phina and my lovely children, Kamso, Nonyelum, Ifeoma and Dimma.

ACKNOWLEDGEMENTS

I wish to acknowledge the Shell Petroleum Development Company (S.P.D.C) of Nigeria Limited for providing data, facilities and financial support for this research.

I will like to use this medium to gratefully acknowledge those who have helped to make this thesis a reality. First of all, I recognise my supervisor, Dr A.W. Mode, for his fruitful discussions, criticisms and guidance. With great honour and respect, It is my wish to also acknowledge Professor Kalu Mosto Onuoha, who first gave me some insight into the rudiments of basin analysis.

I also wish to acknowledge my industrial supervisor at the Shell Petroleum Development Company of Nigeria Limited, Dr Juergen Frielingsdorf for his supervision of this work. He taught me how to use the Petrel and Petromod softwares amongst other invaluable lessons. Prior to working with Dr Frielingsdorf, Segun Obilaja helped me to conceptualize the framework of this project. I am indeed very grateful to these highly experienced geologists.

I am very grateful to other staffs of S.P.D.C, exploration department, who have in one way or the other contributed to the success of this work. Such staffs include; Charles Anowai, Ade Adesida and Otuka Umahi, and others too numerous to mention.

I wish to thank the Vice chancellor of the Anambra State University, Uli, Professor I.P. Orajaka, who gracefully approved a one-year study leave to enable me undertake this project. I also wish to acknowledge the support of my colleagues at the Department of Geology of the Anambra State University Uli, for their concern, prayers, encouragement and understanding.

I am also very grateful to the sales representative of Petromod (Schlumberger), Dr Alexander Neber for releasing the Petromod II 1-D Express software used for the burial history modelling.

It is my pleasure to acknowledge my parents, Sir and Lady Andrew O. Odumodu for their vision in my education. Without them, I wouldnôt have come this far.

Special thanks goes to Phina, my wife and my kids; Chikamso, Chinonyelum, Ifeoma and Chidimma for their prayerful surport and understanding. Their love has been the motivating force pushing me to achieve my goals and aspirations.

Above all, I am grateful to the almighty GOD for his care, wisdom and the good health I enjoyed in the course of this study.

Chukwuemeka Frank Odumodu

ABSTRACT

Reservoir and bottom hole temperatures from seventy wells in the Eastern Niger Delta suggests that two leg dogleg geothermal patterns characterize the geothermal gradients pattern of the Central Swamp and the Coastal Swamp in contrast to the single gradient patterns seen in the Shallow Offshore.

In the shallow/continental sections in the Niger Delta, geothermal gradients vary between 10 - 18 ^{o} C/Km onshore, increasing to about 24 ^{o} C/Km seawards. In the deeper (marine/parallic) section, geothermal gradients vary between 18 ï 45 ^{o}C/Km. The average geothermal gradient for the various depobelts is 19 ^{o}C/Km for the Central Swamp, 17^{o}C/Km for the Coastal Swamp and 20^{o}C/Km for the Shallow Offshore. Geothermal gradients in the Eastern Niger delta increase eastwards, northwards and seawards from the Coastal Swamp. Vertically, thermal gradients in the Niger Delta show a continuous and non-linear relationship with depth, increasing with diminishing sand percentages. As sand percentages decrease eastwards and seawards, thermal gradient increases. Thermal conductivies also decreases with depth from about 2.3 W/mK in the continental sands to 1.56 W/mK in the parallic and continuous shaly sections. Isothermals constructed at three depth levels: 1000m, 2000m, and 3000m shows that depressed temperatures occur in the western and north central parts and elevated temperatures in the eastern and northern parts of the study area, respectively.

Heat flow computed from 1 ï D modelling software and calibrated against BHT and reservoir temperatures suggests heat flow variations in the Niger Delta to range from 29 ï 55 mW/m^2 (0.69 ï 1.31 HFU) with an average value of 42.5 mW/m^2 (1.00 HFU). Lower heat flows (< 40 mW/m^2) occur in the western and north central parts of the parts of the study area, and is likely to be influenced by high sedimentation rates. Higher heat flows (40 - 55 mW/m^2) occur in the eastern and northwestern parts of the study area. Radiogenic heat production from crustal rocks and shaleøs may account for the heat flow in the east. Hydrothermal convection is likely to have elevated the heat flow in the northwest.

The hydrocarbon maturity modelling results show vast differences in timing and levels of kerogen transformation into petroleum. Result suggests that the potential source rocks (Paleocene, Eocene, Oligocene and partially the Lower Miocene) have attained maturity status to generate hydrocarbons. The depth to the onset of the oil window decreases from the west to the east and to the northwest.

TABLE OF CONTENTS

LIST OF FIGURES

LIST OF TABLES

CHAPTER ONE

1.0 INTRODUCTION

1.1 General Introduction

A good knowledge of the geothermal gradients, subsurface temperature distribution and heat flow regime is invaluable in understanding the thermal maturation patterns of sediments as well as in unravelling the past thermal regimes in an area. The maturation of disseminated sedimentary organic matter into petroleum and its conversion to oil and natural gas is usually controlled by the temperature history of the sedimentary basin.

It is well established that the thermal history of a sedimentary basin is closely related to the mechanisms of basin formation (Sleep, 1971; McKenzie, 1978) and the development of suitable environments for the maturation of hydrocarbons. The implication for petroleum exploration is that the present day temperature field contributes to the probability of occurrence of economic hydrocarbon reserves. It is therefore appropriate to assess carefully the present thermal regime in the Niger Delta basin, where hydrocarbon exploration has been going on since the late 1950s. The database from which geothermal gradients, subsurface temperature and heat flow variations were estimated came from about seventy wells in the Niger Delta.

The Niger Delta is considered as one of the most prolific hydrocarbon provinces in the world, and recent oil discoveries in the deep-water areas suggest that the region will remain a focus of exploration activities for a long time to come (Corredor *et al*, 2005). In this study, the present day temperature data will serve as the basis for studying the thermal structure of the Niger Delta basin.

1.2 Location of the Study Area

The study area lies between longitudes 6°30′E - 8°00′E and latitudes 4°00′N - 5°00′N. This is approximately between Easting 460,000.00-620,000.00 and Northing 8,000. - 112, 000.00 lying within the Eastern parts of the Niger Delta. The area spans about three depobelts: the Central Swamp, the Coastal Swamp and the Shallow Offshore depobelt of the Eastern Niger Delta of Nigeria. (Fig.1.1). The list of wells used for the study is shown in table 1.1.

1.3 Statement of the Problem

The Niger Delta sedimentary basin of Nigeria contains more than 12km of marine and deltaic sediments. Recent interests in drilling high-risk depths and targets such as the turbidite and channel fill facies of the Akata Formation, requires a good knowledge of the geothermal gradients and subsurface temperature variations. This study will therefore help in predicting temperatures prior to drilling, so that high temperature drilling bits, as well as well mud cementing programmes suitable for drilling such high-risk targets could be designed. This study will also be useful in basin analysis for evaluating the hydrocarbon maturation status. This work is therefore aimed at characterizing the thermal structure of the Niger Delta as well as illustrating its hydrocarbon maturation status. The processes responsible for the recognised thermal anomalies will also be highlighted.

Again conflicting views exists concerning possible source rocks in the Niger Delta. Some workers attribute the generated hydrocarbons as being sourced solely from Akata Formation with little or no contribution from the Agbada Formation (Evamy et al, 1978; Bustin, 1988 and Stacher, 1995), while others suggest variable

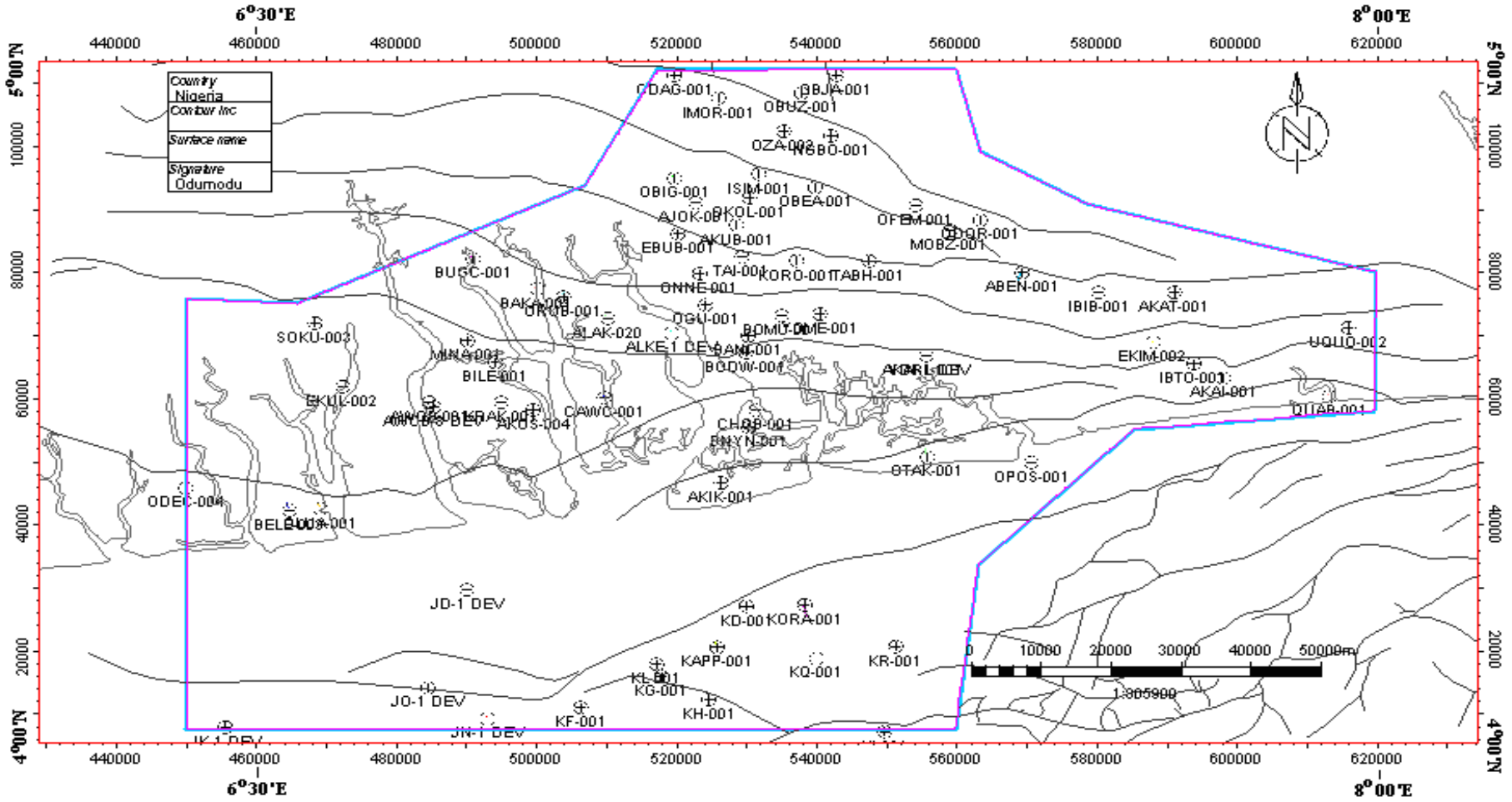

Figure 1.1: Map of the study area showing the three depobelts, wells used for the study and the the regional faults

TABLE 1.1: LIST OF WELLS USED IN THE STUDY				
S/N	**Well Names**	**OML**	**Class of well**	Depobelts
1	AKATA-001	13	E	Central Swamp
2	ABAK ENIN-001	11	E	,,
3	AKUBA-001	11	E	,,
4	AJOKPORI-001	11	E	,,
5	EBUBU-001	11	E	,,
6	ISIMIRI-001	11	E	,,
7	IMO RIVER-001	11	D	,,
8	MOBAZI-001	11	E	,,
9	NGBOKO-001	11	E	,,
10	KOROKORO-001	11	A	,,
11	IBIBIO-001	13	A	,,
12	OBEAKPU-001	11	D	,,
13	OBIGBO-001	11	E	,,
14	ODAGWA-001	11	A	,,
15	ODORO IKOT-001	11	E	,,
16	OFEMINI-001	11	E	,,
17	OKOLOMA-001	11	E	,,
18	ONNE-001	11	E	,,
19	OZA-002	11	A	,,
20	TABANGH-001	11	E	,,
21	TAI-001	11	E	,,
22	AKAI-001	13	E	,,
23	AKASO-004	18	A	Coastal Swamp
24	AKIKIGHA-001	11	E	,,
25	ALAKIRI EAST-001	11	E	,,
26	ALAKIRI-020	18	A	,,
27	AWOBA-001	24	E	,,
28	AWOBA-008	24	E	,,
29	BAKANA-001	18	E	,,
30	BANIELE-001	11	E	,,
31	BELEMA-003	25	E	,,
32	BILLE-001	18	E	,,
33	BODO WEST-001	11	E	,,
34	BOMU-001	11	E	,,
35	BONNY NORTH-001	11	E	,,
36	BUGUMA CREEK-001	18	E	,,
37	CAWTHORNE CHANNEL-1	18	A	,,
38	CHOBIE-001	11	E	,,
39	EKIM-002	13	E	,,
40	EKULAMA-002	24	A	,,
41	IBOTIO-001	13	E	,,
42	KRAKAMA-013		A	,,
43	MINAMA-001	18	E	,,
44	ODEAMA CREEK-004	29	A	,,
45	OGU-001	11	E	,,

TABLE 1.1: LIST OF WELLS USED IN THE STUDY				
S/N	**Well Names**	**OML**	**Class of well**	Coastal Swamp
46	OPOBO SOUTH-004	11	A	,,
47	ORUBIRI-001	18	E	,,
48	OTAKIKPO-001	11	E	,,
49	OLUA-001	25	E	,,
50	QUA IBO-001	13	E	,,
51	SOKU-003	23	E	,,
52	UQUO-002	13	E	,,
53	YOMENE-001	11	E	,,
54	YORLA-001	11	E	,,
55	KORONAMA-001	72	E	Shallow Offshore
56	KAPPA-001	72	E	,,
57	KR-001	72	E	,,
58	KF-001	72	E	,,
59	KG-001	72	E	,,
60	KH-001	72	E	,,
61	KD-1	72	E	,,
62	KI-001	71	E	,,
63	KQ-001	72	E	,,
64	KL-001	72	E	,,
65	JA-001	74	E	,,
66	JD-001	74	E	,,
67	JK-001	74	E	,,
68	JK-002	74	E	,,
69	JN-001	74	E	,,
70	JO-001	74	E	,,

contributions from both formations (Lambert-Aikhionbare and Ibe, 1984) and even from deeper sources (Haack et al, 1997; Stephens et al, 1997)

This work therefore evaluates the hydrocarbon maturation status of Miocene to Paleocene source rocks using the burial and thermal history of the basin.

1.4 Scope of Previous Studies

The Niger delta sedimentary basin of Nigeria has been a focus of so many geological studies because of the petroleum potentials of the area. Most of these studies range from sedimentological / stratigraphic, biostratigraphic, paleontological, geophysical to petroleum geology. However few geothermal studies that have been done in Niger Delta include the works of Nwachukwu (1976), Avbovbo (1978), Evamy *et al* (1978), Chukwueke *et al* (1992), Brooks *et al* (1999), Akpabio *et al* (2003) and Ogagarue (2007). Subsurface temperatures variations and heat flow in the adjacent Anambra basin has also been studied by Onuoha and Ekine (1999).

Nwachukwu (1976) examined about 1000 well logs from the Niger Delta basin and discovered that the geothermal gradients are lowest over the centre of the Niger Delta, approximately about 0.7 to 1.0^{o}F/100ft, and increase to about 3^{o}F/100ft in the Cretaceous rocks on the north. Evamy *et al* (1978), in his study on the hydrocarbon habitat of the Tertiary Niger Delta, investigated the relationship between sand percentage, depth and temperature. In that study, they showed that geothermal gradient increases with diminishing sand percentage from less than 1.0^{o}F/100ft (1.84^{o}C/100m) in the continental sands to about 1.5 ^{o}F/100ft (2.73 ^{o}C/100m) in the paralic section, to a maximum of about 3.0^{o}F/100ft (5.47^{o}C/100m) in the continuous shales of the Niger Delta. Avbovbo (1978) utilized electric logs (Bottom Hole Temperatures) and production reservoir temperatures data from southern Nigeria

basin to determine geothermal gradients in the Niger Delta. His geothermal gradient map based on one hundred and sixty temperature depth plots showed an increase in temperature gradient to the North-east, with the highest gradient of 3.00^{o}F/100ft occurring in the Awgu-Enugu-Nsukka axis of the Anambra Basin, fairly high temperature gradients of about 1.60 to 2.60^{o}F/100ft in the Calabar-Onitsha ï Benin axis of the Coastal region and low gradients of about 1.20 to 1.40 ^{o}F/100ft in the Warri-Port-Harcourt areas of the Niger Delta, while in the offshore areas the maximum temperature gradient is about 1.80 ^{o}F/100ft. He also showed that geothermal gradients are quite higher at the flanks. The maximum temperature gradient at the northeastern flank is about 2.60 ^{o}F/100ft and 2.20 ^{o}F/100ft at the eastern flank. Chukwueke *et al* (1992) in their study of the sedimentary processes, eustatism, subsidence and heat flow in the distal part of the Niger Delta, has shown that geothermal gradients determined from 33 wells range between 19 - 32^{o}C / km while heat flow varies from 45 - 85 mWm^{-2}.

Brooks *et al* (1999), conducted regional heat flow measurements at 112 sites on the continental margin, offshore Nigeria, for the primary purpose of determining basal heat flow for thermal maturation studies of the petroleum systems. The result of their study shows that heat flow in the area ranged between 18.8 - 123.7 mWm^{-2}, with an average of 58.2 mWm^{-2}, and a predominance of heat flow between 40 and 70 mWm^{-2}. Ogagurue (2007) determined heat flow estimates from twenty-one wells in the western Niger Delta Basin. The heat flow estimates vary between 27.6 mWm^{-2} - 68.3 mWm^{-2}, with a simple average of 43.92 mWm^{-2}. He concluded that the north-central part of the study area is characterized by high heat flow, which decreases towards the Niger Delta coast. Akpabio *et al* (2003) determined geothermal gradients in the Niger Delta using continuous temperature logs from 260 wells and discovered

that geothermal gradients in the continental section are lowest (0.82^{o}C/100m) in the central part of the delta, increases seaward to 2.62^{o}C/100m, and northward to 2.95 ^{o}C/100m. Also in the marine/paralic section, the geothermal gradients range from 1.83^{o}C/100m to 3.0 ^{o}C/100m at the central parts of the delta, to between 3.5 ^{o}C/100m and 4.6 ^{o}C/100m northwards and 2.0^{o}C/100m and 2.5 ^{o}C/100m seawards. Onuoha and Ekine (1999) studied subsurface temperature variations and heat flow in the adjacent Anambra Basin and calculated geothermal gradients and heat flow estimates that varies between 25 - 49 ± 1^{o}C/km, and 48 - 76 ± 3mWm^{-2} respectively.

1.5 Purpose and Scope of Present Research

The aim of this research is to study subsurface temperature distributions, geothermal gradients, thermal conductivity, heat flow variations, burial history and hydrocarbon maturation modelling in the Central Swamp, Coastal Swamp and Shallow Offshore depobelts of the Eastern Niger Delta.

The technical objectives set for this study include;

i. To produce temperature / depth profiles of some of the wells in the two depobelts

ii. To estimate the geothermal gradients in the various depobelts

iii. To produce reliable subsurface temperature distribution maps and geothermal gradient maps.

v. To estimate the heat flow variations in the depobelts

vii To assess the burial history and hydrocarbon maturation

iv. To assess the timing and depth of hydrocarbon generation

Seventy wells, which include exploration, appraisal, and development wells, owned by the Shell Petroleum Development Company of Nigeria Limited were used for this study (Table 1.1)

In this study, subsurface temperatures and geothermal gradients were evaluated using production reservoir temperature logs supplemented by corrected bottom hole temperature data. The choice of reservoir temperature data is predicted on the fact that they are generally considered alongside with continuous temperature logs as being closer to formation equilibrium temperatures. The continuous temperature logs were not used because they are available only for very few fields such as Bomu, Ekulama and Opobo South, within the study area.

The temperature and burial history of a sedimentary basin is crucial in accurately evaluating its hydrocarbon maturation status. This study is therefore necessary so that it can provide some qualitative and quantitative information on the thermal status of these three depobelts in the eastern part of the Niger Delta. In this study the factors influencing the variations in geothermal gradients, temperature distribution patterns and certain geological and structural features of these parts of the delta will be highlighted.

This study is also significant in the sense that this study will facilitate the exploration studies in this part of the delta and also in the deep play prospects of the offshore Niger Delta. It has been noted that the deeper, over pressured shales of Akata Formation have not been drilled. Drilling in such areas requires an accurate assessment of the hazard risks associated with drilling in high-pressure, high-temperature conditions. This study will also be necessary for designing well mud and cementing programmes for drilling in such a high-risk area.

CHAPTER TWO

2.0 GEOLOGIC AND STRUCTURAL SETTING

2.1 Background Geological Information of

2.1.1 Lithostratigraphy the Niger Delta

The Tertiary Niger Delta covers an area of approximately 75,000 sq km and consists of a regressive clastic succession, which attains a maximum thickness of 12,000m (Orife and Avbovbo, 1982). The Niger delta is located in the Gulf of Guinea, Central West Africa, at the culmination of the Benue Trough (Figure 2.1) and is considered one of the most prolific hydrocarbon provinces in the world (Corredor *et al*, 2005). The Anambra basin and Abakaliki High to the north, the Cameroun volcanic line to the east, the Dahomey Embayment to the west and the Gulf of Guinea to the south define the boundaries of the Niger Delta. Burke (1972) remarked that the siliciclastic system of the Niger Delta began to prograde across pre-existing continental slope into the deep-sea during the Late Eocene and is still active today. The lithostratigraphy of the Tertiary Niger Delta (Figure 2.2 and 2.3) can be divided into three major units: Akata, Agbada and Benin formations, with depositional environments ranging from marine, transitional and continental settings respectively. The Akata, Agbada and Benin formations overlie stretched continental and oceanic crusts (Heinio and Davies, 2006). Their ages range from Eocene to Recent, but they transgress time boundaries. These prograding depositional facies can be distinguished mainly on the basis of their sand-shale ratios.

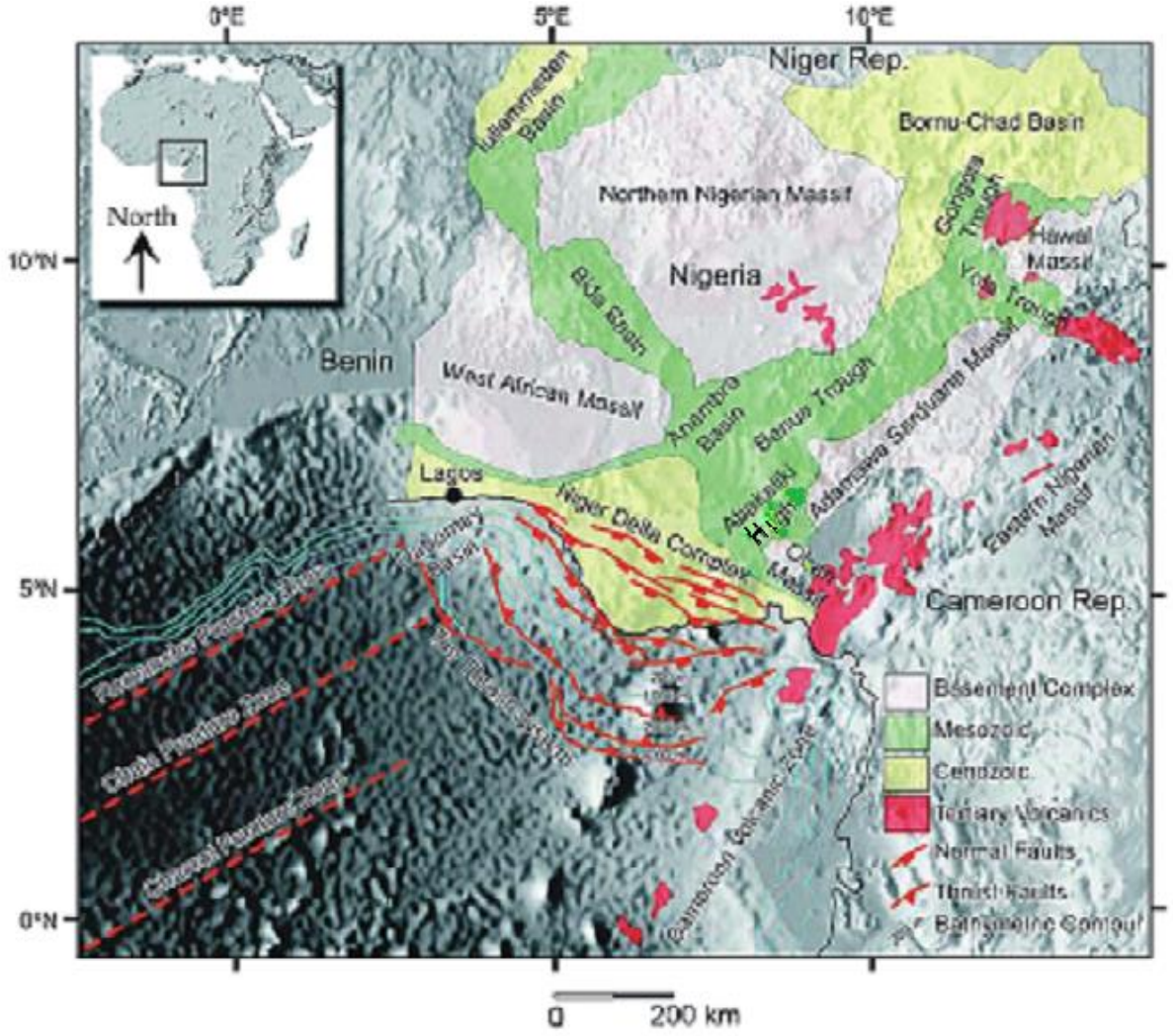

Figure 2.1: Map of Nigeria showing the Niger Delta Complex, the Anambra Basin & the Benue Trough (After Corredor et al, 2005)

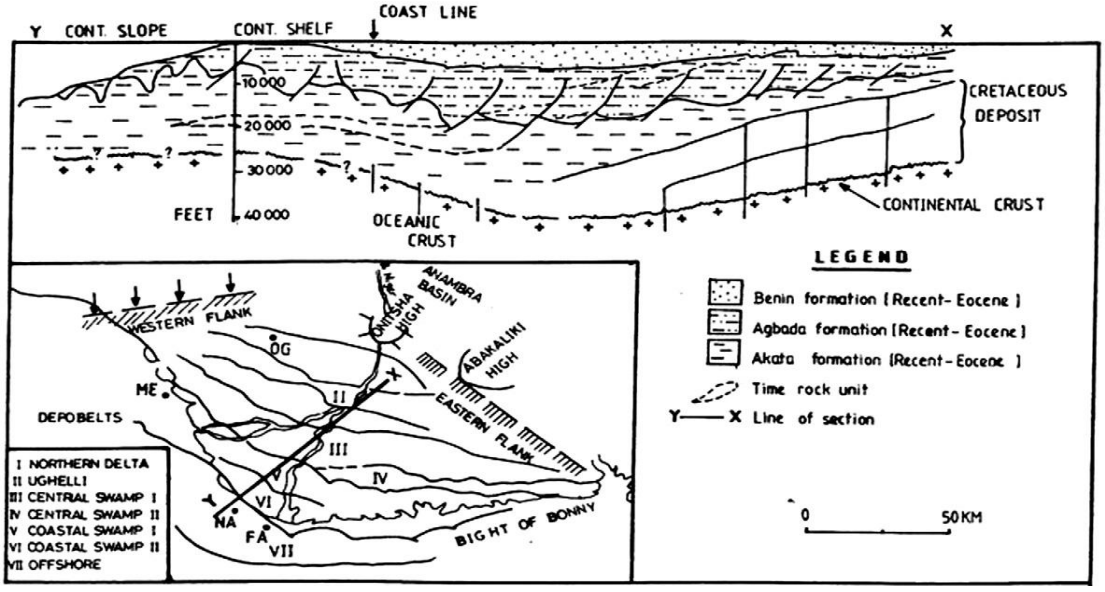

Fig 2.2: Niger Delta: Stratigraphy and Depobelts (Ekweozor and Daukoru, 1984)

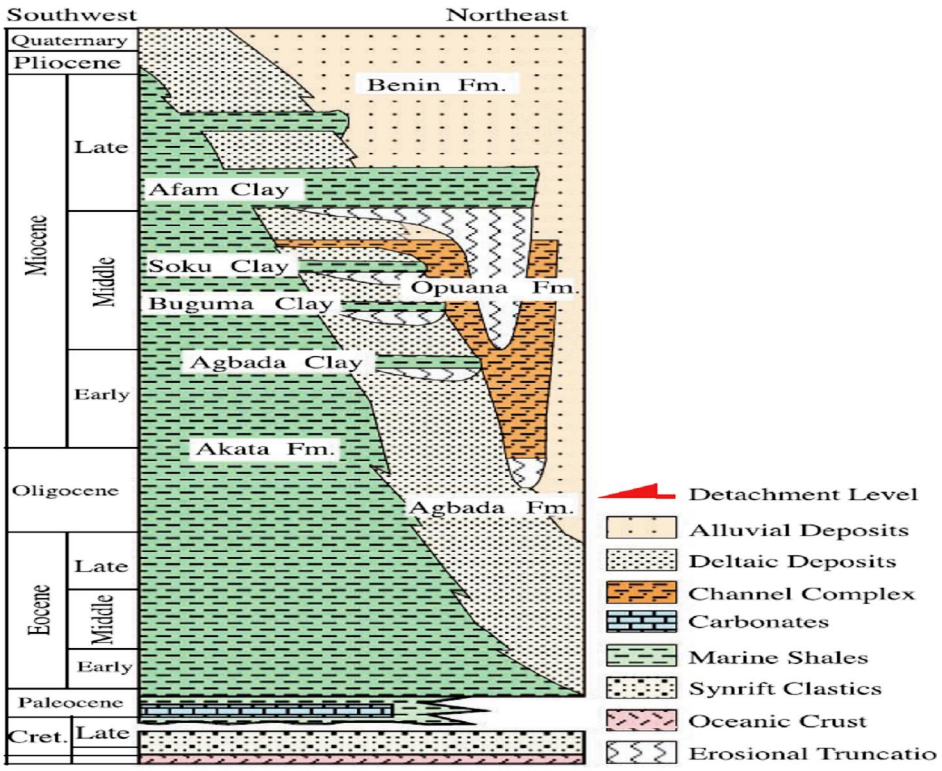

Fig. 2.3: Regional Stratigraphy of the Niger Delta (Lawrence et al, 2002; Corredor et al, 2005

2.1.1.1 The Akata Formation

The Akata Formation is the basal sedimentary unit of the delta. It consists of uniform dark grey over-pressured marine shales with sandy turbidites and channel fills. Its age ranges from Late Eocene to Recent. In deep-water environments, these turbidites are the potential reservoirs. Whiteman (1982) suggested that the Akata Formation may be about 6,500m (21,400 ft) thick, while Doust and Omatsola (1990) suggested that the thickness ranges from 2000 m (6600 ft) at the most distal part of the delta to 7000 m (23,000 ft) beneath the continental shelf. Corredor *et al* (2005) also suggested a thickness of about 5000m (16,400 ft) for the deep fold and thrust belts in the offshore Niger Delta. The Akata Formation has generally been regarded as the main source rock for oil in the delta.

2.1.1.2 The Agbada Formation

This is the major petroleum-bearing unit in the Niger Delta. It overlies the Akata Formation and consists of alternations of sand and shale layers. The Agbada Formation is characterized by paralic to marine-coastal and fluvial-marine deposits mainly composed of sandstone and shale organized into coarsening upward off-lap cycles (Pochat *et al*, 2004). According to Corredor *et al* (2005), the Agbada Formation consists of paralic siliciclastics that are more than 3500 m (11,500 ft) thick and they represent the actual deltaic portion of the succession that accumulated in delta front, delta-top set and fluvio-deltaic environments. The first occurrences of shale with marine fauna usually characterize the top of the Agbada Formation while the deepest significant sandstone body characterizes the base. The Agbada Formation can be subdivided into upper, middle and lower units. The upper unit is made up of 60 - 40 percent sand. The middle unit consists of 50 ï 30 percent sand and is the main

objective of oil and gas exploration in the delta. The lower unit is made up of 20 percent sand inter-bedded with under-compacted shales.

2.1.1.3 The Benin Formation

Onshore and in some coastal regions, the Benin Formation overlies the Agbada Formation. The Benin Formation consists of Late Eocene to Recent deposits of alluvial and upper coastal plain deposits that are up to 2000 m (6600 ft) thick (Avbovbo, 1978).

2.1.2 Depositional Belts

Depositional belts or ñdepobeltsò consists of a series of off-lapping siliciclastic sedimentation cycles or mega-sedimentary belts. Evamy *et al* (1978) referred to this structure as, ñmega structureò while Doust and Omatsola (1990) were the first to call them ñdepobeltsò. Five regional depobelts can be discerned along the north ï south axis of the delta, each with its own sedimentation, deformation and petroleum history. These depobelts include: the Northern Delta, the Greater Ughelli, the Central Swamp I & II, the Coastal Swamp and the Offshore depobelts (Figure 2.2). Each of these depobelts is bounded by large-scale regional and counter-regional growth faults (Evamy *et al*, 1978; Doust and Omatsola, 1990; Pochat *et al*, 2004). The activity in each belt has progressed in time and space toward the south-southwest through stepwise alluvial progradation facilitated by large-scale withdrawal and forward movement of the underlying shale. The interplay of subsidence and supply rates resulted in deposition of discrete depobelts ï when further crustal subsidence of the basin could no longer be accommodated, the focus of sediment deposition shifted seaward, forming a new depobelt (Doust and Omatsola, 1990).

2.2 Regional Structural Setting

The Niger Delta remains the best-studied part of Nigeriaôs continental margin because of its rich hydrocarbon resources. An averaged section of the Niger Delta as drawn by Thomas (1999) is shown in figure 2.4, illustrating the diapiric structures on the continental slope and rise as well as the faulting of the Oligocene and younger formations.

In the Niger Delta, the continental shelf is about 50 to 80 km in width and the shelf break occurs at depths between 150 to 200 m (Fig 2.5). The continental slope, which is steeper, extends from the shelf break to a distance of 2-3 km, where the more gently sloping continental rise starts. The continental rise continues downslope to the abyssal plains of the Gulf of Guinea with water depths greater than 4.5 km. In the continental margin, from the outer shelf (shallow water) to the deep slope (deep water) of the Niger Delta, three distinct structural domains (Figure 2.5) have been observed from previous studies. These structural zones are:

(I) an upper extensional domain dominated by growth faults beneath the continental shelf and upper slope;

(II) a translational domain or an intermediate zone characterized by mud diapirism, and

(III) a lower compressional domain characterized by imbricate toe of slope thrusts.

According to Cohen and McClay (1996) as well as Morgan (2004), this structural configuration is caused by gravitationally driven delta tectonics, where the Agbada Formation is collapsing on a detachment in the Akata Formation.

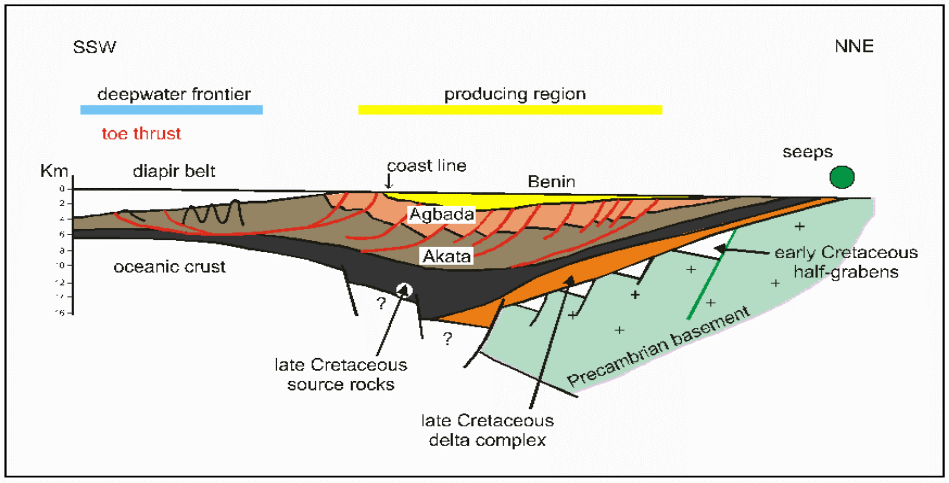

Fig. 2.4: Averaged section of the Niger Delta (After, Thomas, 1995,

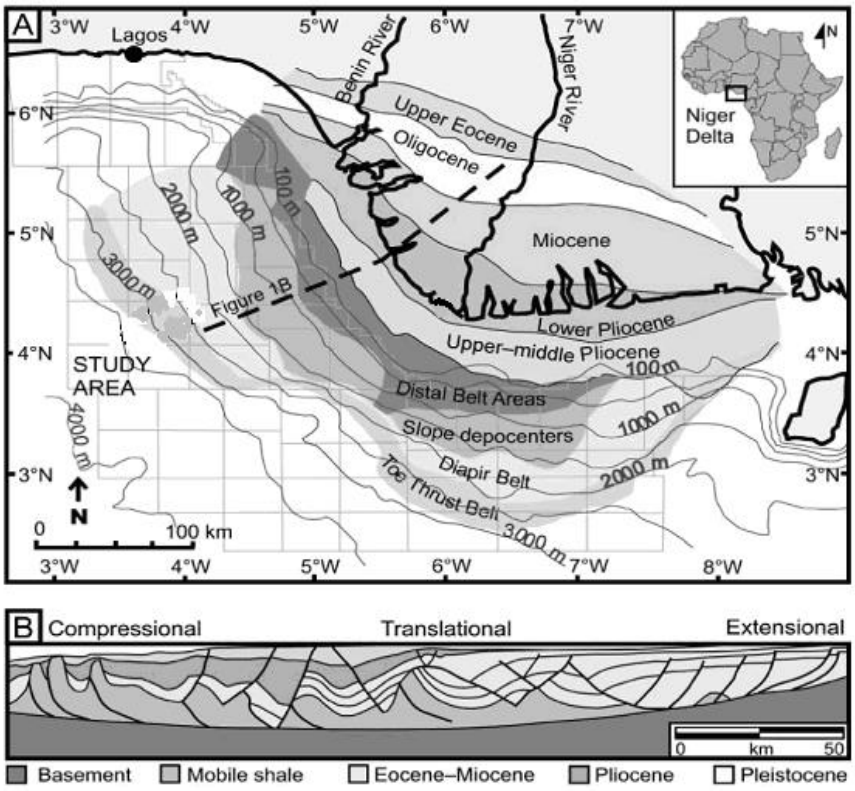

Fig. 2.5; Structural domains of the continental shelf, slope and rise of the offshore Niger Delta (After Cohen and McClay, 1996

2.2.1 Structural Evolution of the Niger Delta

Several workers including Burke *et al* (1971), Whiteman (1982) and Olade (1975) has summarized the structural and tectonic setting of the Niger Delta. According to these authors, the structural evolution of the Niger Delta began with the formation of the Benue trough in the Early Cretaceous as a failed arm of a triple rift junction associated with the opening of the South Atlantic. Olade (1975) contends that the initial stage of the evolution involves the rise of a mantle plume in the region of the present Niger Delta, which led to the doming and rifting in the Benue region, developing an RRR triple junction. Three major tectonic phases or epirogenic movements were suggested by Murat (1972) to have influenced the geologic history of the Benue Trough system, which he subdivided into three paleogeographic areas or sub-basins; the Abakalikiï Benue Trough, the Anambra Basin and the Niger Delta basin.

The initial rifting resulted to rapid subsidence and deposition of the Asu River Group during the Albian times. During the Cenomanian, a mild deformational event led to the compressive folding of the Asu River Group and restriction of the Odukpani Formation to the Calabar flank. Continued mantle upwelling and rifting during the Early Turonian resulted to the deposition of the Ezeaku Formation. When mantle upwelling finally ceased and migrated westward by the Santonian, the trough collapsed.

The second tectonic phase started during the Santonian as a gentle widespread compressive folding, uplifting the Abakiliki-Benue Trough. The Anambra Basin and the Afikpo Syncline subsequently subsided and were filled by two deltaic sedimentary cycles through to Palaeocene. The last tectonic phase resulted from the uplift of the Benin and Calabar flanks during the Paleocene ï Early Eocene (Murat,

1972). These movements initiated the subsidence and progressive outbuilding of the Eocene ï Holocene sediments of the Niger Delta along the Northeast-Southwest fault trend of the Benue Trough.

The structural evolution of the Niger Delta has been controlled by basement tectonics as related to crustal divergence and translation during the Late Jurassic to Cretaceous continental rifting. It has also been influenced by isostatic response of the crust to sediment loading. The Niger Delta has been rapidly subsiding because of sediment accumulation, flexural loading, and thermal contraction of the lithosphere (Onuoha, 1982, 1986; Onuoha and Ofoegbu, 1988). According to Caillet and Batiot (2003), throughout the geological history of the delta, its structure and stratigraphy have been controlled by the interplay between rates of sediment supply and subsidence. Subsidence itself has been controlled both by driving subsidence of the basement as well as differential sediment loading and compaction of unstable shales.

2.2.2 Structural Patterns of the Niger Delta

Evamy *et al* (1978) described the fault typeôs common in the Niger Delta. These faults include (a) structure building faults, (b) crestal faults (c) flank faults (d) counter regional growth faults as well as antithetic faults (Figure 2.6.) The structure building faults define the up-dip limit of major rollover structures. They are essentially concave in the down-dip direction and repeat each other en echelon. They also define the boundaries of depobelts or megastructures. The counter regional faults as their name implies are those faults that possesses a counter regional hade, including as well the antithetic faults. Large counter regional faults define the southern limits of depobelts. Crestal faults also occur within rollover structures. These crestal faults are characterized by a lesser curvature in a horizontal direction

and are generally steeper in the vertical direction. They display less growth, which also tends to be less continuous. The flank structures occur at the southern flanks of major structures and show some major rollover deformation at shallow levels. These faults show southerly dips at depth. K-type faults are mainly flank faults, which are very closely spaced resulting to a multiplicity of narrow fault blocks. The K faults are very common in SPDCôs offshore K- field.

The occurrence of synsedimentary faults, which deforms the delta beneath the Benin Formation, presents a very striking structural feature in the Niger Delta (Fig. 2.7). These synsedimentary faults are also known as growth faults while the anticlines associated with them are known as rollover anticlines. According to Whiteman (1982), they are called growth faults because they are frequently initiated around local depocentres and grow during sedimentation, thereby allowing a greater amount of sediment to accumulate in the down thrown block compared to the up thrown block. Caillet and Batiot (2003) suggested that growth faults were triggered by the movement of the deep-seated, over pressured, ductile marine shales and aided by slope instability.

Whiteman (1982) also defined a growth fault as a fault that offsets an active surface of deposition. Most growth faults in the Niger Delta are frequently crescent in shape with the concave side facing the down thrown side usually seawards. Most growth faults show a marked flattening with depth. They can be described as being listric in shape. These growth faults affect the Agbada and the Akata formations, and dies out below the base of the Benin Formation. These growth faults exhibit throws of several thousands of feet at the top of the Akata Formation whereas they die out to nothing at the base of the Benin Formation. In depth, growth faults may become thrusts and displacement may exceed many thousand feets in toe thrust zones. . As

noted by Doust and Omatsola (1990), the magnitude of throws on growth faults bounding depobelts is such that much of the paralic succession on the downthrown side is younger than that on the up thrown side. Within depobelts, growth faults form boundaries of macrostructures, each characterized by its own sand-shale distribution pattern and structural style.

Growth faults present a migratory path for hydrocarbons generated in the Akata and Agbada formations, thereby enabling them to migrate and accumulate in the reservoir sands within the Agbada Formation. The growth faults also act as seals to migration. When the throw of the fault exceeds the sand thickness, the fault zone serves as a seal but this depends on the amount of shale smeared into the fault plane.

Rollover anticlines always occur in association with the growth faults and it is in these structures that oil and gas in the Agbada reservoir sands have been noted.

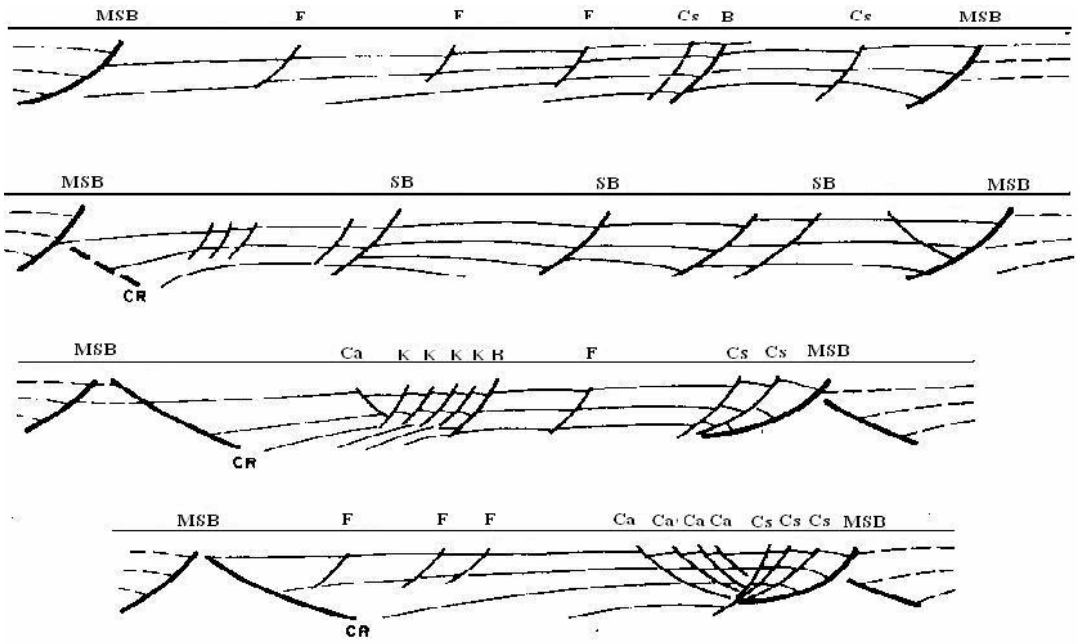

Fig. 2.6 : Megaunits and associated sedimentary fault types (Evamy et al, 1978)

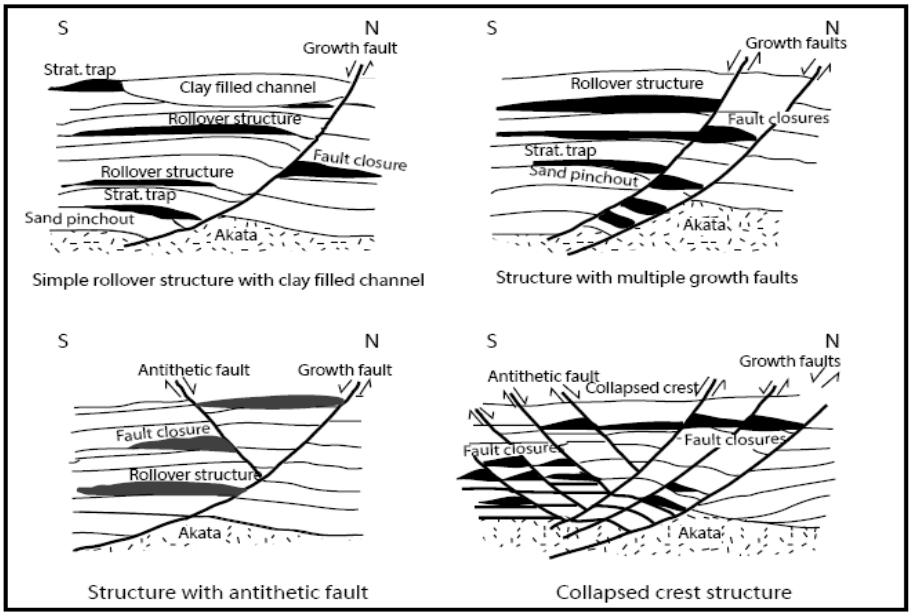

Fig. 2.7: Examples of Niger Delta field structures and associated traps (Doust and Omatsola, 1990, Turtle et al, 1999)

2.3 Source Rocks of the Niger Delta

The source rocks responsible for the hydrocarbon accumulation in the Niger Delta has been widely discussed in literature (e.g. Weber and Daukoru, 1975; Frost, 1977; Evamy *et al*., 1978; Ejedawe *et al*, 1979; Ekweozor *et al*, 1979; Ekweozor and Okoye, 1980; Ekweozor and Daukoru, 1984; Lambert Aikhionbare and Ibe, 1984; Bustin, 1988; Doust and Omatsola, 1990; Stacher, 1995; Haack *et al*, 1997). Some of these authors attributed the generated petroleum solely to the source rocks of the Akata Formation, while others suggests variable contributions from the marine interbedded shales in the lower Agbada Formation and the marine Akata Shale and possibly a Cretaceous source.

These controversies as to the possible source rocks in the Niger Delta were generated by the known poor source rock qualities of the Agbada Formation and the Akata Shale. According to Lambert-Aikhionbare and Ibe (1984), the Agbada shales contain moderate total organic carbon and type II to II-III kerogen. These source rocks give low rock eval pyrolysis yields (i.e. hydrogen index < 200mgHC/g organic carbon) and vitrinitic, gas prone kerogens (Nwachukwu and Chukwura, 1986; Bustin, 1988). Evamy *et al* (1978) and Stacher (1995) suggested that the Agbada Formation does not have the sufficient thickness and maturity to be a potential source rock.

The Akata shales have been poorly sampled because of their great depths and also due to the undercompacted and overpressured sediments. The source rocks contain a lot of terrigenous organic matter even though they were deposited in a more open marine than a deltaic environment (Bustin, 1988). The paucity of known good to excellent oil-prone source rocks is responsible for the petroleum occurrence in the delta being attributed to the large volume of source rocks rather than to the organic richness (Bustin, 1988).

A recent study by Haack *et al* (1997) suggests a correlation between oils and source rock in the Early Tertiary. In this work, the Upper Cretaceous ï Lower Palaeocene and Upper Eocene are suggested as potential source rocks. Stephens et al (1997) found a source potential in the Oligocene in the southeastern Niger Delta, offshore Equatorial Guinea.

2.4 Hydrocarbon Properties of the Niger Delta

The physical and chemical properties of the Niger Delta crude oils are highly variable, even to the reservoir scale. According to Whiteman (1982), the oil within the delta has an API gravity range of 16 ï 50 ^{o} API, with the lighter oils having greenish colours. It is also noted that about fifty-six percent of the oils in the delta have API gravity between 30^{o} and 40^{o}.

Evamy *et al* (1978) classified Niger Delta crude oil into light and medium gravity crudes. The light crudes are characteristically paraffinic and waxy, with pour points from ï 7 to 32 ^{o}C (20 to 90 ^{o}F). Their wax contents are about 20%, but commonly around 5 %. They occur in the deeper reservoirs. The medium crudes are dominantly naphthenic, non-waxy, with pour points less than ï 25 ^{o}C (-13 ^{o} F). The medium gravity crudes has a specific gravity that is greater than 0.90 (< 26 ^{o}API).

Evamy *et al* (1978) also noted that the distribution of crudeôs according to their tank-oil specific gravity and pour point shows the heavy, low pour point crudes to be consistently above the lighter, high pour-point varieties. The quality of crude oil in the Niger Delta has also been shown to be more dependent on temperature rather than depth. Evamy *et al* (1978) has shown that the heavy naphthenic oils are paraffinic oil that have undergone bacterial transformation or biodegradation in the shallow cooler reservoirs and belong to the same family as the paraffinic waxy oils that occur in deeper high

temperature reservoirs. Based on the fact that biodegraded oils occur only in shallow traps within the temperature regime that bacteria can survive, they suggested that a late migration within no noticeable subsidence of the trap after its emplacement. Matava *et al* (2003) also showed that compositional variations in Niger delta crudes results from migration rather than source rock organic matter input or thermal maturity.

The concentration of sulphur in the Niger Delta crude oil is low, between 0.1% and 0.3%, with a few samples having concentrations as 0.6% (Nwachukwu *et al*, 1995).

CHAPTER THREE

3.0 BACKGROUND ON THERMAL STUDIES

3.1 Thermal Studies

Geothermal studies is useful in understanding many of the geological and geophysical phenomena that is being witnessed on the earth, such as earthquakes and volcanism as well as the earthôs magnetic field and the plasticity of earthôs material at depth. Heat flow studies also give us insight into the thermal history and geodynamic origin of sedimentary basins. According to Jessop and Majorowicz (1994), the thermal history of a basin depends on its tectonic origin and the circumstances of its development. The dissipation of excess heat associated with basin formation and the transfer of the continuous heat supply from the basement depend on the thermal properties of the strata and their water content. The thermal conditions of a sedimentary basin is usually influenced by the heat flow from the underlying basement and the thermal conductivity of the sedimentary cover or overprinted by other processes such as fluid flow (Forster, 2001)

Present-day temperature data is most often used in studying the thermal structure of the earth. The thermal gradient and thermal conductivity values of rock types in an area have been used to obtain estimates of heat flow variations in an area. The variations in heat flow in a sedimentary basin are influenced by several factors, which include:

I Basement Heat flow

II Radioactive Heat Production in sediments

III Effect of Sedimentation

IV Deeply buried salt structures

V Fluid flow through sediment

I. Basement Heat Flow

Basement heat flow is primarily controlled by the mechanics of the basin-forming rift-extension event and subsequent subsidence caused by the cooling of the lithosphere (McKenzie, 1978; Sclater and Cerlerier, 1987). Heat flow decreases with time as the lithosphere gradually approaches a quasi-steady state (Sclater and Christie., 1980). Beardsmore and Cull, (2001) observed that the heat generated through the radioactive decay of unstable elements, such as uranium, thorium and potassium contained in the crustal rocks has a significant contribution to the total heat flow coming from the basement. The continental crust is also known to produce several tens of time more radiogenic heat than the oceanic crust.

II Radiogenic Heat Production in Sediments

Clastic sediments such as shale contain quite a lot of radiogenic heat-producing elements such as thorium, uranium and potassium. The sediments contribute its radiogenic heat to the total heat flux travelling up in the column. The contribution of radiogenic heat to seafloor heat flow is proportional to the total thickness of the sediments.

III Effects of Sedimentation

Sedimentation influences surface (Seafloor) heat flow (Hutchison, 1985; Wang and Davies, 1992). All agree on an inverse relationship between sedimentation and sea floor heat flow (i.e. faster sedimentation rate, lower heat flow and vice versa).

IV Deeply buried Salt structures

Two factors commonly control salt-induced heat flow anomalies (OôBrien and Lerche, 1984; Corrigan and Sweat, 1995). These factors are: the depth of burial and the thickness or height of the salt body relative to its width. A tall piercing diapiric plug would cause a large heat flow anomaly whereas a laterally extensive, bedded salt

body would not show any anomaly. Nagihara *et al* (1992) observed that diapiric induced heat flow anomalies are localized directly above the salt body.

V Fluid flow through sediments

The sedimentary thermal regimes can be perturbed by the vertical migration of pore fluids and seeps on the sea floor. Anderson *et al* (1991) observed that heat flow measurements made close to the upward migration path of the seeps shows that the values are higher than those beside it.

3.2 Heat Transfer Mechanisms

Three basic ways exist through which heat can be transferred through rocks. These include convection, conduction and advection. Convection involves heat transfer by which the motion of the fluid carries heat from one place to another. Convection currents are set up in the fluid because the hotter part of the fluid is not as dense as the cooler part, so there is an upward buoyant force on the hotter fluid, making it rise while the cooler denser fluid sinks. In conduction, the substance itself does not flow; rather vibrations transfer heat energy internally, from atom to atom within a substance. Conduction is most effective in solids. Advection involves convective energy transfer through fault planes.

In the Akata and Agbada formations, the predominant heat transfer mechanisms are conduction and advection through some major faults. Because of fresh water circulation, the predominant heat transfer mechanism in the Benin Formation is convection.

3.3 Determination of Static Formation or Virgin Rock Temperatures

The temperature logs used in determining static (equilibrium) formation temperatures include (i) Bottom hole temperature logs (ii) Continuous temperature logs and (iii) Production Reservoir temperature logs.

The Continuous Temperature logs and the Production Reservoir temperature logs have been considered in a lot of studies as being close to the static formation temperature. Forster (2001) observed that continuous temperature logs reflect true formation temperatures because of the fact that the time prior to the logging was enough for the borehole to regain thermal equilibrium after the drilling process.

Bottom-hole temperatures are routinely recorded during wire-line logging operations and thus are usually the commonest type of subsurface temperature measurements available from hydrocarbon exploration activities. Nagihara and Smith (2005) described the method from which bottom-hole temperatures were obtained. According to them, bottom hole temperature measurement is obtained shortly after the well has been shut in. After drill fluid circulation ceases, a string of logging tools, which includes a temperature censor, is lowered. When the tool string returns to the surface, the maximum-recorded temperature is reported in the log header, along with the time the well is shut in and the time the tool string reached the bottom. BHT measurements can be made at several depths in a well while the well is deepened during drilling. It has been noted in several studies that bottom-hole temperature values are considerably lower than the true formation temperature, or virgin rock temperature, because of the cooling effect of the drill-fluid circulation (Forster, 2001; Nagihara and Smith, 2005 & 2008; Cory and Brown, 1998; Chulli *et al*, 2005). Nagihara and Smith (2008) reported that temperature difference between bottom-hole temperature and virgin rock temperature as being dependant on many

factors involved in the fluid circulation such as borehole size, depth of the formation, formation thermal properties, and the timing of the bottom hole temperature measurement relative to the shutting in of the well. If the borehole is left undisturbed for sometime after drilling, the temperature inside and around it will gradually recover to its pre-drilling state. This recovery can take weeks or months and so it is not logistically possible to keep the well shut for a full recovery. So multiple BHT measurements for a short period of time (1-2 days) at a particular depth can reveal the temperature recovery trend which can be theoretically extrapolated to determine the equilibrium temperature.

There are several methods for estimating static formation temperatures from bottom-hole temperatures. These include: (I), using the Hornerôs plot method of Bullard (1947) and (ii) correcting BHT data based on CTL (Continuous temperature logs) and PRT (Production reservoir) temperature logs as references for correction.

The Hornerôs method has been the most widely used technique and requires two or more BHT measurements at different times and at the same depth to monitor the return to equilibrium temperature after drilling has ceased (Cory and Brown, 1998). According Nagihara and Smith (2005), the BHT measurements obtained at different times should show the well bore temperature slowly recovering towards its pre-drilling state. The Hornerôs plot method is given by the following equation:

$$T_{equil} = T_{BHT} - M \ln \left[\frac{t_{shut-in} + t_{circ}}{t_{shut-in}} \right] \text{----------(1)}$$

Where T_{equil} represents the equilibrium temperature (°C), T_{BHT} represents the bottom hole temperature (°C), $t_{shut-in}$ represents the shut in time, t_{circ} represents the circulation time and M represent the Horner slope. A Horner

slope is produced by plotting T_{BHT} values against the corresponding $In\left[(t_{shut-in} + t_{circ}) / t_{shut-in}\right]$ values for a particular run. The slope M and intercept T_{equil} can be determined using linear regression. Therefore for each run in a well where two or more BHTs are measured at the same depth but at different shut-in times, a Horner plot can be used to estimate the equilibrium temperature.

According to Cory and Brown (1998) some quality control that must be applied to BHT data before it is used in estimating equilibrium or static formation temperature include that: (1) Each sequence of BHT measurements recorded at the same depth during a logging run generally shows a smooth increase in temperature as the shut-in time increases. Any BHT, which showed an irregular increase or decrease, thereby disrupting the pattern should be removed from the dataset. (2) The accuracy of the Horner plot should increase with the increasing shut-in time. BHTs measured after a short shut-in time period are unsuitable for the Horner plot method. BHTs measured with a shut-in time < 2 hours should be removed. (3) The circulation time is not a sensitive parameter in the Horner plot method (Luheshi, 1983; Brigaud *et al*, 1992) A circulation time of 2 hours is mostly been assumed in some studies.

Chapman *et al* (1984) utilized the Horner plot method to correct bottom hole temperatures data to static formation temperatures in the Uinta basin. The relation is given as:

$$T_{B(t)} = T_{B(\alpha)} + A \log \left(\frac{t_c + t_e}{t_e}\right) \text{----------(2)}$$

The ordinate intercept on the semi-log plot of $(t_c + t_e)/t_e$ versus T, gives the estimate of $T_{B(\alpha)}$, which is the equilibrium or static formation temperature.

Leblanc *et al* (1981) suggested a method of correcting bottom hole temperatures based on Middleton (1979) curve matching technique whereby thermal stabilization curves derived from an assumed thermal diffusivity are superimposed on actual data to estimate a true formation temperature. Leblancôs relation is given as:

$$BHT\ (0,t) = T_m + \Delta T\left[e^{-a^2}/_{4Kt}\right] \text{----------(3)}$$

Where $\Delta T = T_f - T_m$

T_m = the temperature of the drilling mud before circulation

T_f = the formation temperature

a = the drill hole radius

K = the formation rock diffusivity constant

t = the total time of mud circulation at the depth of measurement,

and T_f = the formation temperature

Luheshi (1983) proposed a relation for determination of formation temperature T_f from bottom hole temperature $T_{(a,t)}$, which is space and time dependent. Luheshis relation is given as:

$$T_{(a,t)} = T_f + (Q/4\pi\kappa)In\left(\frac{t_2}{t_1 + t_2}\right) \text{ ---------- (4)}$$

Where $t_2 = t - t_1$, is the shut in time after the end of mud circulation?

t , is the duration of drilling and, t_1 the total mud circulation time at the depth of measurement. κ, is the diffusivity of the formation rock type, a is the borehole radius while $T_{(a,t)}$ i.e. Q is the heat flow at the depth of measurement.

The above relation is valid when $T_{(a,t)}$ measured at depth is more than ten times borehole radius above the bottom of the well and $a^2/4kt_2$ is less than unity.

Shen and Beck (1986) utilized laplace transforms to derive analytical models for BHT stabilization, in which drilling mud circulation effects, thermal property contrast between the formation and the borehole mud and presence of radial or lateral fluid flow are considered.

The other method is based on a statistical approach that uses continuous temperature logs (CTL) and Production reservoir temperatures (PRT) as references for correcting bottom-hole temperatures.

3.4 Geothermal Gradients and Heat Flow Determinations

There are two basic approaches in calculating thermal gradients. These include the thermal resistance or Bullardôs method and the simple gradient method (Chapman *et al*, 1984).

Thermal resistance is defined as the quotient of the thickness Δz and a characteristic thermal conductivity k and is given by the equation

$$T_B = T_o + q_o \sum_{z=0}^{n} \left(\frac{\Delta z}{k}\right) \quad \text{---------- (5)}$$

Where (T_B) is the temperature at depth z = B, T_o, the surface temperature at z = 0 q_o, the surface heat flow and $(\Delta z/k)$, the thermal resistance, which is summed for all rock units from the surface to the depth B.

Heat flow (q_o) can be calculated as the slope of the plot of the consecutive values of T_B versus the summed thermal resistance (R_i) to the measurement depth.

The steps required in using this method to estimate heat flow and subsurface temperatures in a sedimentary basin include;

i. A set of bottom hole temperatures (T_B) are compiled and corrected for drilling disturbances.

ii. Thermal conductivity values must be measured or determined for all representative rocks in the basin

iii. Sum the thermal resistance at each well from the surface to the depth of the BHT observation and solve using equation 6 above.

The simple gradient method (Klemme, 1975) is an alternative approach to analysing BHT data. Thermal gradients are calculated as two point differences using a single BHT and an estimate of the mean annual ground temperature or through regression techniques on multiple bottom hole temperatures at different depths (Chapman *et al*, 1984). A major advantage of this method is its convenience. The simple gradient method is given by equation 6 as shown below.

$$T_B = T_o + \left(\frac{\partial T}{\partial Z}\right) \times B \quad \text{---------- (6)}$$

$$q_o = K \frac{\partial T}{\partial Z} \quad \text{---------- (7)}$$

Houbolt and Wells (1980) developed a method for calculating heat flow between two depth points by assuming an empirical relationship between subsurface temperature and one way sound travel time. Leadholm *et al* (1985), also used this method to predict thermal conductivity of rocks so as to model organic maturation on the Norwegian continental shelf. The relation is given as:

$$Q = a\left[\left(t_L - t_u\right)^{-1} \times In\left(\frac{c + T_L}{c + T_U}\right)\right] \quad \text{---------- (8)}$$

Where, Q is the relative heat flow in Boderij unit (BU), which is equal to $77\, mWm^{-2}$ in SI unit. $a, c,$ are constants having values 1.039 and 80.031 respectively,

T_L, t_L are the subsurface temperature and one-way travel time, respectively, at a deeper depth level of any chosen interval within the well. T_U, t_U, are the temperature and one-way travel time at the shallower depth level of the chosen interval.

The following relations give the geothermal gradient (g_i) and the effective thermal conductivity (k_i) of the interval respectively:

$$g_i = \left[(T_L - T_{L-1}) / (h_L - h_{L-1}) \times 100 \right] \quad \text{---------- (9)}$$

and $(k_i = 77V / 1.039(80.031 + T_i))$ ---------- (10)

where h_L, h_{L-1} are the depths (m) corresponding to T_L and T_{L-1} respectively, V, is the acoustic velocity in m/sec.

The velocity of sound waves in a formation can be estimated from a sonic log using the relation:

$$V_{(m/s)} = \left(\frac{1000000}{\Delta t} \right) \times 0.305 \quad \text{---------- (11)}$$

Where Δt is the interval transit time, in $\mu \sec ft^{-1}$, which is read from the sonic log. The one way travel time $t_{(\sec)}$ at a particular depth, $Z_{(m)}$ can also be calculated from the following relation:

$$t_{(\sec)} = \frac{Z_{(m)}}{V_{(m/s)}} \quad \text{---------- (12)}$$

3.5 Thermal Conductivity Estimation

Thermal conductivity is a physical property describing transfer of heat through the material. The thermal conductivity or rocks is one of the major factors that affect temperatures in sedimentary basins and therefore should be addressed in

basin analysis. (Norden and Forster, 2006). Knowledge of thermal conductivity is important in understanding and modelling of the temperature in sedimentary basins Differences in thermal conductivity may affect a basin in such a way that the thermal structure may change laterally and vertically even if heat flow into the basin is regionally the same. In geothermal studies, assessments of thermal conductivities of rocks in an area are either accomplished using the direct measurement or the indirect measurement. Different methods have been used for the direct measurement of thermal conductivity, for which the two main techniques are the stationary divided bar method and the transient needle probe method (Sass et al, 1971 and Brigaud & Vasseur, 1989). The indirect method may be accomplished using one of the wide ranges of formulae based on particle-fluid volume relationship and the corresponding individual thermal properties. (Sass et al, 1971).

Different models of thermal conductivity have been developed (Farouki, 1981; Somerton, 1992). One of the models, the geometric mean model is simple and is used to calculate the thermal conductivity of sediments (Midttomme and Roaldset, 1998). The basic geometric mean equation applied to sedimentary rocks is:

$$k = k_w^{\phi} k_s^{(1-\phi)} \quad \text{---------- (13)}$$

Where k is the thermal conductivity of the sample $(Wm^{-1}k)$, k_w is the pore fluid (water) thermal conductivity $(Wm^{-1}k)$, k_w, is the solid matrix conductivity $(Wm^{-1}k)$ and ϕ is the porosity. Two other basic models, the arithmetic and harmonic mean models are also widely used.(Mckenna et al, 1996 ; Midttomme and Roaldset, 1998).

Majorowicz and Jessop (1981) obtained an effective thermal conductivity(k_e) estimates based on net rock analysis and heat conductivity values for different rock types using the following equation;

$$k_e = \sum_i di \Big/ \sum_i \frac{d_i}{k_i} \quad \text{---------- (14)}$$

Where k_i is the conductivity of rock types in a discrete layer I, and d_i, is the thickness of the ith layer.

They showed that their effective thermal conductivity relation could give more reliable results than conductivity estimates based on measured data from only the intervals in which core samples are available. This method is very representative of the whole column of rocks drilled through. In the above equation, the porosity of the rock types, which may contain some fluids, were not considered. Some methods of calculating the effective thermal conductivities that considers the effect of porosity and pore fluids exist. The effective thermal conductivity (k_e) proposed by Huang (1971) is given by the equation;

$$k_e = \alpha k_s + \beta (k_e + k_r) \quad \text{---------- (15)}$$

Where α = the solid ï solid heat transfer coefficient

β = the fluid ï solid heat transfer coefficient

$k_s =$ Solid fraction conductivity

$k_f =$ fluid content conductivity

k_r = radioactive conductivity

The heat transfer coefficient depends on porosity and a geometric factor n, which has a value of zero for pure solids, unity for consolidated porous material and greater than unity for unconsolidated porous material.

Beck (1976) proposed a relation that gives an effective thermal conductivity (k_e) for fluid-filled sedimentary rocks drilled through by a well as:

$$k_e = \left[(2r+1) - 2\phi(r-1)/(2r+1) - \phi(r-1)\right] \quad \text{---------- (16)}$$

Where $r = k_s/k_f$ = the conductivity ratio; k_s = thermal conductivity of the solid matrix; k_f = the thermal conductivity of the pore fluid; ϕ = the porosity of the sedimentary rock. For very low porosity rocks with small conductivity ratios, the above relation reduces to;

$$k_e = k_s\left[1 - \phi(r-1)\right] \quad \text{---------- (17)}$$

3.6 Transformation of Organic Matter into Hydrocarbons

Three main stages have been recognized in the transformation of organic matter and kerogen. These include; (I) Diagenesis, (II) Catagenesis, (III) Metagenesis

Diagenesis can be divided into early diagenesis and late diagenesis. Early diagenesis includes all the processes that take place prior to deposition and during the early stages of burial, under conditions of relatively low temperature and pressure. The changes here are biological, physical and chemical. Biological agents are mainly responsible for diagenetic transformations. Chemical transformations occur by catalytic reactions on mineral surfaces. Compaction and consolidation takes place here. There is a decrease in water content and an increase in temperature. During this time, biopolymers form.

Biopolymers + CO_2 + H_2O ---------- (18)

Later Diagenesis is the transformation occurring during and after lithification. Polycondensation takes place here. (i.e. there is a loss of superficial hydrophilic functional groups such as OH and COOH). Geopolymers are created.

Kerogen + CH_4 ---------- (19)

End of this phase is marked by a temperature of 60 ^oC and vitrinite reflectance level (R_o) = 0.6%. R_o depends on organic matter types. At the end of

diagenesis, sedimentary organic matter is mainly composed of kerogen, which is insoluble in organic solvents.

Catagenesis is a zone in which thermally influenced transformations occur in kerogens. It is temperature dependent and occurs under reducing conditions. The dominant agents are temperature and pressure. It requires minimum temperatures maintained over millions of years and requisite pressure, derived from a few kilometers of overlying rocks and gas pressure as the decomposition of kerogen progresses. Certain characteristics that occur at this stage include;

- the structureless immature kerogen is unstable
- rearrangement of the kerogen structure occurs
- elimination of some groups
- Residual kerogen becomes increasingly compact and aromatic. The loss of aliphatic components and formation of benzene ring compounds through dehydrogenation reactions causes an increase in the aromatic character of kerogen.
- the C ï O and C ï C bonds break to generate and release hydrocarbons, resulting in a decrease in hydrogen content
- H/C and O/C ratios decrease significantly

Hydrocarbon generation during catagenesis can be divided into two zones.

I. The main zone of oil generation (or the oil window) (Table 3.1, Fig 3.1a)

The breakage of C ï O bond in kerogen yields or produces low to medium molecular weight liquid hydrocarbons. As temperature increases, high molecular weight liquid hydrocarbons are first to evolve, after which lower molecular weight hydrocarbons are produced.

II. Wet Gas zone

Thermally induced cracking of C-C bonds in kerogen yields light gaseous hydrocarbons or gas condensate. Gaseous hydrocarbons consist of C_1 to C_5 compounds. C_5 members can be liquids at normal surface conditions. Gas condensate refers to gases from which liquid hydrocarbons condense at the surface during commercial recovery and the liquid is known as condensate.

Metagenesis or Dry gas zone is the zone in which liquid hydrocarbons are cracked at high temperatures to yield dry gas methane and pure carbon (i.e. $CH_4 + C$). The temperature range is > 150 ^oC and Ro > 2.0%. The wet gas zone and the dry gas zone constitutes the gas window (Table 3.1, Figure 3.1b

Table 3.1: Various stages in the formation of Petroleum hydrocarbons (Frielingsdorf, 2009)

Stages of Petroleum formation	**Temperature**	**Maturity Vr%**		**Hydrocarbon Type**
	0	0	immature	
		0.2	immature	biodegredation
Diagenesis	50	0.4	immature	
	60	0.6	oil window	black heavy Oil
Catagenesis		0.8	oil window	black Oil
		1	oil window	black Oil
		1.2	oil window	light Oil
	150	1.4	gas window	volatile oil
		1.6	gas window	Condensate rich
		1.8	gas window	Dry gas rich
	200	2	gas window	Dry gas
Metagenesis		2.2	gas window	Dry gas
		2.4	gas window	Dry gas
	240	2.6	overmature	Dry gas
		2.8	overmature	Dry gas
		3	overmature	
		3.2	overmature	
		3.4	overmature	
		3.6	overmature	
		3.8	overmature	
		4	overmature	

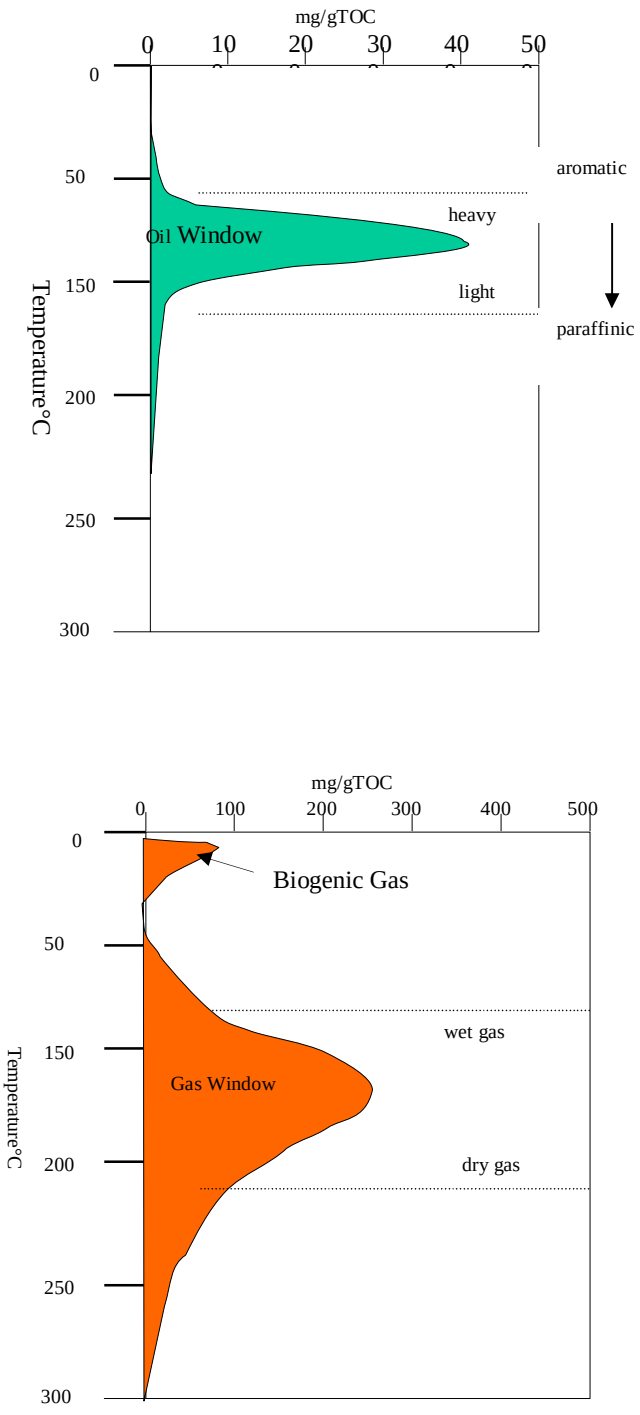

Fig. 3.1: (a) The oil window and (b) the gas window(Frielingsdorf, 2009)

3.7 Time and Temperature: kinetics of maturation

The nature of organic matter and its thermal history determines the maturation of kerogen into hydrocarbons (Tissot and Welte, 1984). According to Connan (1974) and Pigott (1985), the most important factors influencing organic matter maturation include amount and type of organic matter, temperature, time as well as pressure.

The effects of time and temperature on thermal reactions occurring in sediments during burial are first order reactions which obey the Arhenius equation, describing the intensive variable K as:

$$K = A \exp(-E / RT) \quad \text{---------- (21)}$$

Where K is the rate constant, A is the frequency factor, E is the activation energy, R is the universal gas constant (joule mole $^{-1}K^{-1}$) and T is the temperature.

In order to quantify the amount of evolved oil and gas, it is necessary to determine the constants and specify T. The Time ï Temperature Index (TTI) method of calculating maturity as used by Lopatin (1971) and Waples (1980) as well as the classic level of organic metamorphism (LOM) of Hood et al (1975) are all applications of Arhenius equation used to quantify the time ï temperature dependency on source rock maturity.

The model used in this study utilizes a broad distribution of Arhenius rate constants to calculate vitrinite maturation, then correlates maturation with reflectance. Sweeney and Burnharmôs Easy % kinetic model of calculating source rock maturity was used in this study which correlates the oil window for mixed type II / III kerogen.

3.8 Thermal Maturity Modelling

Basin modelling is a powerful tool for the evaluation of the temperature and maturity evolution and hence petroleum generation and migration from potential source rocks in sedimentary basins (Tissot et al, 1987). It is an integrated study that takes into account all geological, geophysical and geochemical processes that takes place during the entire geological history of the basin. Maturity modelling is a major part of basin modelling. Maturity models are used in describing the behaviour of individual thermal indicators with regard to hydrocarbon generation of potential source rocks. Maturity modelling can be described as the simulation of geohistory, thermal history and hydrocarbon generation.

3.7.1 Burial History Analysis

Burial History is a term used to describe plots showing the depth of burial of a given sedimentary formation as a function of post-depositional time (Seiver, 1983). It also shows the changes that take place in the sedimentary section as well as the gradual thinning of each formation in accordance to its assumed rate and extent of compaction. Geohistory analysis is another term that is often used to describe burial history (subsidence and uplift) and related processes like decompaction / compaction and the analysis of removed sections. Geohistory analysis quantifies subsidence and sediment accumulation / erosion through time of a well section or an outcrop section. A geohistory diagram is used to analyse the subsidence history of a surface point in relation to its present day elevation.

3.7.2 Thermal History

Thermal History is the expression of the temperature intensive property as it varies through time and its determination is very vital to both maturity and kinetic calculations (Metwalli and Pigott, 2005). Thermal history is a very important aspect of basin modelling, as the maturity and generation of hydrocarbon are mainly dependent on temperature. Temperature and time are utilised in thermal history modelling of a sedimentary basin. Temperature is used in determining the maturity and generation level whereas time is used for the charge history of the structural traps. Thus a reconstruction of the heat flow evolution over time and the change in geothermal gradient with time and depth is necessary. This is done by setting boundary conditions which includes:

- Basal Heat Flow (HF) ï lower thermal boundary
- Paleo water depth (PWD) or upper thermal boundary
- Sediment water interface temperature (SWIT) ï upper thermal boundary

The boundary conditions define the basic conditions for the temperature development of all layers, especially the source rock and, consequently for the maturation of organic matter through time. With these boundaries and the thermal conductivity of each lithology, a paleotemperature profile can be calculated at any event.

3.7.3 Heat Flow Estimation

It is important to know the heat flow history of a sedimentary basin in order to assess the generative potential of kerogens as well as the amount and timing of the petroleum generated in the sedimentary rocks. The heat flow history is usually derived from geological consideration and only heat flow values at maximum burial and present day are useful for thermal maturity modelling.

For the reconstruction of thermal histories and the evaluation of source rock maturation and petroleum generation, a corresponding heat flow history has to be assigned to the geological evolution. The paleo heat flow is an input parameter. . Basins affected by crustal thinning and rifting processes (Mckenzie 1978, Jarvis and Mckenzie, 1980, Allen and Allen 1990) usually experience high heat flows during the basins initiation. Iliffe et al (1999) as well as Carr and Scotchman (2003) also attest to the fact that elevated heat flows are required for rifting events and such a model is preferred to the constant heat flow model. The finite rifting model is thus the most widely accepted theory and the general model involves two phases:

(I) rifting phase: stretching, thinning and faulting of the crust accompanied by increased heat flow due to upwelling of the asthenosphere;

(II) subsidence phase: post rift exponential thermal decay owing to re-establishment of thermal equilibrium in the mantle, lithosphere and asthenosphere.

3.7.4 Geochemical Parameters

Geochemical parameters that are specified for each source rock interval include:

- The total organic carbon (TOC) content
- The Hydrogen Index (HI) and
- The Kerogen kinetics

The ability of a potential source rock to generate and release hydrocarbons is dependent upon its contents of organic matter, which is evaluated by total organic carbon (TOC) content, expressed as weight percentage organic carbon (Hunt, 1996) The total organic carbon content and Rock eval pyrolysis data specifies the quantity and quality of organic matter available within the source rocks. This information is used for calculation of generated hydrocarbons that have been transformed from

organic matter in the source rock. Peters (1986) has shown that TOC can be used to describe potential source rocks as shown in table 3.2.

Rock eval pyrolysis, was developed by Espitalie *et al* (1977) and is commonly used to determine the hydrocarbon generative potential of organic matter. A flame ionization detector (FID) senses any organic compounds generated during pyrolysis. The measured parameters include S1; free hydrocarbons present in the rock that volatized at a moderate temperature, S2; the hydrocarbons generated by pyrolytic degradation of the kerogen and S3; oxygen ï containing volatiles, i.e., carbon dioxide and water. Another important parameter is the temperature, known as Tmax, corresponding to the maximum of hydrocarbon generation during pyrolysis. Kerogen types are characterized using two indices; the hydrogen index (HI = S2 × 100 / TOC) and the oxygen index (OI = S3 × 100 / TOC). The indices are independent of the abundance of organic matter and are strongly related to the elemental composition of kerogen. The organic matter type or the kerogen type can be distinguished by plotting the oxygen index against the hydrogen index. This is known as the Van Krevelen diagram. Peters (1986) has also shown that using the hydrogen index (HI) the following products (gas + oil) will be generated from source rocks at a level of thermal maturation equivalent to R_o = 0.6%. (Table 3.3)

Table 3.2: Using TOC to assess the source rock generative potentials (Peters, 1986)

TOC (Wt. %)	**Source rock quality**
<0.5	Poor / non source
0.5 ï 1	Fair / Marginal
1ï 2	Good
2 - 4	Very Good
> 4	Excellent

Table 3.3: Using the Hydrogen index to assess the type of hydrocarbon generated(Peters, 1986)

HI (mg HC/gC_{org})	**Source potential**
0 - 150	Gas
150 - 300	Mixed (Oil + Gas)
300+	Oil

CHAPTER FOUR

4.0 DATA ANALYSIS

4.1 Basic Data Used

The basic data used for this study include;

1. Temperature data sets, such as:

(i) Bottom - hole temperatures (BHT) measurements taken during logging runs.

(ii) Production reservoir températures

(2) Stratigraphic and biostratigraphic age data; given as MFS (Maximum Flooding Surfaces) and SB (Sequence Boundary)

(3) Sand percentages

(4) Porosity logs, such as the sonic log

4.1.1 Collection and Analysis

The bottom-hole temperature (BHT) data were sourced from well logs. The reservoir data were obtained from ARPR (Annual Review of Petroleum Resources) data file, the shell database, Petrotrek, and well file reports in the Shell Library. Continuous temperature temperatures data were collected from Petrotrek. The continuous temperature logs from Petrotrek were not used because they were recorded when the temperatures have not stabilized from drilling perturbations and as such are not close to static formation temperatures. The lithologic, biostratigraphic, sand percentages data, as well as porosity logs were also obtained from the Petrotrek file.

4.1.2 Analytical Software

Softwares used include Excel, Petromod 1D basin modelling package), ArcGIS and Petrel (a mapping software).

4.2 Temperature Data

The temperature data used are mainly reservoir and corrected bottom-hole temperature data.

4.2.1 Temperature Corrections

Reservoir temperature data and corrected bottom-hole temperature data were used to characterize the thermal regime of parts of the Eastern Niger Delta. Reservoir temperatures are noted as providing direct measurements of temperatures at depth that are fairly reliable. (Husson *et al*, 2008a). Bottom-hole temperatures data are usually acquired before thermal equilibrium was reached. Empirical (Bullard, 1947, Horner, 1951) and statistical (Deming and Chapman, 1988) correction techniques exist, but they require some information that is not available, such as circulation time and shut in time (Table 4.1 and Appendix 1). In this study the routine technique generally used for hydrocarbon exploration purpose was adopted due to the general lack of data. The equilibrium or static formation temperature was therefore calculated by simply increasing the BHT by 10% ΔT

Where $\Delta T = T_b - T_s$ ---------- (21)

and T_b is the temperature at depth while T_s is the surface temperature, which is assumed as 27^{o}C and 22 ^{o}C for the Central and Coastal swamps as well as the Shallow Offshore respectively. This technique was used by Husson *et al* (2008a) for correcting BHT data in the north-western part of the Gulf of Mexico.

4.2.2 Temperature Scales and Conversion Factors.

All the data used were originally recorded in Fahrenheit scale but were converted in this study to the Celsius scale. The Fahrenheit scale has a fundamental interval of 180 ^{o}F. It starts from 32 ^{o}F and ends at 212 ^{o}F. The Celsius scale starts from 0 to 100 ^{o}C, having an interval of 100^{o}C.

The conversion scales used for conversion of Fahrenheit to Celsius and vice-versa is given as follows:

$$C = (F - 32) \times \frac{5}{9} \quad \text{---------- (22)}$$

$$F = C \times \frac{9}{5} + 32 \quad \text{---------- (23)}$$

TABLE 4.1: BOTTOM HOLE TEMPERATURE (BHT°C) DATA FROM LOG HEADER									
S/N	Well Names	Time circulation stopped	Time logger on bottom	Shut in time	BHT(oF)	Depth(FT)	BHT(oC)	Depth(m)	BHT©
						0			
1	**Abak - Enin -1**		30/08/1975	2	140	4520	60	1483	63
		10-9-75/06:00	10-9-75/10:00	4	164	9010	73.33	2956	78
			10/9/1975	6	164	9010	73.33	2956	78
			10/9/1975	9	164	9010	73.33	2956	78
			10/9/1975	13	164	9010	73.33	2956	78
			10/9/1975	16	164	9010	73.33	2956	78
		20/09/75/14:00	20-9-75/20:00	6	184	9438	84.44	3096	90
			22/09/1975	5	168	9408	75.56	3087	80
			22/09/1975	8	168	9408	75.56	3087	80
			22/09/1975	10	168	9408	75.56	3087	80
2	**Ajokpori-1**		19/02/1967		108	4005	42.22	1314	44
			3/3/1967		171	10837	77.22	3555	82
			5/3/1967		173	11235	78.33	3686	83
3	**Akai-1**	18-4-87/20:30	14-4-87/06:20		132	5018	55.56	1646	59
		02/05/87/22:15	3-5-87/10:30		179	8697	81.67	2853	88
		02/05/87/22:15	3-5-87/13:12		179	8697	81.67	2853	88
		5/13/1987	13-5-87/23:30		195	9198	90.56	3018	97
		16-5-87/22:00	19-5-87/09:54		209	9943	98.33	3262	105
4	**Akaso-4**								
5	**Akata-1**		12/4/1953		102	4065	38.89	1334	40
			4/6/1953		150	7000	65.56	2297	70
			2/7/1953		160	8185	71.11	2685	75
			22/07/1953		239	10787	115	3539	124
			7/10/1953		245	11104	118.3	3643	127
			7/10/1953		245	11111	118.3	3645	127
6	**Akikigha-1**	13-09-1987/13:00	13-9-87/18:41	5:41	112	5002	44.44	1641	46
		25-9-87/03:00	25-9-87/20:30	17:30	159	9000	70.56	2953	75
		25-9-87/03:00	25-9-87/15:45	12:45	156	9012	68.89	2957	73
		25-9-87/03:00	25-9-87/10:00	7	154	9001	67.78	2953	72
		25-9-87/03:00	26-9-87/00:15	21:15	163	9008	72.78	2955	78
		5-10-87/17:00	6-10-87/04:00	12	187	10455	86.11	3430	72
		25-9-87/03:00	26-9-87/02:30	11:30	232	14234	111.1	4670	109
		25-9-87/07:45	26-9-87/02:30	6:45	232	14234	111.1	4670	109
		5-10-87/17:00	6-10-87/14:15	21:15	194	10464	90	3433	96
		5-10-87/17:00	6-10-87/09:00	16	191	10468	88.33	3434	94
7	**Akuba-1**		12/2/1967		172	10380	77.78	3406	83

4.2.3 Determination of Geothermal Gradients

The basic equation for the determination of geothermal gradients as given by Bradley (1975) is as follows:

$$Geothermal \quad Gradient \quad = \frac{T_d - T_s}{X} \times 1000 \quad \text{----------(24)}$$

Where T_d and T_s are temperatures below and at the surface respectively, while X is the formation depth. The temperatures are in degrees Celsius and depth is given in meters and the thermal gradient is in degrees Celsius per kilometre (^{o}C/Km).

4.2.3.1 Mean Annual Surface Temperature

A good knowledge of the surface temperature is important in the determination of the geothermal gradient in a sedimentary basin because the surface temperature provides a boundary condition. The mean annual surface temperature is an approximation of the temperature at the air-sediment boundary. Accordingly, an equilibrium surface temperature of 27 ^{o}C (80 ^{o}F) was used for the Central Swamp and the Coastal Swamp. A seabed surface (i.e. mudline) temperature of 22 ^{o}C was also applied to the Shallow Offshore. In offshore areas, because of the intervening water column, the air temperatures does not truly reflect temperature at the top of the sediment column and therefore may give spurious results in geothermal gradient calculations. The mean air temperature at the water surface in the deep offshore is considerably higher than the seabed or mudline temperature. The seabed temperature was used as the surface temperature because the depths to the seabed surface for these shallow offshore wells range from 17 to 50m and therefore shows no significant change of temperature with water depth. Figure 4.1 is a simple temperature-depth ocean water profile for low to middle latitudes, which shows how temperature decreases with increasing water depth. This figure was obtained from the web site; http://www.windows.ucar.edu/tour/link=/earth/water/images/temperature_depth_jpg é . This is corroborated by Figure 4.2, showing bottom water temperature as a function of water depth obtained by Brooks *et al* (1999) at heat flow measurement sites, offshore Nigeriaôs continental margin. In offshore areas, the geothermal gradients are usually calculated using mud-line temperature as the surface temperature. The mud-line is usually determined from the temperature-depth ocean water profile as the water depth at which the field or well is located. (Figure 4.1)

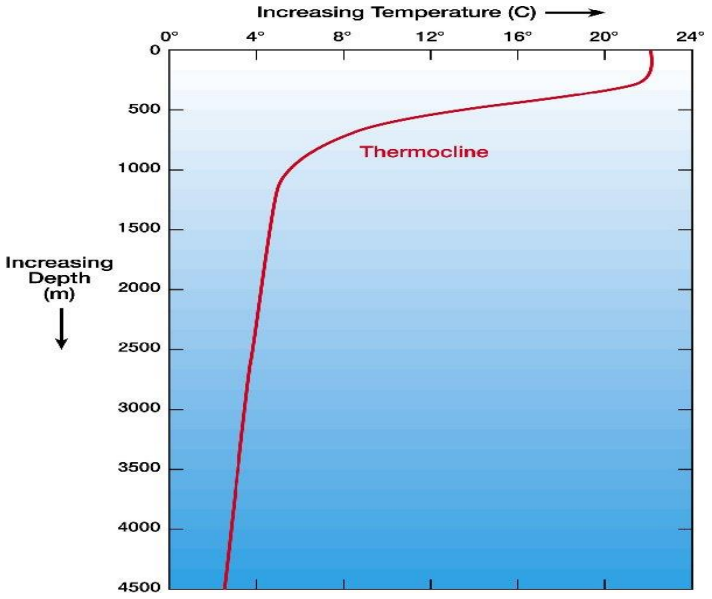

Fig. 4.1: A simple temperature- depth ocean water profile (from http:// www.Windows.ucar.edu.tour/link=/earth/Water/temp.htm&edu=high

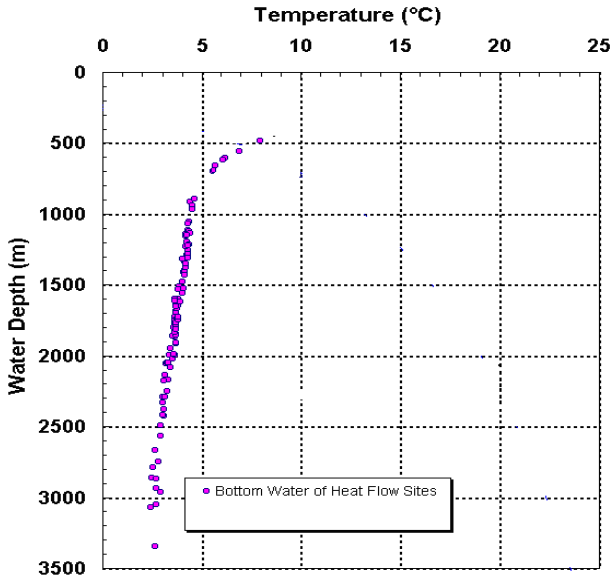

Fig. 4.2; Bottom water temperature as a function of depth, at heat flow sites on Nigeria's offshore continental margin (Brooks et al, 1999)

4.2.3.2 Methodology

Two models were utilized in studying the geothermal gradient patterns in parts of the Eastern Niger Delta. These include;

(i) A constant geothermal gradient model

(ii) A variable geothermal gradient model

In the first model, a single linear regression of temperature versus depth is considered as a convenient first order approximation (Appendix II) while in the second model, the temperature-depth data sets are well fit by two constant gradients at depth (Appendix III). In this model an upper or shallow thermal gradient and lower or deeper thermal gradient were determined. In this case, a sharp break in thermal gradient occurs at depth. This will give a considerable better fit than that given by a single linear regression.

To calculate geothermal gradients, reservoir temperature (RT) and (BHT) data from each well was loaded into an excel spreadsheet. The BHT depth data was then converted to a true vertical depth (TVD ï SS) using directional survey data from log headers. The Reservoir temperature data from ARPR file had already been converted to a sub-sea true vertical depth. An excel macro was used to plot data from each well, field and depobelt on a temperature-depth graph. Each plot was examined and a gradient line or series of gradient lines was visually established and drawn through the points. The mean annual surface temperature at the air-sediment interface and the temperature at the seabed-water interface (i.e. the mud-line) were used as the shallowest point. For each of the well data, after establishing the gradient lines, values were extracted from each plot to calculate a gradient and the 100^{o}C and 150^{o}C isotherm depth. If dogleg gradients are observed, the temperature of the deepest point, above the deepest dogleg was recorded, and the gradient of this last step was used to calculate the temperatures at 1000m, 2000m, 3000m and the depth at which temperatures of 100^{o}C and 150^{o}C were attained.

4.2.4 Temperature and Geothermal Gradient Mapping

The temperature field in a linear regression (i.e. average geothermal gradient model), were computed using the following relation:

$$T_{(z)} = Z_{g} + T_{s} \quad \text{----------} \quad (25)$$

Where Z is the formation thickness, g is the geothermal gradient and T_s, is the seabed or surface temperature.

In the second case, (i.e. variable geothermal gradient model), temperatures were well fit by two constant geothermal gradients. Temperatures are thus computed using the following equation:

$$T_{(z)} = T_s + g_1 z + g_2 (z - z_0) \text{ ---------- (26)}$$

Where g_1 is the upper thermal gradient, g_2, is the lower thermal gradient, z_0 is the rupture depth and z is the formation thickness.

The estimated temperatures may also be presented in temperature maps showing the temperature fields at specific depths of 1000m, 2000m, and 3000m. An alternative way to examine the temperature-depth relationship is the isothermal maps. Isothermal maps involve mapping the depth to a constant temperature such as 100^{o}C and 150^{o}C. Geothermal gradient maps can also be presented as average geothermal gradient map and geothermal gradient map of the shallow section (continental sandstones) and for the deeper marine/paralic section. These maps were contoured using Petrel 2007 software.

4.3 Sand and Shale Percentages

4.3.1 Method of Determination

Sand and Shale Percentages are usually determined from gamma ray logs, resistivity and spontaneous potential logs. For this study, the sand and shale percentages for all the wells were retrieved from the shell database known as Petrotrek.

4.3.2 Sand Percentage Mapping

The sand percentage data were averaged for certain depth intervals such as: 0 ï 4000ft (0 ï 1312m) and 4000 ï 9200 ft (1312 ï 3000 m) for each of the wells. The average sand percentages for all the entire project area were then contoured using Petrel 2007 software.

4.4 Thermal Maturity Modelling

In this work, PetroMod 1-D modelling software package (Version 11, 2009) made by IES Germany were used to reconstruct the burial and thermal history,

evaluate the hydrocarbon potentials as well as the timing of petroleum generation across the Coastal Swamp, the Central Swamp and Shallow Offshore of the Eastern Niger Delta.

4.4.1 Burial History Analysis

4.4.4.1 Model Construction

According to Underdown and Redfern (2007), the conceptual model used in basin modelling is derived from the geological evolution of the basin under consideration and is thus based on the geological framework of the study area. This therefore gives the temporal framework that is required to structure the input data for computer simulation. Stratigraphic analysis provides one of the most important inputs to the conceptual model. The sedimentation history is then subdivided into a continuous series of events, each with a specified age and duration of time. Each of these stratigraphic events represents a time span during which deposition (sediment accumulation), non-deposition (hiatus) or uplift and erosion (unconformity) occurred. The model for the Niger Delta basin used in this study contains a maximum of 7 events (layers) and is summarized in tables 5.09, 5.10, 5.11, 5.12. Models were constructed from Paleocene (65 Ma) to Recent.

4.4.1.2 Input Parameters

In order to carry out a burial history reconstruction the following input data are required.

- Depositional thickness
- Depositional age in Ma (millions of years)
- Lithological Composition
- Thickness and age of eroded intervals
- Petroleum Systems Essential Elements (Underburden, Source Rocks, Reservoir rocks, Seal Rock and Overburden rock
- Possible source rock properties (TOC & HI)
- Applicable kinetics

Depositional thicknesses and absolute ages in many of the different stratigraphic units were defined using biostratigraphic data and Shell Development Company of Nigeria Limited Cenozoic Geological data table (Table 4.2). A generalised stratigraphy and tectonic history of the Niger Delta and the Benue Trough is shown in table 4.3. The thicknesses of sedimentary layers not penetrated by wells

were estimated from available data from surrounding wells (Table 4.4). The lithological composition of the stratigraphic units was obtained from the sand/shale percentage data. The petrophysical properties of the lithologies were provided by the modelling package.

4.4.2 Thermal History

Thermal History is the expression of the temperature intensive property as it varies through time and its determination is very vital to both maturity and kinetic calculations (Metwalli and Pigott, 2005). Thermal history is a very important aspect of basin modelling, as the maturity and generation of hydrocarbon are mainly dependent on temperature. Temperature and time are utilised in thermal history modelling of a sedimentary basin. Temperature is used in determining the maturity and generation level whereas time is used for the charge history of the structural traps. Thus a reconstruction of the heat flow evolution over time and the change in geothermal gradient with time and depth is necessary. This is done by setting boundary conditions which includes:

- Basal Heat Flow (HF) ï lower thermal boundary
- Sediment water interface temperature (SWIT) ï upper thermal boundary

The boundary conditions define the basic conditions for the temperature development of all layers, especially the source rock and, consequently for the maturation of organic matter through time. With these boundaries and the thermal conductivity of each lithology, a paleotemperature profile can be calculated at any event.

4.4.3 Paleobathymetry

The paleobathymetry or the paleo-water depth (PWD) data are used to reconstruct the total subsidence that has occurred within a basin. Paleobathymetry is used for subsidence calculation and to display burial curves with respect to sea level. It has no influence on the temperature and geochemical calculations. The estimated values of paleobathymetry for the Niger Delta used in the models are shown in table 4.5

Table 4.2; NIGER DELTA CENOZOIC GEOLOGICAL DATA TABLE

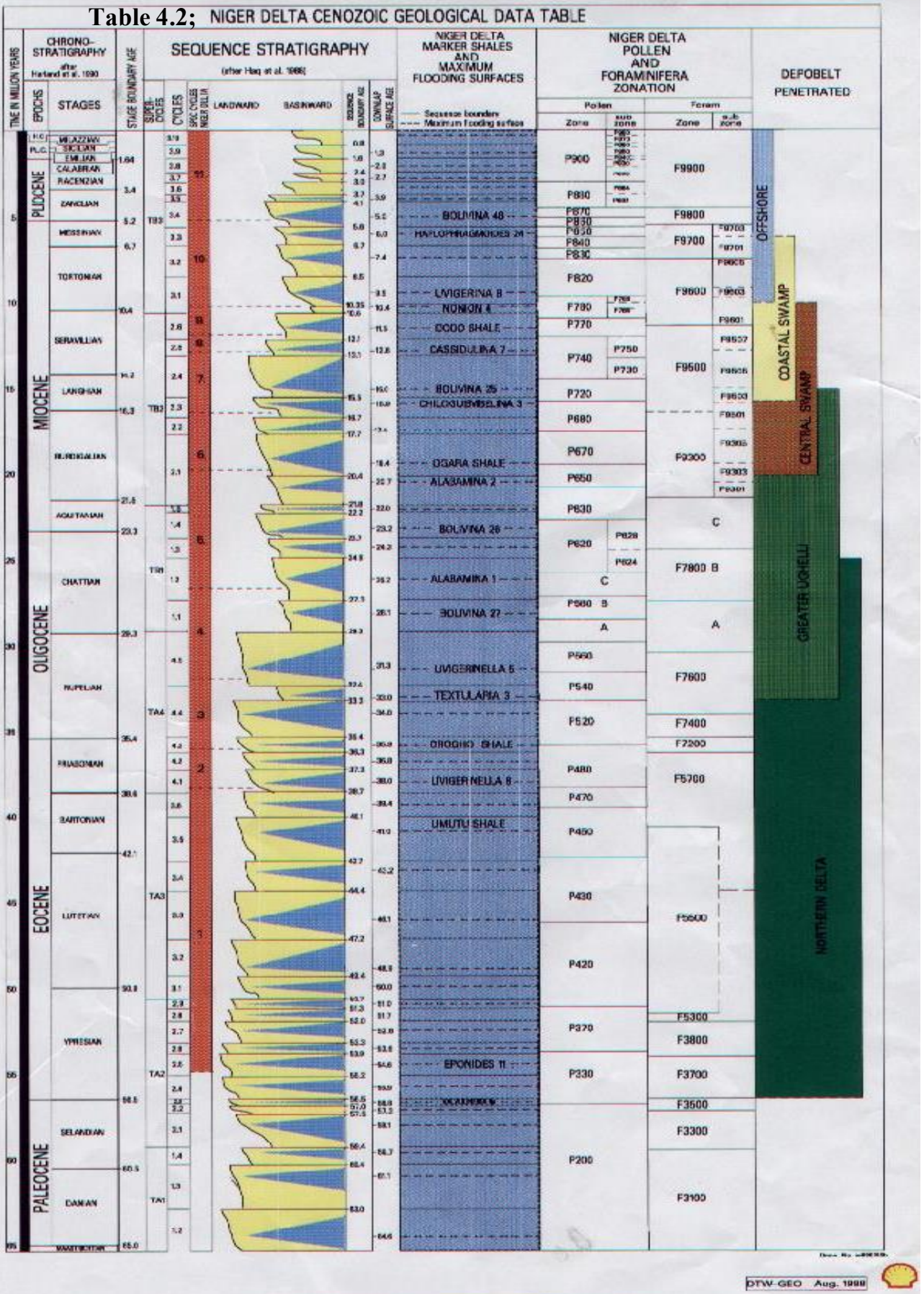

Niger Delta Cenozoic Chronostratigraphic Chart

Table 4.3: Generalized Stratigraphy and Tectonic History of the the Tertiary Niger Delta.

Tectonic Events		Heat Flow	Age			Time (Ma)	Stratigraphy: Niger Delta Depobelts	Stratigraphy: Benue Trough AnambraBasin
				Holocene				
				Pleistocene		1.64	Offshore	Benin Formation
			TERTIARY	Pliocene	Placenzian	3.4		
					Zanclian	5.2		
			NEOGENE	Miocene	Messinian	6.7		Ogwashi Asaba Formation
					Tortonian	10.4		
					Serravilian	14.2	Coastal Swamp	
					Langhan	16.3		
					Burdigalian	21.5	Central Swamp	
					Aquitanian	23.3		
Postrift	Subsidence/ Prograding Delta/ rapid sedimentation	Thermal cooling	PALEOGENE	Oligocene	Chatian	29.3	Greater Ughelli	
					Rupelian	35.4		
				Eocene	Priaborian	38.6	Northern Delta	Ameki Formation
					Bartonian	42.1		
					Lutetian	50.0		Imo Shale
					Ypresian	56.7		
				Paleocene	Thanetian	58.5		Nsukka Formation
					Selandian	60.5		
					Danian	65.0		
Synrift	Drift	Slow Decreasing Heat flow	CRETACEOUS LATE Senonian	Maastrichtian		70.6		Ajali Sandstone
				Campanian				Mamu Formation
				Santonian		83.5		Enugu/Nkporo Shale
						85.6		Awgu Shale
	Break up	Peak Heat flow		Coniacian		89.3		
				Turonian		93.5		Ezeaku Shale
				Cenomanian		99.6		Odukpani Formation
	Benue Rift Uplift and erosion	Slow Rising Heat flow	Early	Albian		112		Asu River Group
				Aptian		125		Awi Formation
Pre - Rift	Graben formation			PRECAMBRIAN				BASEMENT

Table 4.4: Model used to estimate the thickness of the Miocene, Oligocene, Eocene and the Palaeocene sediments.

Location	**Source rock name**	**Top depth (m)**	**Bottom depth (m)**	**Thickness(m)**
Nsit -1	Oligocene	1207	2146	939
	L. Eocene	2146	2264	118
	Paleocene	2264	2412	148
Etinan -1	Miocene	1129	1568	459
	Oligocene	1568	2297	729
Midim -1	Miocene	328	1175	847
	Oligocene	1175	2920	1745
	U. Eocene	2920	3076	156
Edik - 1	L. Miocene	411	556	145
	Oligocene	556	639	83
	Eocene	639	957	318
	Palaeocene	957	1812	855
Akaso	U. Eocene	5300	6000	700
	L. Eocene	6000	7000	700
	Palaeocene	6700	7400	700
Uge ST	Oligocene	3410	4220	810
	U.Eocene	4220	5401	1181
Summary Estimates				
Source rock name	**Thickness (m)**			
L.Miocene	340			
Oligocene	842			
Eocene	635			
Paleocene	568			

Table 4.5: Paleobathymetry of sediments in the Niger Delta as used for input in the modelling

Epoch		Age	Water Depth
Holocene		0	0
Pliocene	Placencian	3.6	30
	Zanclean	5.33	10
Miocene	Serravillian	13.82	150
	Langhan	15.97	300
Oligocene		33.9	100
Eocene		48.6	80

4.4.4 Heat Flow

It is important to know the heat flow history of a sedimentary basin in order to assess the generative potential of kerogens as well as the amount and timing of the petroleum generated in the sedimentary rocks. The heat flow history is usually derived from geological consideration and only heat flow values at maximum burial and present day are useful for thermal maturity modelling.

For the reconstruction of thermal histories and the evaluation of source rock maturation and petroleum generation, a corresponding heat flow history has to be assigned to the geological evolution. The paleo heat flow is an input parameter, which is commonly difficult to define. Following published concepts on heat flow variations, basins affected by crustal thinning and rifting processes (McKenzie 1978, Allen and Allen 1990) usually experience elevated heat flows during the basins initiation. For all simulations the scenario adopted is thus; a steadily increasing heat flow history from a value of 60 mWm^{-2} at 125Ma. A maximum heat flow value of 90 mWm^{-2} was assigned for the heat flow experienced at 85Ma, the break-up phase of the basins initiation (Figure 4.3). Assuming a gradual cooling, as proposed by theoretical stretching models (Mckenzie, 1978), the heat flow then declines to its lower present day values. The present day heat flow is then adjusted until the calculated present day temperature field fits the observed thermal structure constructed from well log temperature measurements. To match present-day heat flow, as calibrated against temperature data, lower heat flow values of c. 29 ï 55 are needed.

4.4.5 Calibration Parameters

In this study, corrected bottom-hole temperatures (BHT) and reservoir temperatures (RT) were used for the calibration of the temperature history of the basin. The measured temperature values were compared with calculated temperature values. The model uses the Easy% Ro algorithm of Sweeney and Burnham (1990) to calculate vitrinite reflectance. This is the most widely used model of vitrinite reflectance calculation and is based on a chemical kinetic model that uses Arhenius rate constants to calculate vitrinite elemental composition as a function of temperature. No vitrinite reflectance data were made available. The results of the simulation include a calculated Easy $\%R_o$ of Sweney and Burham (1990).

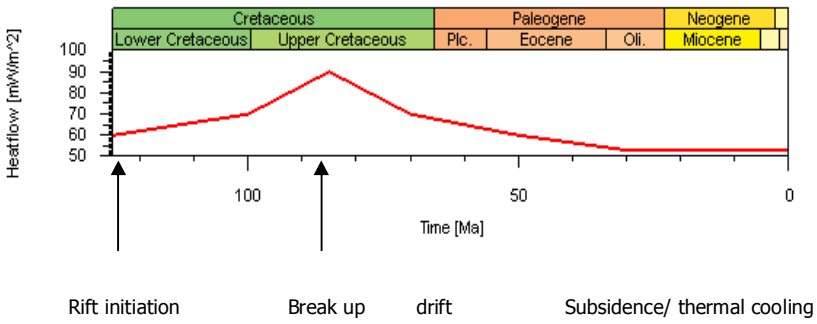

Fig. 4.3. Heat flow history model of the Niger Delta used in the present study

4.4.6 Petroleum Geochemistry

4.4.6.1 Organic matter content and quality

The geochemical and petrologic characteristics of organic matter provide data that must be considered in evaluating potential source rocks (Bustin, 1988). The total organic carbon content (TOC) and rock-eval pyrolysis measurements gives information on quality and quantity of organic matter. This information is used for calculation of hydrocarbons that have been transformed from organic matter in the source rocks. TOC and rock-eval pyrolysis data were not given for any particular well. However TOC and rock eval data exists in literature for most of the stratigraphic units in the Niger delta, and also for older Tertiary and Cretaceous rocks of the adjacent Anambra Basin and the Benue Trough. The geochemical evaluation used in this study is based on geochemical data available in literature (Bustin, 1988; Udo and Ekweozor, 1988; Ekweozor and Okoye, 1980, Ekweozor and Daukoru, 1994) as well as from some confidential records. The average source rock values for the various stratigraphic units in the Niger Delta are given in table 4.6. For the modelling study, the Upper Miocene, Lower Miocene, Oligocene, Eocene and Palaeocene are considered as effective source rocks. For the calculation of kerogen transformation, the kinetic dataset of Burnham (1989) for type II / III kerogen was used.

A marked decrease in total organic carbon content occurs in the source rocks of the Niger Delta from a mean of 2.2% in late Eocene strata to 0.90% in Pliocene strata.(Bustin, 1988). Udo and Ekweozor (1988) similarly has obtained an average TOC of 2.5% and 2.2% for the Agbada - Akata shales in two wells in the Niger Delta. The variation of the total organic carbon (TOC) with age is shown in figure 4.4a. The total organic carbon (TOC) content is thus greater in Upper Eocene to Oligocene strata, followed by lower and middle Miocene and Upper Miocene ï Pliocene strata. Organic petrography suggests that the organic matter consists of mixed maceral components (85 ï 98%) vitrinite with some liptinite and amorphous organic matter (Bustin, 1988). There is no evidence of algal matter.

Table 4.6: Source rock properties of Tertiary sediments of the Niger Delta (Compiled from Bustin, 1988 and Confidential data)

Epoch	TOC (%)	HI(mgHCg^{-1}TOC	Kerogen type
Pliocene	0.87 -0.90	50 - 55	III / IV
Upper Miocene	0.80 ï 0.85	57 ï 60 (100)	II / III
Middle Miocene	1.2 ï 1.3	70 ï 75 (100)	II / III
Lower Miocene	1.4 ï 1.5	60 ï 80 (100)	II / III
Oligocene	1.6 - 1.7	85 -100 (150)	II / III
Eocene	1.8 ï 2.3	72 ï 100 (250)	II / III
Paleocene	2.5	(350)	II / III

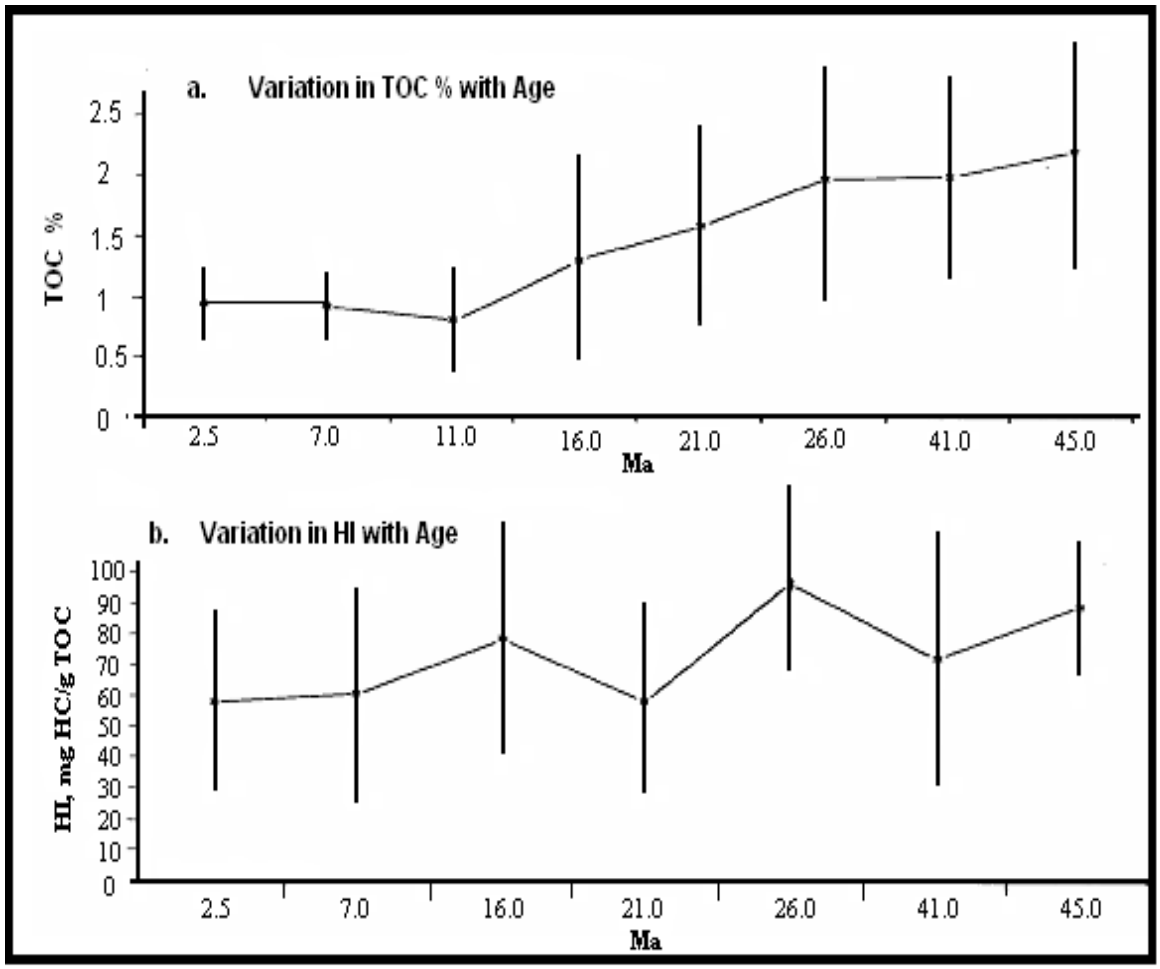

Figure 4.4: (a) Variation in TOC content with age for strata with less than 10% TOC (n =1221).(b) Variation in HI with age for strata with less than 10% TOC (n = 616) (After Bustin, 1988

Bustins (1988) rock eval pyrolysis result suggests that the hydrogen indices (HI) are quite low and generally range from 160 to less than 50mgHC/gTOC. There is also a general decrease in hydrogen index from the Eocene strata to the younger Pliocene sediments (Figure 4.4b), although not as significant as TOC. In Ekweozor and Daukoru (1994) view, an average hydrogen index value of 90 mgHC/gTOC suggested by Bustin (1988) is an underestimation of the true source rock potential because of the matrix effect on whole rock pyrolysis of deltaic rocks. Bustins plot of rock eval determined oxygen index (OI) and hydrogen index (HI) on a Van-krevelan-type (HI/OI) diagram shows that almost all samples plot between type II and type III kerogen (Figure 4.5). Similarly Lambert-Aikhionbare and Ibe (1984) has shown in their elemental analysis (carbon, hydrogen, nitrogen and oxygen) of the kerogens that the kerogen type is mainly type II with varying admixtures of type I and III. (Fig. 4.6)

In general, no rich source rock occurs in the Tertiary succession of the Niger Delta and as conventionally measured; the strata have little or no oil generating potential. According to Bustin (1988), the poor quality of the source rocks has been compensated for by the great volume of the source rocks, the excellent migration routes provided by interbedded permeable sands and the relatively high rate of maturation.

4.4.7 Thermal Conductivities of sediments in the Niger Delta

The sediments in the Niger Delta principally consist of sands and shales in variable proportions. The thermal conductivities of these deltaic sediments generally decreases with depth, varying in the following manner; 1.81 ï 2.26 W/mK for sands, 1.63 ï 2.19 W/mK for shaly sands, 1.56 ï 1.76 W/mK for shales, 1.85 ï 1.95 W/mK for sandy shales and 2.04 ï 2.15 W/mK for equal proportions of shale and sand. The thermal conductivities of these prominent lithologies in the Niger Delta shows a wide variation from well to well. Plots of thermal conductivities and lithology as a function of depth for some wells in the Niger Delta are shown in figures 4.7 a ï d.

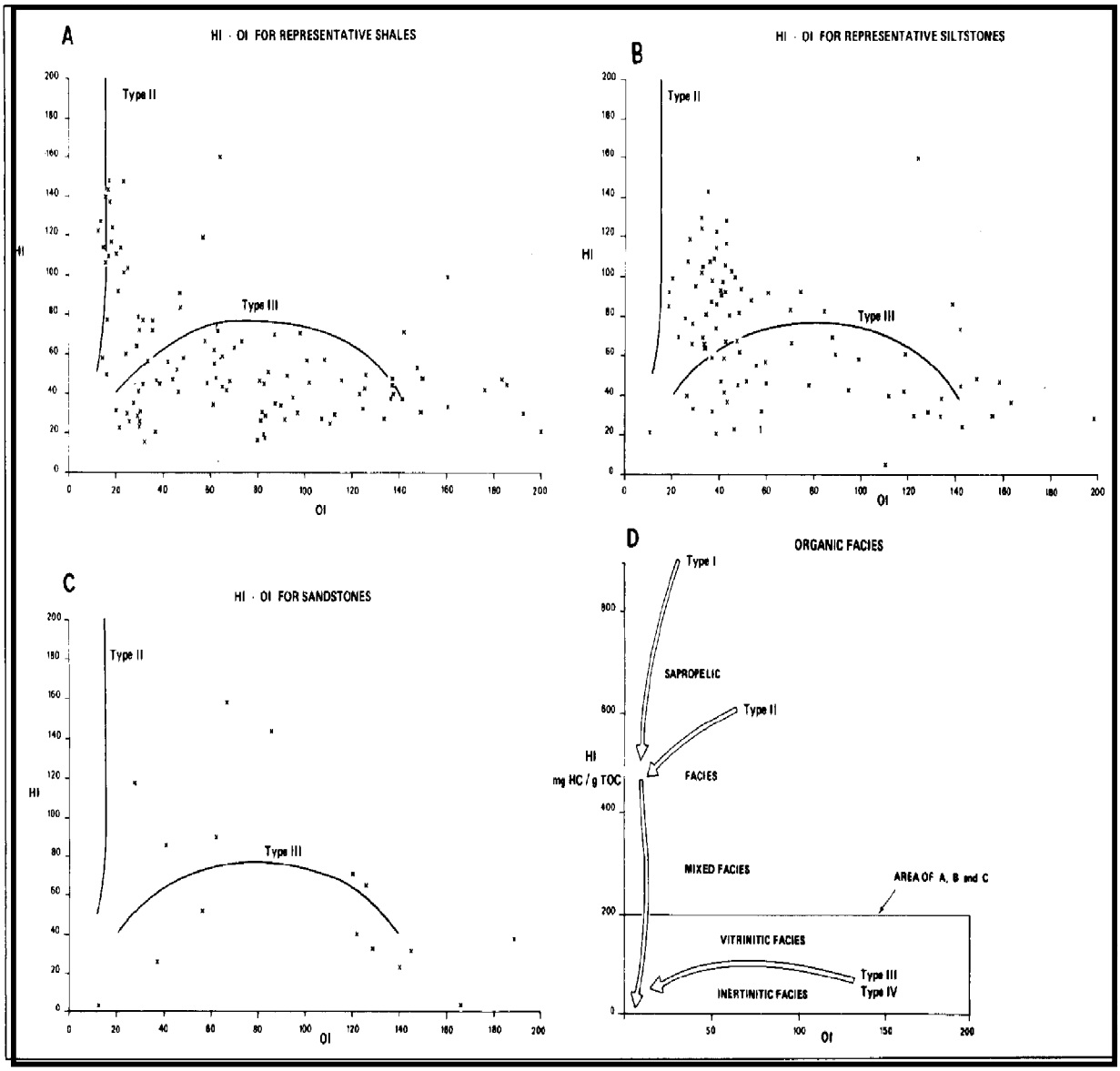

Figure 4.5: HI/OI diagram for (a) Shales (includes all clay rocks);
(b) Siltstones; (c) Sandstones; (d) chemical facies diagram (Bustin, 1988)

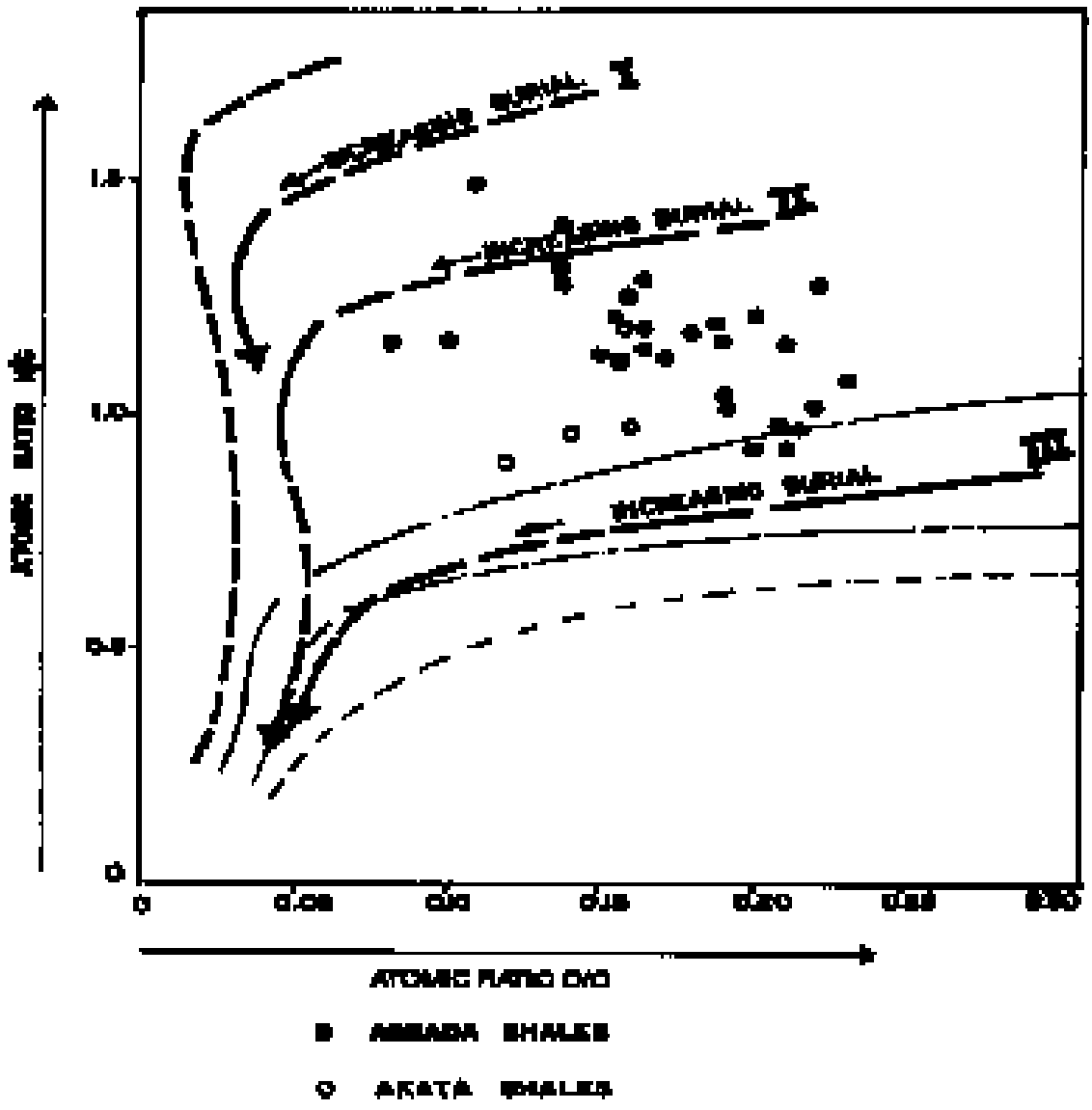

Figure 4.6: Van Krevelens diagram with results of elemental analysis of some kerogen of Agbada and Akata shales of the Niger Delta (Lambert-Aikhionbare and Ibe, 1984)

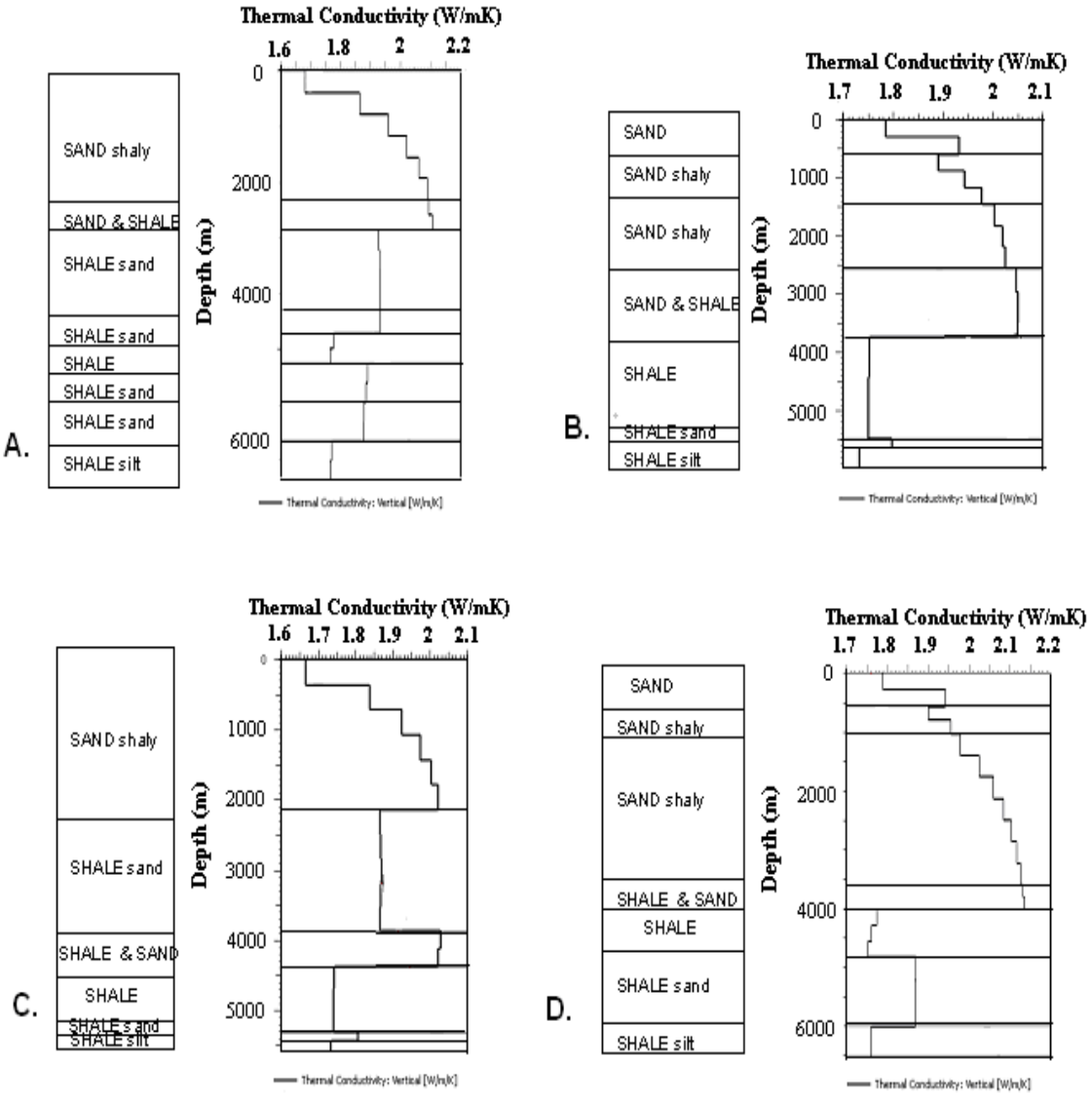

Figure 4.7: Thermal coductivity variations in (a) Akaso – 4 (b) Obigbo – 1 (c) Opobo South – 4 and (d) Kappa – 1 wells in the Niger Delta.

4.4.8 Sedimentation Rates in the Niger Delta

Sedimentation rates (VSE) is usually calculated by dividing the actual thickness (Z_2) of the sedimentary layer by the difference between the age of the bottom and top of the layer.

Sedimentation rate VSE = Z_2 / ϕT ---------- (27)

Where ϕT = t_2 - t_1 ---------- (28)

Sedimentation rates were calculated for Pliocene to Recent sediments in the study area. The result shows that sedimentation rates are highest in the Shallow Offshore and in the western part of the Coastal Swamp (Fig. 4.8). Sedimentation rates in the Shallow Offshore ranges from 200 ï 700 m/Ma while in the western part of the Coastal Swamp it ranges from 100 ï 500 m / Ma. In the Central Swamp and the Eastern parts of the Coastal Swamp, the sedimentation rates vary between 100 ï 300 m / Ma.

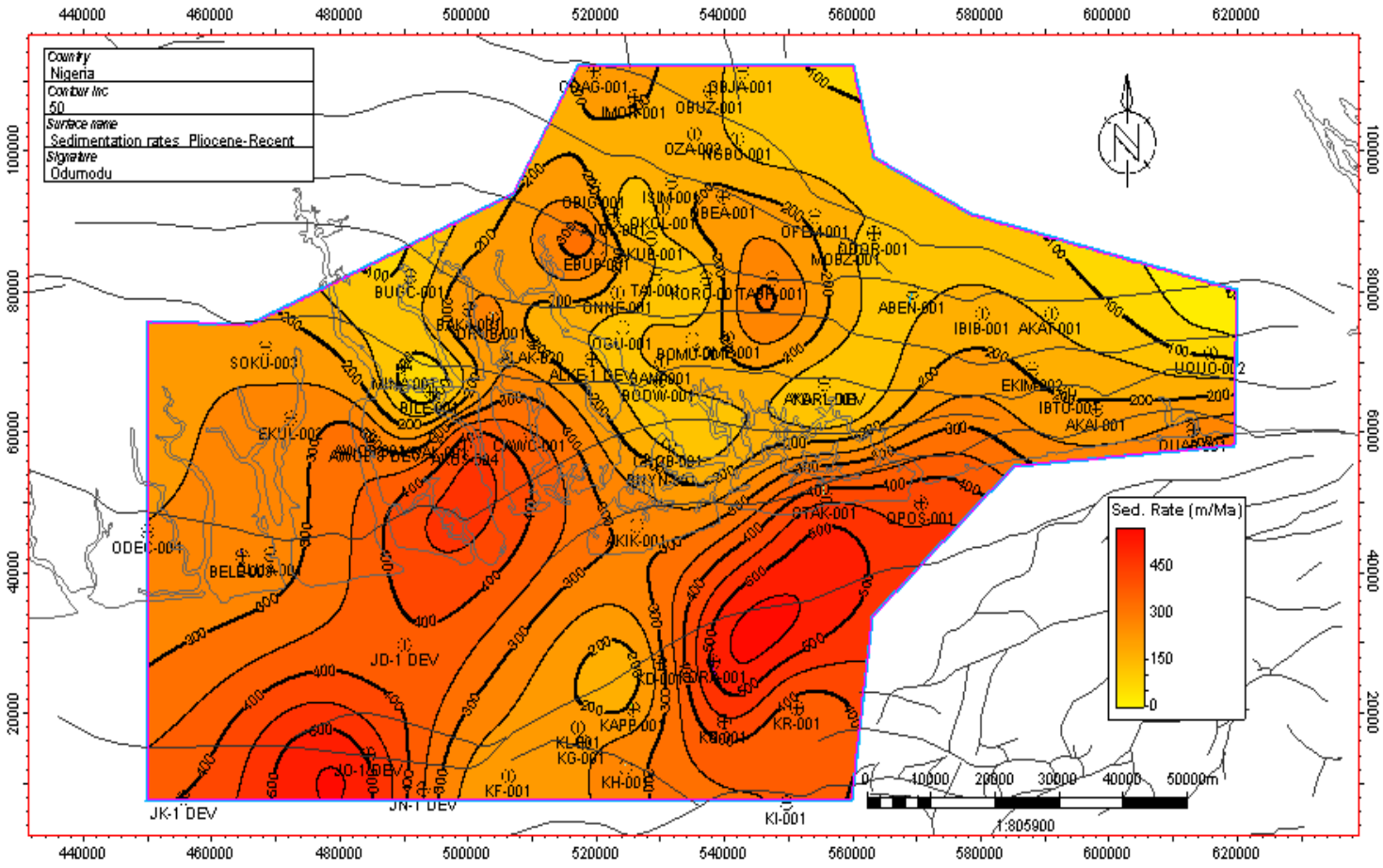

Figure 4.8: Map showing variations in Sedimentation Rates for Pliocene to Recent sediments in the Niger Delta

CHAPTER FIVE

5.0 RESULTS AND INTERPRETATION

5.1 Geothermal Gradients

Geothermal gradients pattern in the eastern part of the Niger Delta were determined using reservoir and corrected bottom-hole temperatures data. The result shows that the Central and Coastal Swamps were characterized by two-leg dogleg geothermal gradients pattern whereas the Shallow Offshore has single leg geothermal gradients pattern. In the two-leg dogleg geothermal pattern, a shallow interval of low geothermal gradient and a deeper interval of higher geothermal gradient are usually observed. The shallow interval of lower geothermal gradient is usually characterized by higher thermal conductivity whereas the deeper interval of higher geothermal gradients exhibits lower thermal conductivities. A sharp break occurs in the two gradient legs of the temperature ï depth profile. The shallow gradient belongs to the continental and/or continental transition (CT) sequence, whereas the deeper gradient belongs to the paralic/marine paralic sequence. The thickness of the lower geothermal gradient interval varies from 700m to 2000 m. The shape of the dogleg depends on the contrast in thermal gradient between the continental and the deeper paralic/marine paralic. If the contrast is low, the dogleg pattern appears close to a single leg model and a gentle curve replaces the kink. The single leg pattern occurs in the Shallow Offshore areas where high percentage interval (70 ï 80%) interval occurs at depths of 2900 ï 3600 m. In the Shallow Offshore, temperature profile or the geothermal gradient pattern show a uniform linear increase with depth.

The geothermal gradients pattern in the Eastern part of the Niger Delta is thus a reflection of the lithological variations in the area. The transition from one leg of the dogleg to another coincides with the change from the continental sandstones to the paralic / marine section. The temperature depth profiles used in calculating the thermal gradients are thus shown in figure 5.1 and in appendix 1. Geothermal gradient maps of the study area are shown in figures 5.2, 5.3 and 5.4.

5.1.1 Geothermal Gradients in the Shallow (Continental) section.

In the Central Swamp depobelt, the geothermal gradient in the continental sandstone is slightly above 10 ^{o} C/Km at the central part around Tabangh, Yomene and Mobazi fields. The geothermal gradients increase eastwards and westwards to

slightly above 18 ^{o}C/Km. In the Coastal Swamp depobelt, the geothermal gradient in the shallow / continental section varies between 10 ^{o}C/km ï 18 ^{o}C/Km in the western and central parts and increases eastwards to 26^{o}C/Km (Fig. 5.2). In the Shallow Offshore, the geothermal gradient in the continental sandstones increases from about 14 ^{o}C/Km at the coastline to about 24 ^{o}C/Km in the J field. The geothermal gradient in the K field averages about 20^{o}C/Km and increases eastwards to about 26 ^{o}C/Km. Geothermal gradients variation within the Shallow (Continental) section are summarized in table 5.1

5.1.2 Geothermal Gradients in the deeper (Marine / Paralic) section

In the deeper (marine/paralic) section, the geothermal gradient varies from between 18 ^{o}C/km to 30^{o}C/km in the west and central part of the Coastal Swamp and increases to 45 ^{o}C/Km at the eastern parts. (Fig.5.3). Northwards in the central parts of the Central Swamp, the geothermal gradients are slightly less than 20 ^{o}C/Km, but increases up to 45 ^{o}C/Km eastwards and westwards. The geothermal gradient in the marine/paralic section of the Shallow Offshore varies between 18 ï 25 ^{o}C/Km in the eastern and central parts and increases eastwards towards the Qua-Ibo field. The geothermal gradients variation in the deeper (marine / paralic) section are summarized in table 5.2

5.1.3 Average Geothermal Gradient variation

In the Coastal Swamp, the average geothermal gradient varies between less than 12 ^{o}C/Km to 20 ^{o}C/Km in the western and central parts and increases eastwards up to 24 ^{o}C/Km towards the Qua Ibo field (Fig. 5.4). In the Central Swamp, the lowest values of average geothermal gradient of 14 ^{o}C/Km occur in the central parts around Tabangh, Mobazi and Yomene fields. The average geothermal gradient increases eastwards to 20 ^{o}C/Km and westwards to and 30 ^{o}C/Km. In the Central Swamp, the highest average thermal gradients of 23 ^{o}C/Km 30 ^{o}C/Km occur at Imo river-1 and Obigbo-1 wells. In the western part of the Shallow Offshore, the average thermal gradient varies between 14 ï 24 ^{o}C/Km from the coastline to further offshore. It also increases eastwards to about 20 ^{o}C/Km in the K field and further eastwards to 26 ^{o}C/Km

Table 5.1: Summary of Geothermal Gradient variations for the Shallow Section (Continental Sandstones) across the depobelts in the study area

	Depobelt	*Abbreviation*	*Geothermal Gradient $^{o}C/Km$*	
			Low	*High*
1	Shallow Offshore	S_{HO}	14	26
2	Coastal Swamp	C*so*	10	26
a.	Western part	C*so(a)*	10	18
b.	Central part	C*so(b)*	10	18
c.	Eastern part	C*so*©	10	24
3	Central Swamp	C*sw*	10	20

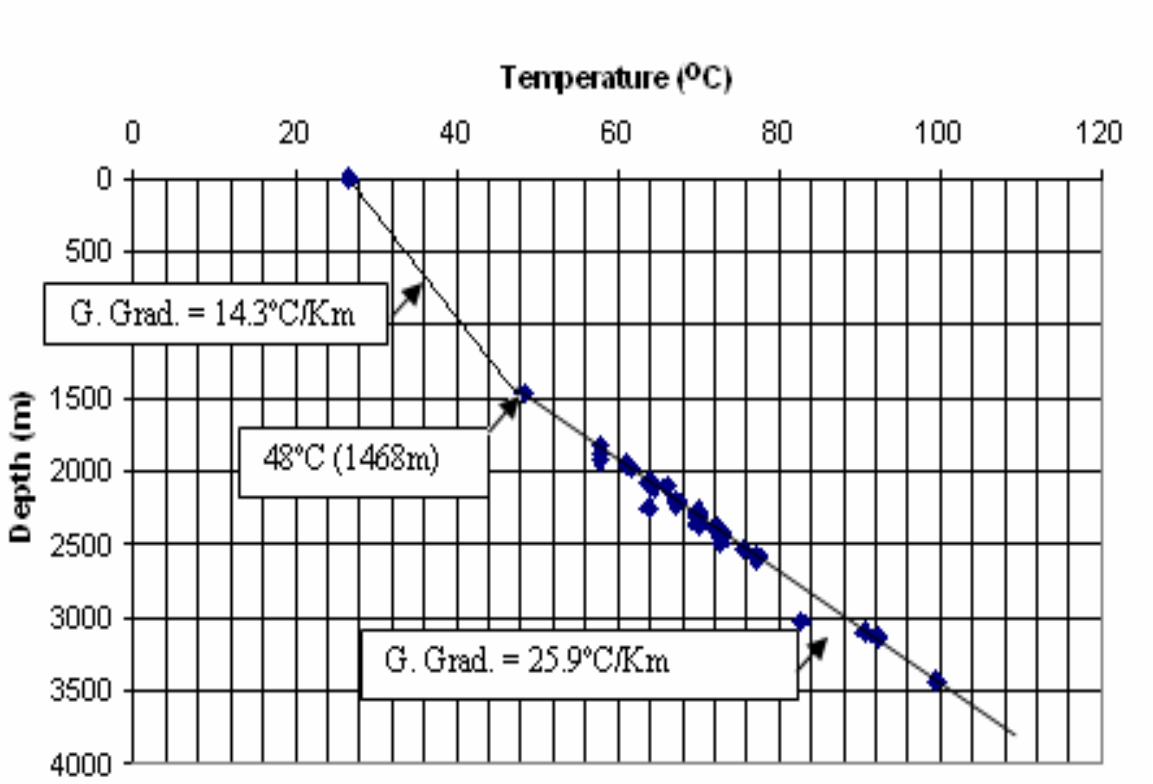

FIG. 5.1: Temperature-Depth plot for Bomu field

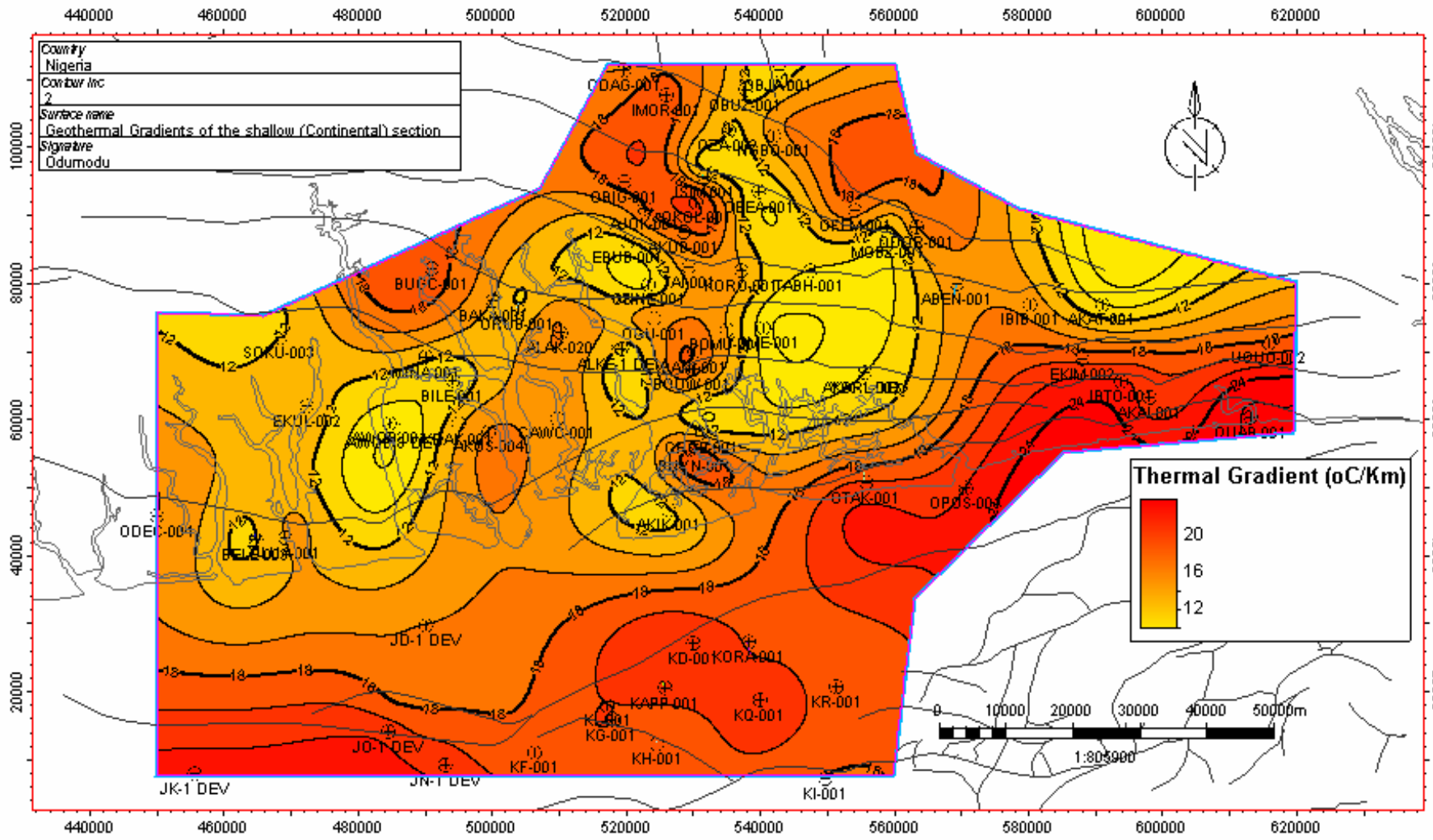

Figure 5.2 : Geothermal Gradients map of the Shallow (Continental) section

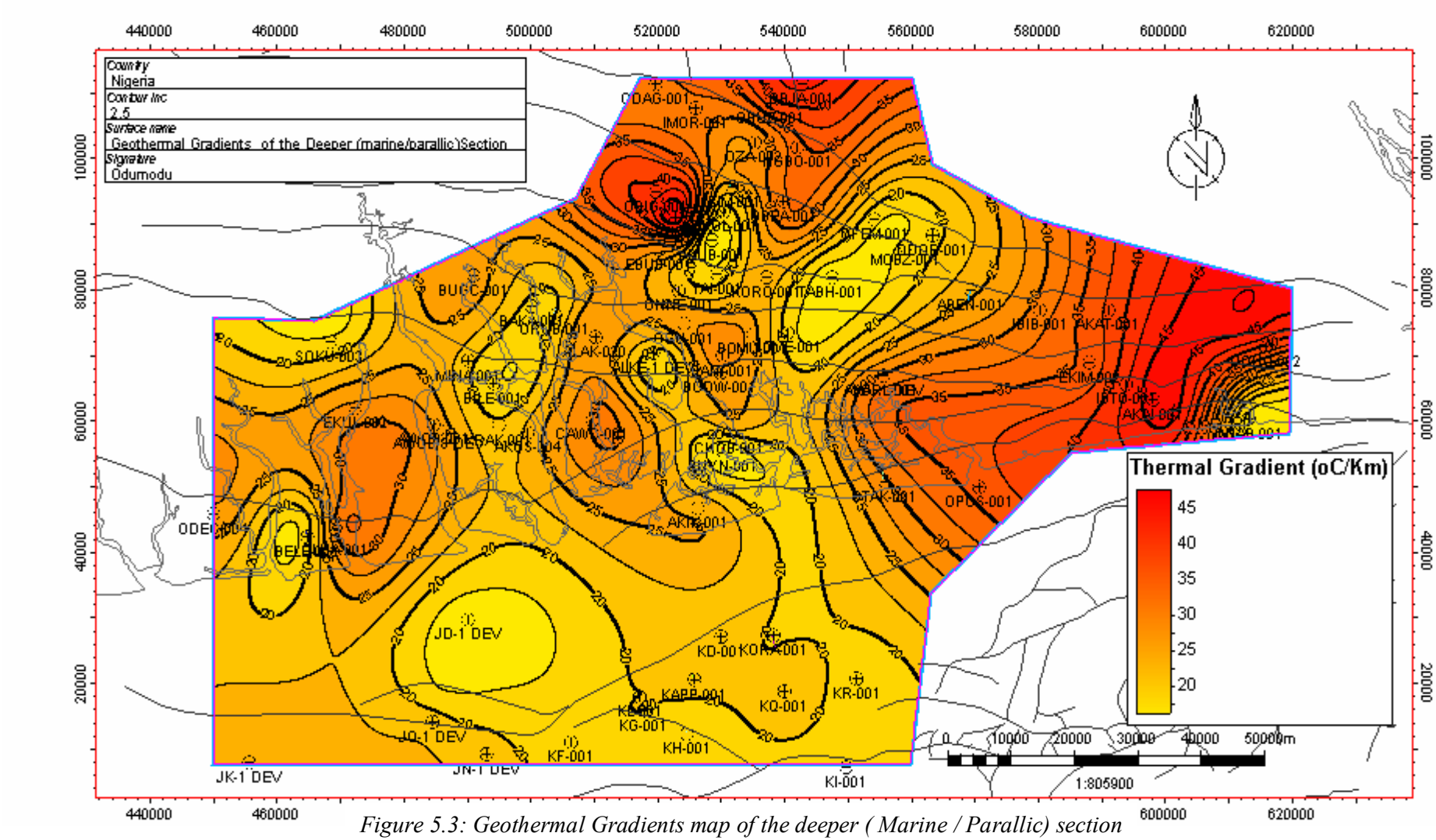

Figure 5.3: Geothermal Gradients map of the deeper (Marine / Parallic) section

Table 5.2: Summary of Geothermal Gradient variations for the deeper (paralic/ marine section across the study area

	Depobelt	*Abbreviation*	*Geothermal Gradient $^{o}C/Km$*	
			Low	*High*
1	Shallow Offshore	S_{HO}	18	20
2	Coastal Swamp	C*so*	20	45
a.	Western part	C*so(a)*	18	30
b.	Central part	C*so(b)*	20	30
c.	Eastern part	C*so(c)*	30	45
3	Central Swamp	C*sw*	18	45

Table 5.3: Summary of Average Geothermal Gradient values for the depobelts across the study area

	Depobelt	*Abbreviation*	*Geothermal Gradient* $^{o}C/Km$	
			Low	*High*
1	Shallow Offshore	S_{HO}	14	26
2	Coastal Swamp	C*so*	12	24
a.	Western part	C*so(a)*	12	18
b.	Central part	C*so(b)*	16	20
c.	Eastern part	C*so(c)*	20	24
3	Central Swamp	C*sw*	14	32

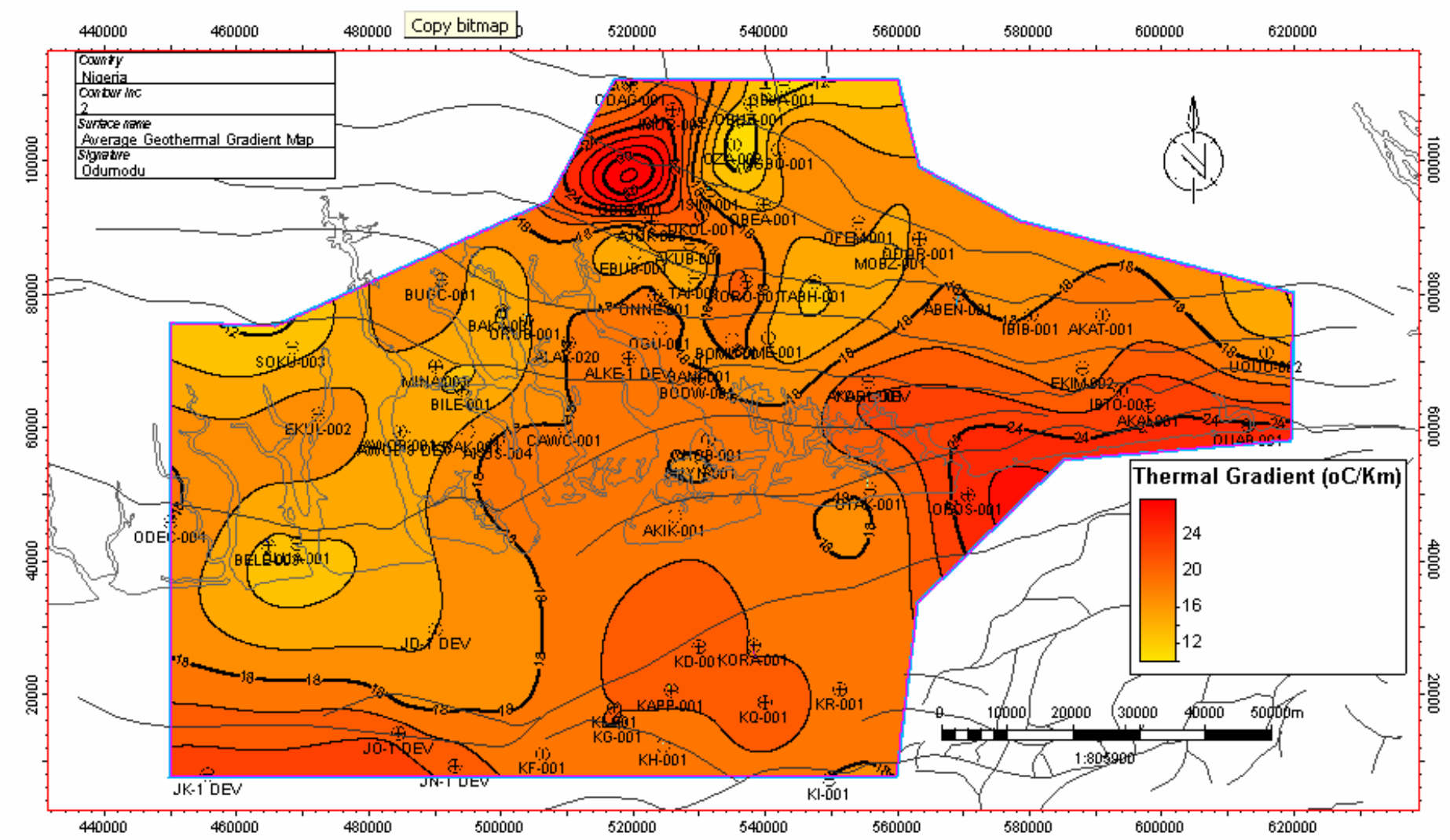

Figure 5.4: Average Geothermal Gradients map of parts of the Eastern Niger Delta

Least square fit to the combined reservoir and corrected bottom hole temperatures data gave the average geothermal gradient for the Central Swamp depobelt of the Niger as 19.3 ^{o}C/km, with a correlation coefficient of about 0.66(Figure 5.5a). The temperature depth relationship in the Central Swamp depobelt can thus be predicted using the following equation:

$$T = 19.3z + 27 \quad \text{---------- (29)}$$

Where T is the surface temperature and z is the depth.

Least square fit to the combined reservoir and corrected bottom hole temperatures data gave the average geothermal gradient for the Coastal swamp depobelt of the Niger as 17.6 ^{o}C/km, with a correlation coefficient of about 0.86. (Fig.5.5b)The temperature depth relationship in the Coastal Swamp depobelt can thus be predicted using the following equation:

$$T = 17.6z + 27 \quad \text{---------- (30)}$$

Where T is the surface temperature and z is the depth.

Least square fit to the combined reservoir and corrected bottom hole temperatures data gave the average geothermal gradient for the Shallow Offshore depobelt of the Niger as 20.4 ^{o}C/km, with a correlation coefficient of about 0.97. (Fig. 5.5c) The temperature depth relationship in the Coastal Swamp depobelt can thus be predicted using the following equation:

$$T = 20.4\ z + 22 \quad \text{---------- (31)}$$

Where T is the surface temperature and z is the depth.

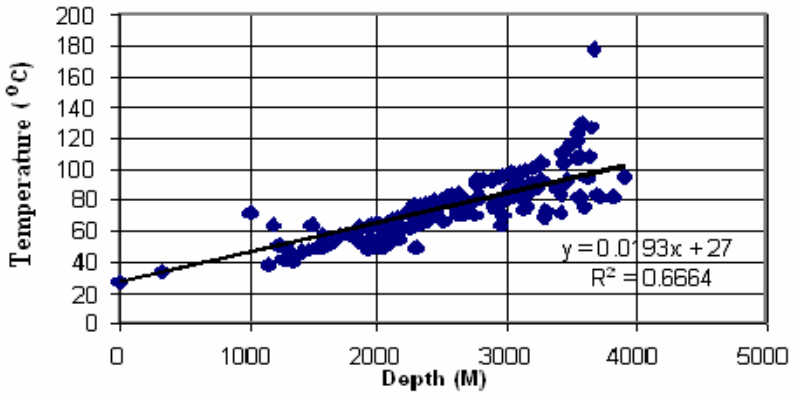

Figure 5.5a: Generalized Temperature - Depth plot for the Central Swamp depobelt

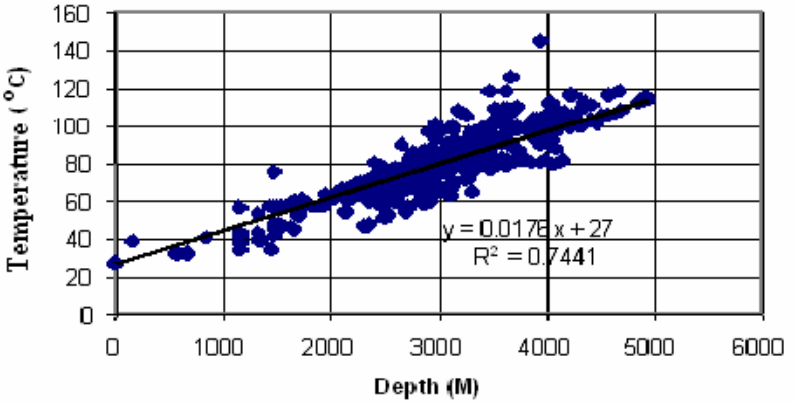

Figure 5.5b: Generalized Temperature - Depth plot for the Coastal Swamp Depobelt of the Niger Delta

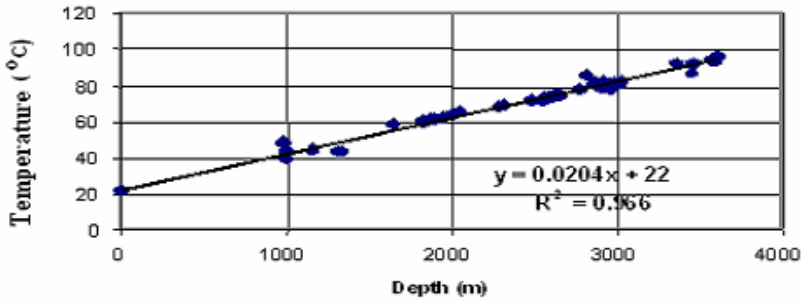

Figure 5.5c: Reservoir Temperature-Depth plot for the Shallow Offshore Depobelt of the Niger Delta

4.1 Subsurface Temperature Variations in the Niger Delta

The regional temperature fields in the Central Swamp, Coastal Swamp and Shallow Offshore depobelts of the Eastern Niger Delta were characterized using data collected from reservoir temperature and corrected bottom-hole temperatures. The estimated temperatures are presented in temperature maps showing the temperature fields at specific depths of 1000m, 2000m, and 3000m. (Fig. 5.6a-c and Fig. 5.7a-c) Mapping the depth to isotherms of 100^{o}C and 150 ^{o}C (i.e. isothermal maps) (Fig. 5.9a and 5.9b) were also utilized in this study to evaluate the temperature-depth relationships of the Eastern Niger Delta. The observed temperature anomalies may be largely attributed to the variations in the thermal conductivity of the sediments, thickness of the formations, net gross or lithological control and depth to the top of the basement. The variable sediment accumulation in the area has resulted in differences in the overall thermal conductivity of the sediment and the temperature fields reflect such differences. The temperature field is also influenced by gross lithological changes or sedimentation rate. Regions of low thermal anomalies correspond with areas of high sand percentage. It is a very well known fact that sands are better conductors than shale and will therefore show lower thermal anomalies. The thickness of the sandy intervals of the Benin and Agbada formations is another factor that influences thermal anomalies in this part of the Niger delta. Minimum temperatures coincide with areas of maximum thickness of the sandy Agbada and Benin formations. This suggests a cooling effect of the continental sands. The convection currents set up in the freely moving groundwater helps in lowering the temperature as well as the cooling effect due to conduction.

5.3 Temperature fields

The temperature fields at three depth levels of 1000m, 2000m, and 3000m were evaluated to understand the variable temperature pattern of the Niger Delta. The average geothermal gradient and variable geothermal gradient models were utilized in computing the temperatures at the three depth intervals. The results of this analysis are shown in tables 5.4, 5.5 and figures.5.6 a-c, 5.7 a-c and Fig 5.8 a-e. The temperatures estimates from the average geothermal gradient model are quite higher than that of the variable geothermal gradient model. Since the average geothermal gradient model overestimates temperatures, the variable geothermal gradient model was used to describe the variations in temperature fields.

5.3.1 Temperature Fields at Depth of 1000m (3048ft)

At shallow depths 1000m (3048ft) (Fig. 5.6a), depressed temperatures of about 39 ï 45 ^{o}C were observed in the western and central part of the Eastern Coastal Swamp. The temperatures become elevated to higher values ranging from 45^{o}C ï 52 ^{o}C in the eastern parts of the Coastal Swamp and up to 56 ^{o}C, northwards in the Central Swamp. Depressed temperatures observed in the western part of the study area, which corresponds to the central part of the Niger Delta, is influenced by the great thickness of sands and great depths to the basement. Convection currents set up by the free movement of groundwater in the continental sandstones also help in lowering the heat being conducted to the surface. The shallow depth to basement, shaliness and closeness to the Cameroun volcanic line could influence the elevated temperatures in the eastern part.

5.3.2 Temperature Fields at Depth of 2000m (6048ft)

At depths of about 2000m (6048 ft) (Fig. 5.6b), depressed temperatures (<55 ^{o}C) are observed in the western part of the study area. Moderate temperatures ranging from 55 to 65 ^{o}C are observed in the central part of the Coastal Swamp. Temperature variations in this area are clearly influenced by lithologic differences. Anomalously high temperatures ranging from 65 to 75 ^{o}C are also observed in the eastern part of the Coastal Swamp and in the Central Swamp depobelt in the north. The higher temperature in the north-western part of the study area (i.e. the Central Swamp) is likely to be influenced by hydrothermal convection of fluids coming up from the underlying over pressured Akata Formation.

5.3.3 Temperature Field at Depth of 3000m (9096ft)

At depths of about 3000m (9096ft) (Fig. 5.6c), the temperature field maintain the same pattern as in shallower interval, but with minor changes. Lower temperatures (70 ï 75 ^{o}C) are observed in the western part of the Eastern Coastal Swamp. Moderate temperatures ranging from 75 to 85 ^{o}C were observed in the central part of the Coastal Swamp. Generally in the Coastal Swamp temperatures become elevated to about 85 -100 ^{o}C in the eastern parts as well as north-westwards in the Central Swamp. The higher temperatures are greatly influenced by lithology.

Table 5.4: Temperature fields (Variable Geothermal Gradient model)

	Depobelt	*Temperature field at 1000m (3048ft) (^oC)*	*Temperature field at 1000m (6096ft) (^oC)*	*Temperature field at 1000m (9144ft) (^oC)*
1	Shallow Offshore	41 ï 45	59 ï 65	78 ï 86
2	Coastal Swamp	39 ï 52	45 ï 76	62 ï 105
a.	Western part	39 ï 42	45 ï 55	62 ï 75
b.	Central part	41 ï 45	55 ï 65	75 ï 85
c.	Eastern part	45 ï 52	65 ï 75	85 ï 105
3	Central Swamp	39 - 50	52 - 72	70 - 105

Table 5.5: Temperature fields (Average or Constant Geothermal Gradient model)

	Depobelt	*Temperature field at 1000m (3048ft) (^oC)*	*Temperature field at 2000m (6096ft) (^oC)*	*Temperature field at 3000m (9144ft) (^oC)*
1	Shallow Offshore	40 ï 50	55 ï 80	70 ï 100
2	Coastal Swamp	40 ï 50	50 ï 75	63ï 100
a.	Western part	40ï 45	50ï 60	63 ï 75
b.	Central part	40 ï 48	60 ï 65	75 ï 85
c.	Eastern part	47 ï 50	65 ï 75	85 ï 100
3	Central Swamp	40 - 58	50 - 90	70 - 105

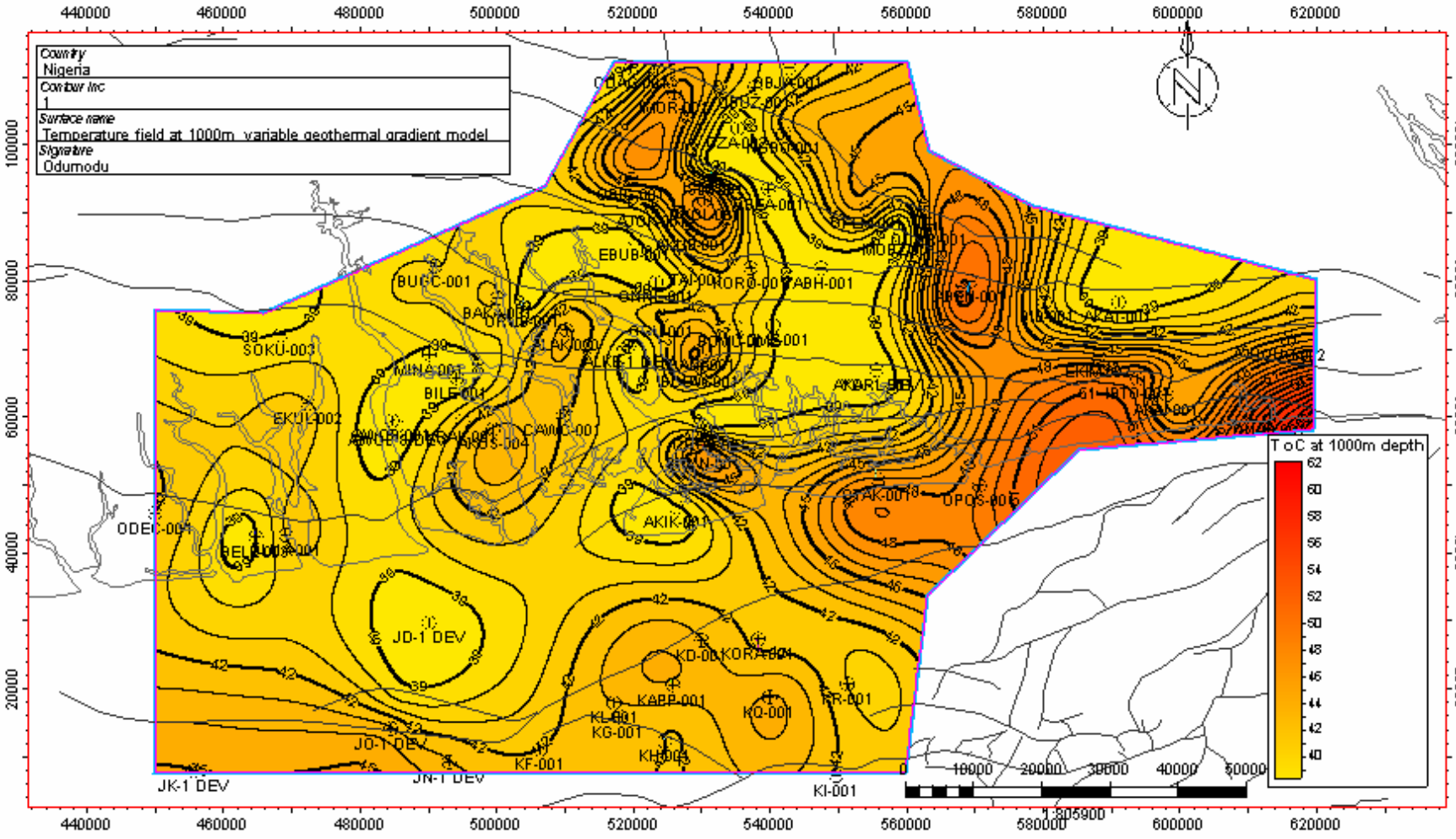

Figure 5.6a : Temperature field at 1000m (Variable Geothermal Gradient model)

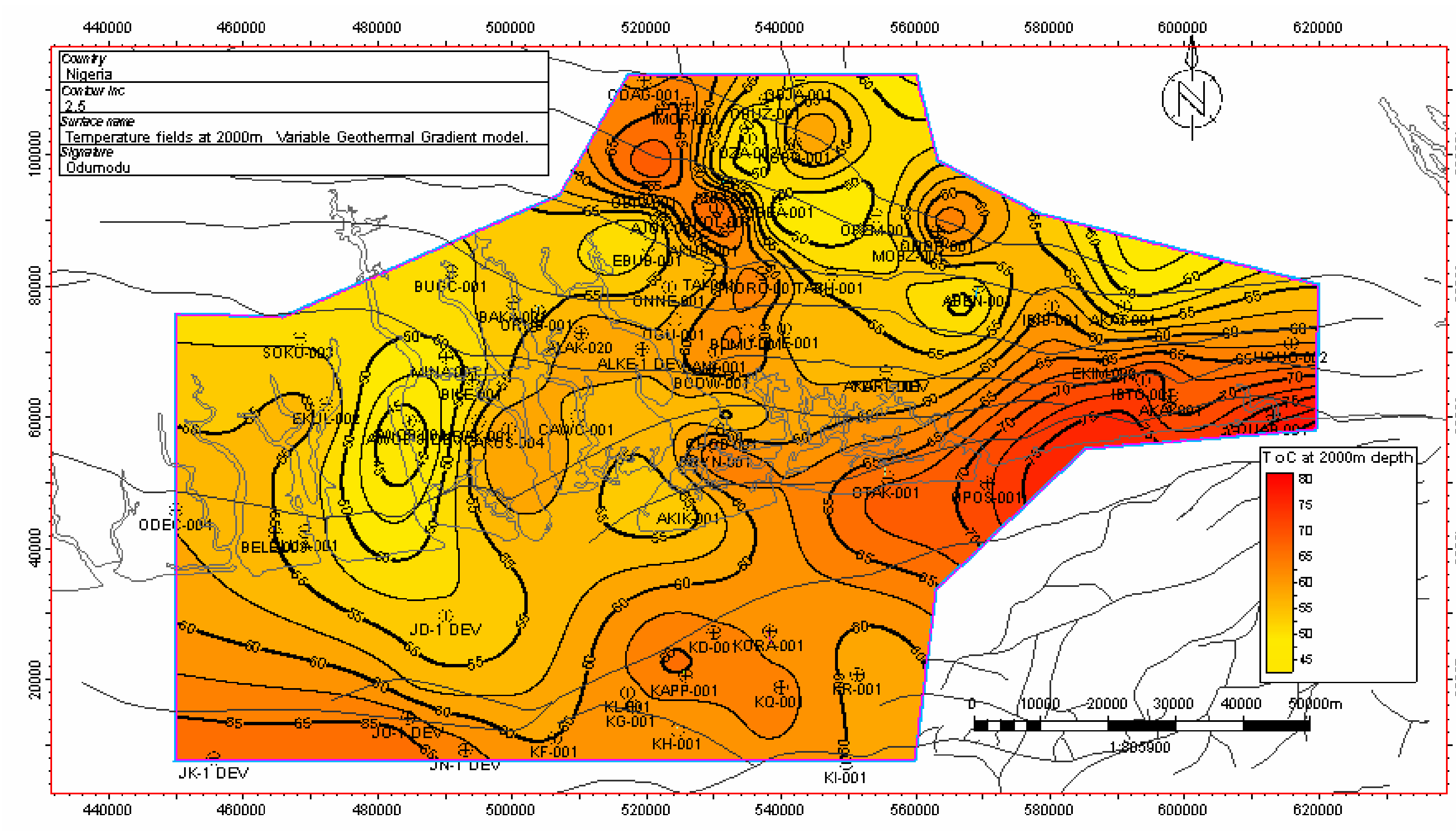

Figure 5.6b : Temperature field at 2000m (Variable Geothermal Gradient model)

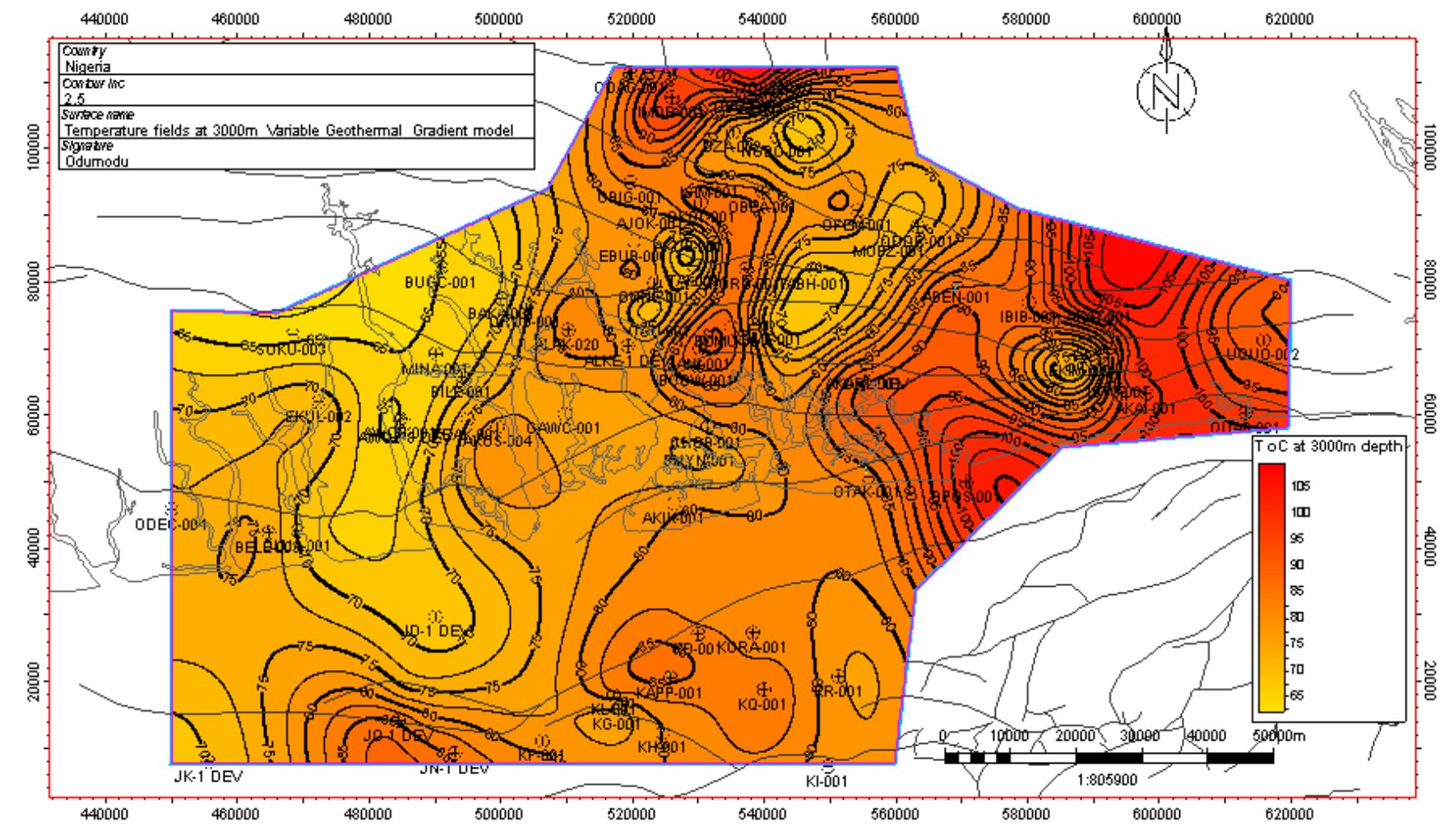

Figure 5.6c : Temperature field at 3000m (Variable Geothermal Gradient model)

a

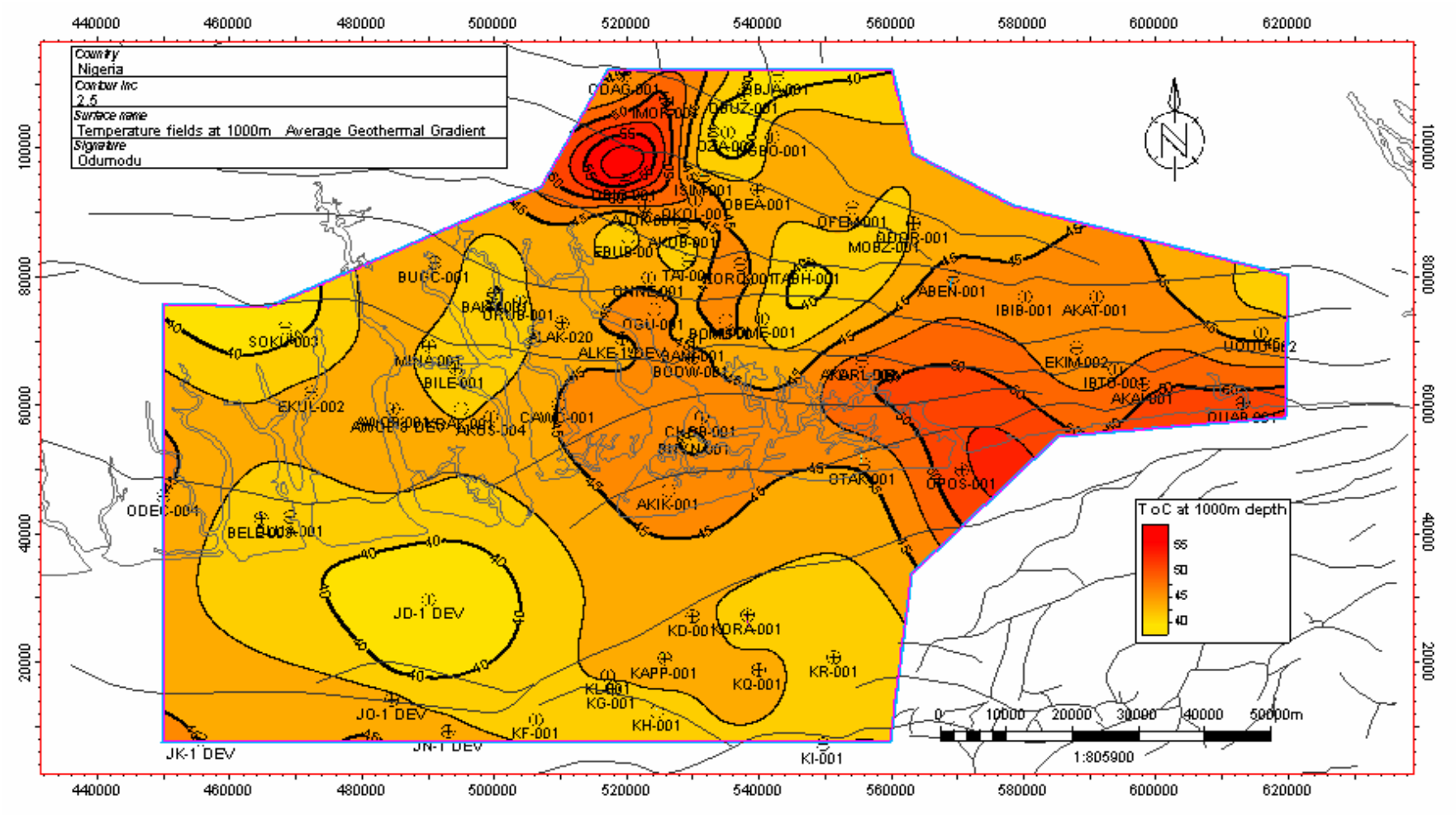

Figure 5.7a : Temperature field at 1000m (Average Geothermal Gradient model)

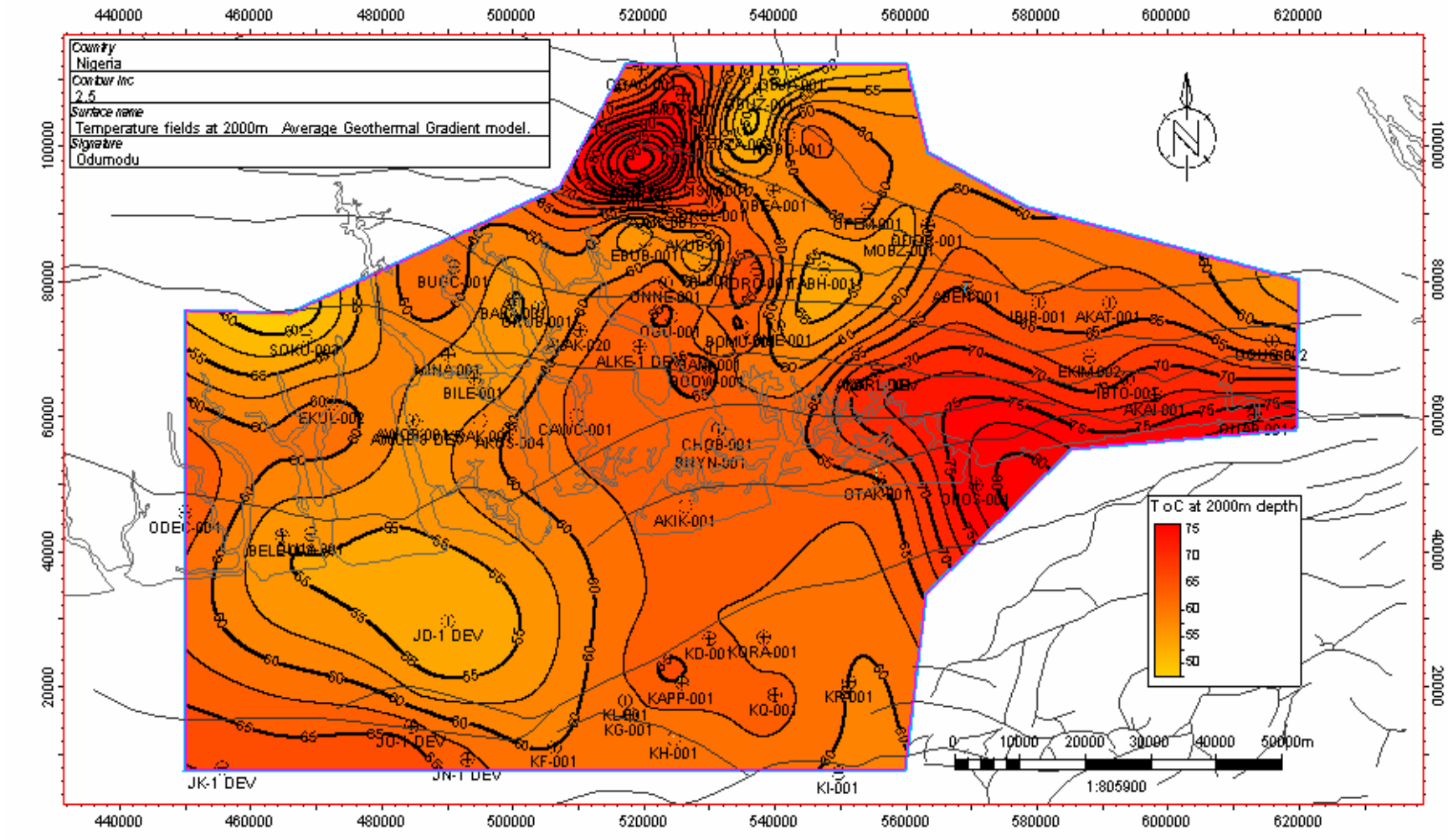

Figure 5.7b : Temperature fields at 2000m (Average Geothermal Gradient model)

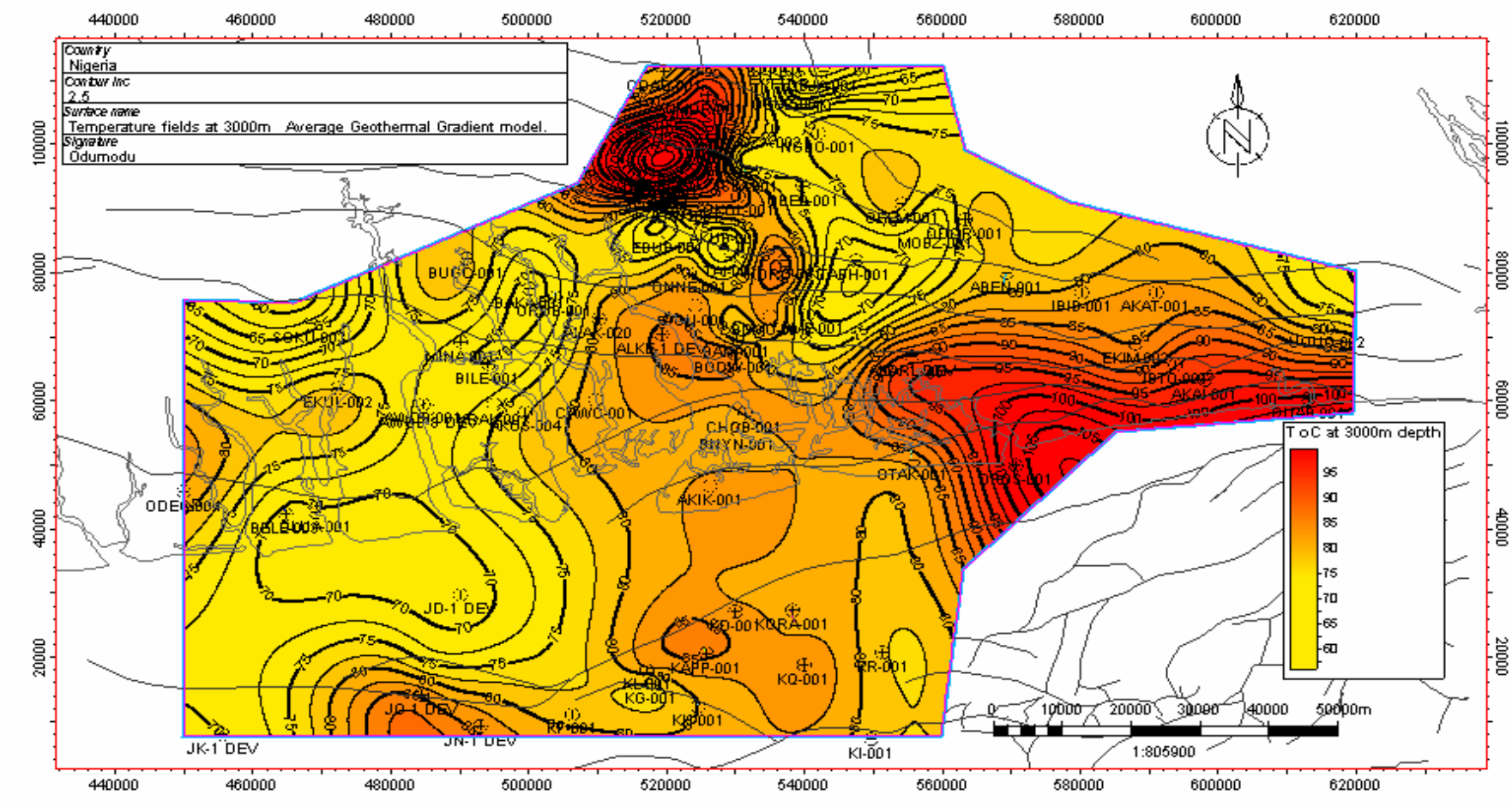

Figure 5.7c : Temperature field at 3000m (Average Geothermal Gradient model

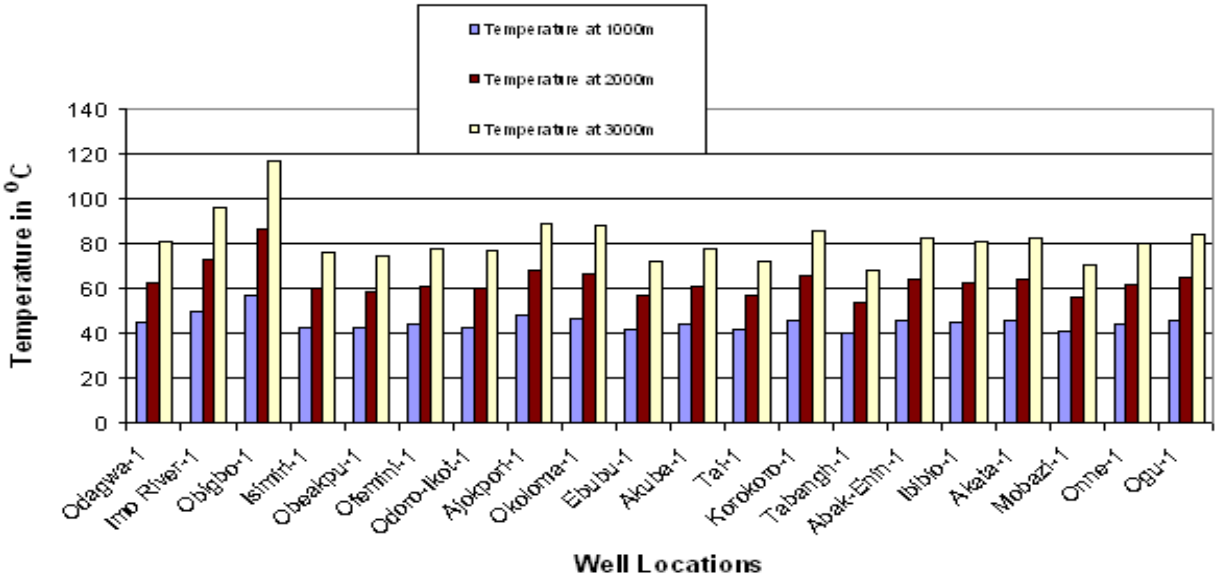

FIG.5.8a: TEMPERATURE VARIATIONS IN THE CENTRAL SWAMP DEPOBELT(AVERAGE GEOTHERMAL GRADIENT MODEL)

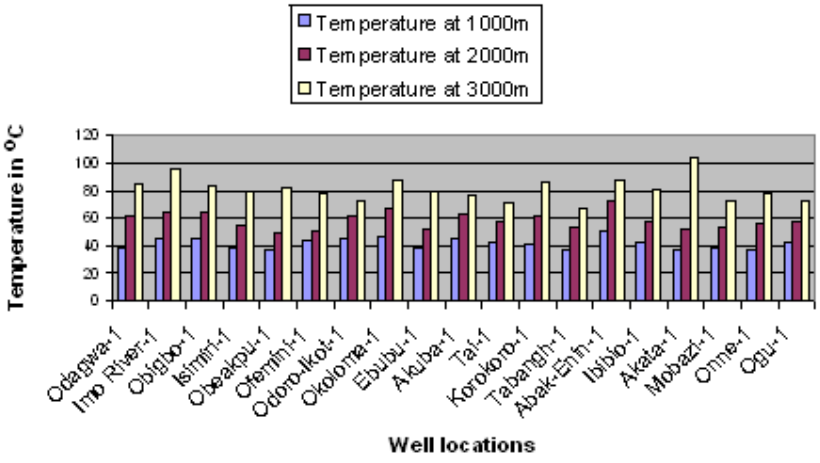

FIG. 5.8b: TEMPERATURE VARIATIONS IN THE CENTRAL SWAMP DEPOBELT (Variable Geothermal Gradient model)

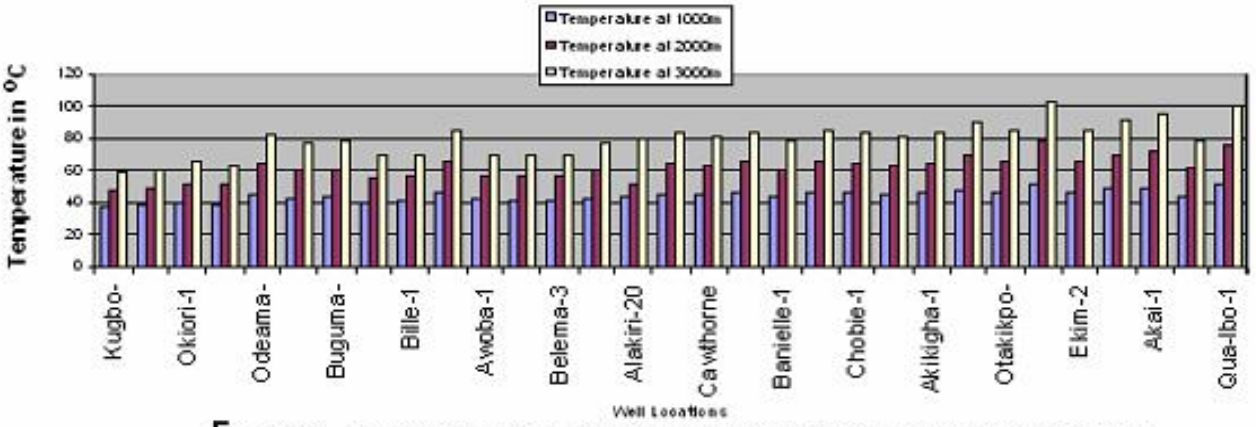

Fig. 5.8c: TEMPERATURE VARIATIONS III THE COASTAL SWAMP DEPOBELT (Average Geothermal gradient model)

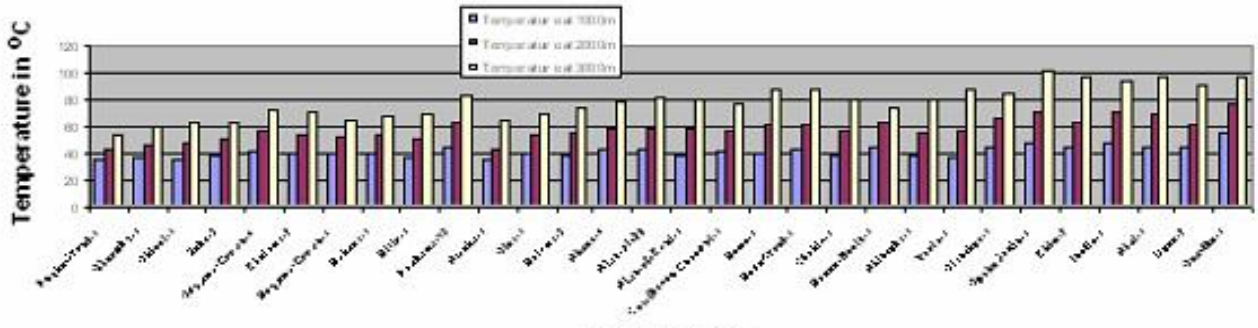

FIG.5.8c: TEMPERATURE VARIATIONS IN THE COASTAL SWAMP DEPOBELT (Variable Geothermal gradient model)

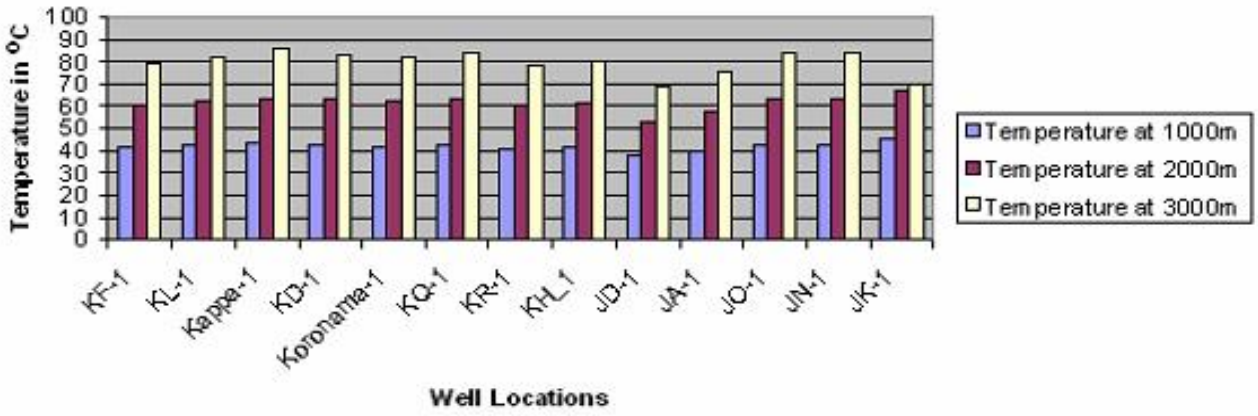

FIG. 5.8e. TEMPERATURE VARIATIONS IN THE SHALLOW OFFSHORE DEPOBELT (Average Geothermal Gradient Model)

5.3.4 Isothermal Maps

Temperature distributions in the study area were also evaluated using 100°C and 150°C isothermal maps (Figures 5.9a and 5.9b, Table 5.6 and 5.7) One remarkable aspect of this mapping is that these isotherms are shallower in areas having higher thermal gradients and deeper in areas with lower thermal gradients. The depths to 100°C isotherm ranges from 4000m to 5000m in the western parts of the Eastern Coastal Swamp. It decreases eastwards from about 4000m to 2800m in the Coastal Swamp. In the central parts of the Coastal Swamp, the depth ranges from 4000m to 5000m, but decreases eastwards and westwards to less than 3000m. In the Shallow Offshore, the depth ranges from 3500 ï 4000m. The depth to 150 °C isotherms shows a similar pattern to the 100 °C isotherm. The shallowest depths to 150°C isotherm occur in the east (4500-5,000m) and in the northwest (4500-5,000m). Greater depths to 150 °C occur in the west (6,000m- 9000m), in the central parts of the Central Swamp (6,000-9,000 m) and in the south (coastal area) (6,000m ï 9,000m).These isotherms are close to the temperatures of 116 °C (240 °F) and 150 °C (300 °F) which Evamy *et al* (1978) considered to represent the top of the oil and gas windows for Tertiary provinces.

Table5.6: Isothermal depths at 100°C (212°F)

	Depobelts	*Abbreviation*	*Depth Range to 100 ° C isotherm (m)*	
			Low	*High*
1	Shallow Offshore	S_{HO}	3645	4084
2	Coastal Swamp	C*so*	2933	5369
a.	Western part	C*so(a)*	3780	5369
b.	Central part	C*so(b)*	3431	5078
c.	Eastern part	C*so*©	2933	3305
3	Central Swamp	C*sw*	3113	5313

Table 5.7: Isothermal depths at 150°C (300°F)

	Depobelts	*Abbreviation*	*Depth Range to 150 °C isotherm (m)*	
			Low	*High*
1	Shallow Offshore	S_{HO}	5981	6809
2	Coastal Swamp	C*so*	4314	9280
a.	Western part	C*so(a)*	5612	8680
b.	Central part	C*so(b)*	5026	9280
c.	Eastern part	C*so*©	4314	4867
3	Central Swamp	C*sw*	4221	6693

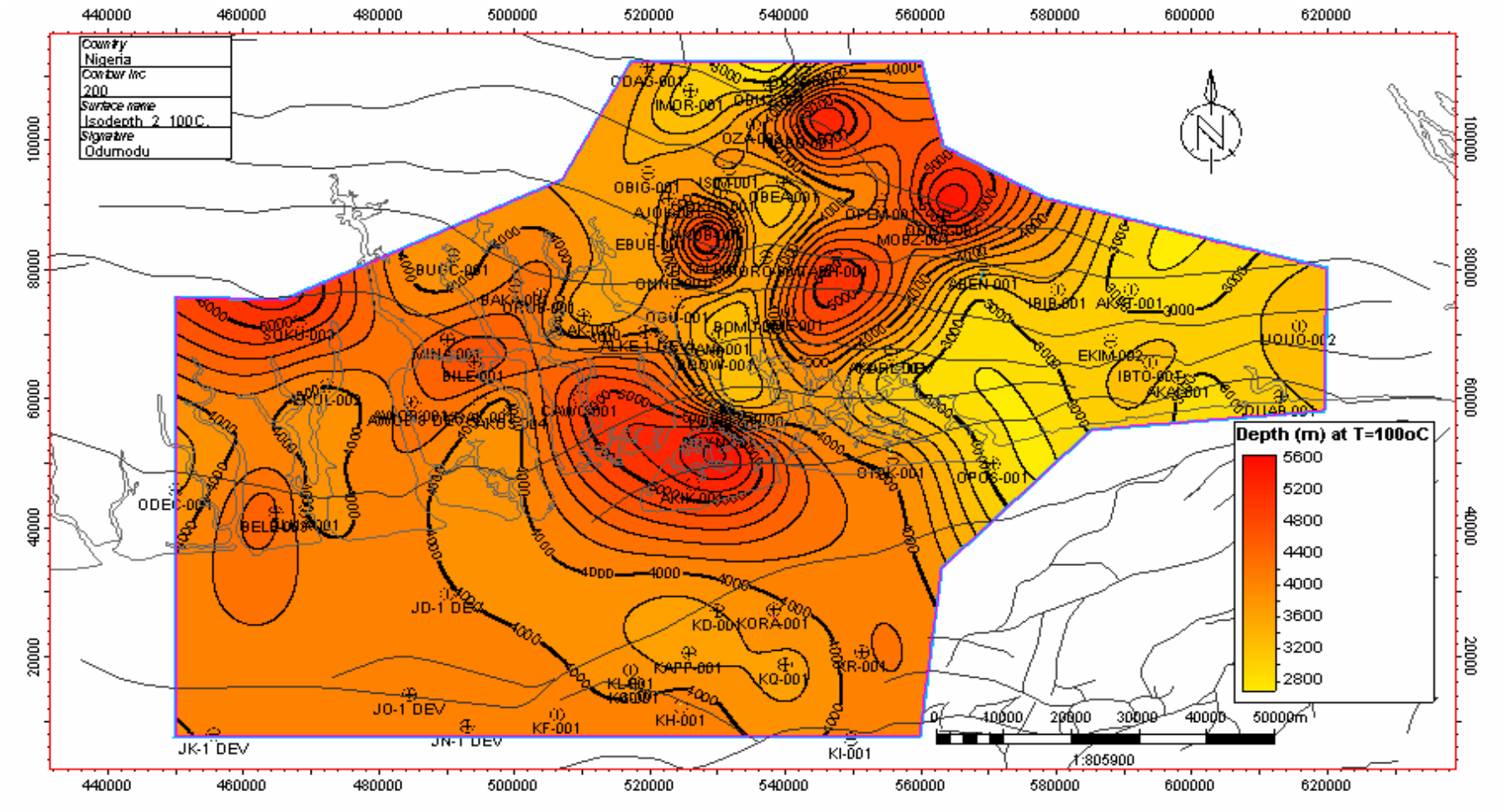

Figure 5.9a: Isothermal depths at 100°C.

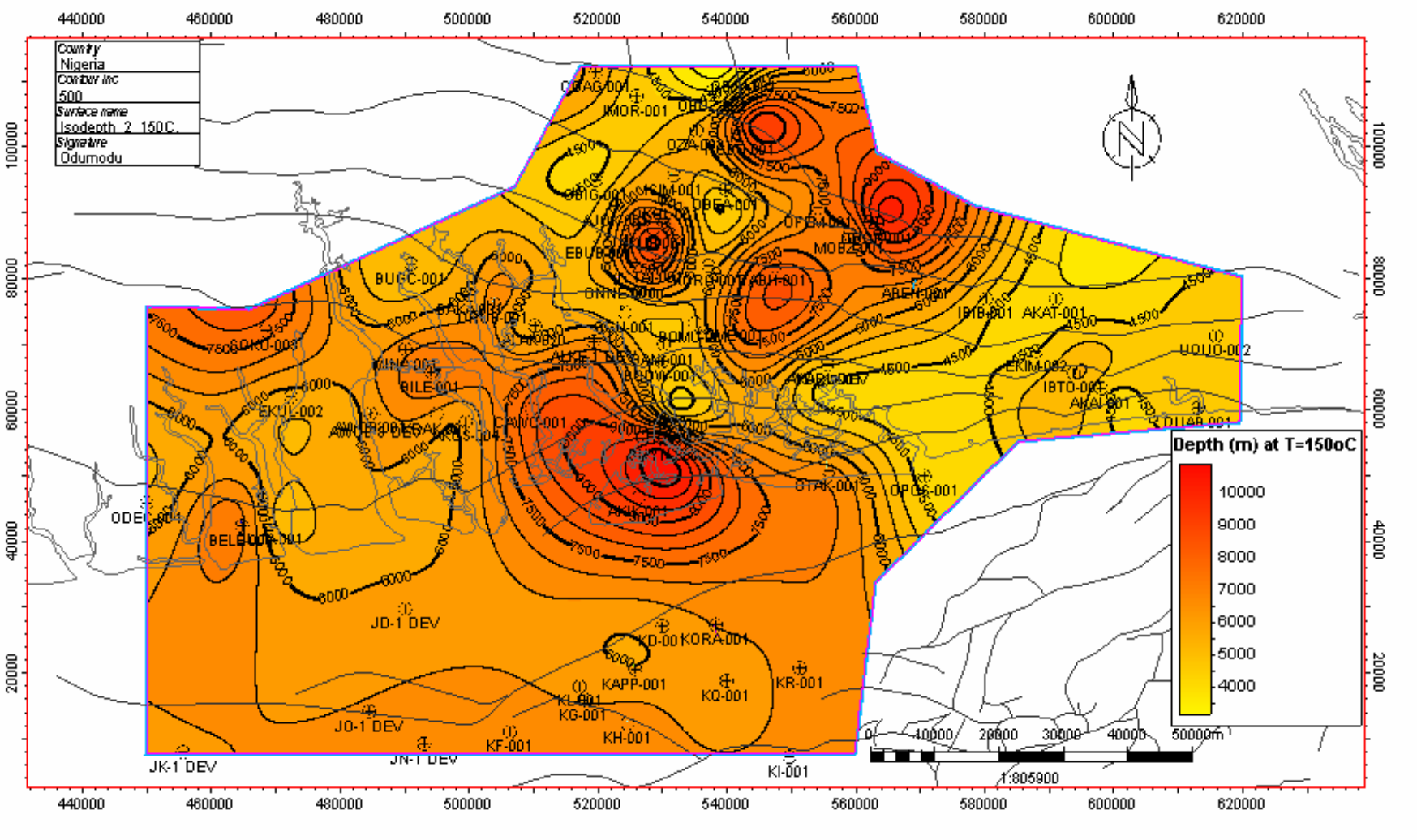

Figure 5.9b: Isothermal depths at 150°C.

5.4 Sand Percentage Distribution in the Niger Delta.

In a vertical section, the sand distribution in the Niger delta consists of 100 ï 70 % for the Benin Formation, 70 ï 30 % for the Agbada Formation to less than 30% for the Akata Formation (Fig. 5.10) This therefore suggests that sand percentages in the Niger delta decreases with depth. The sand percentage map for the depth interval of 0 ï 1312m (Fig. 5.11) also suggests that highest sand percentages of about 95% occur in the centre of the delta around Soku, Ekulama, Awoba and Buguma Creek fields. It all shows that the sand percentage decreases from this part of the Coastal Swamp from a value of 95% to the offshore area to a value of about 75%. It also shows that sand percentages decreases from the western part of the eastern Coastal Swamp, at a value of 95% to the Central Swamp and eastwards at a value of about 80%. Figure 5.11 represents continental deposition that is usually characterized by sand percentages that is greater than 80%. For the depth interval of 1312 ï 3000m (Fig. 5.12), highest sand percentages of about 80% occur at the centre of the delta around Soku, Ekulama, and Awoba and Buguma Creek fields. At this depth interval, sand percentages decreases offshore and eastwards to about 50% and 20% respectively. The sand percentages map generally has an alternating high and low sand percentages distribution in the Niger delta. Pockets of high and low sand percentages occur respectively within low and high sand percentages regions. These maps may therefore indicate a regional trend in the depositional pattern of the delta.

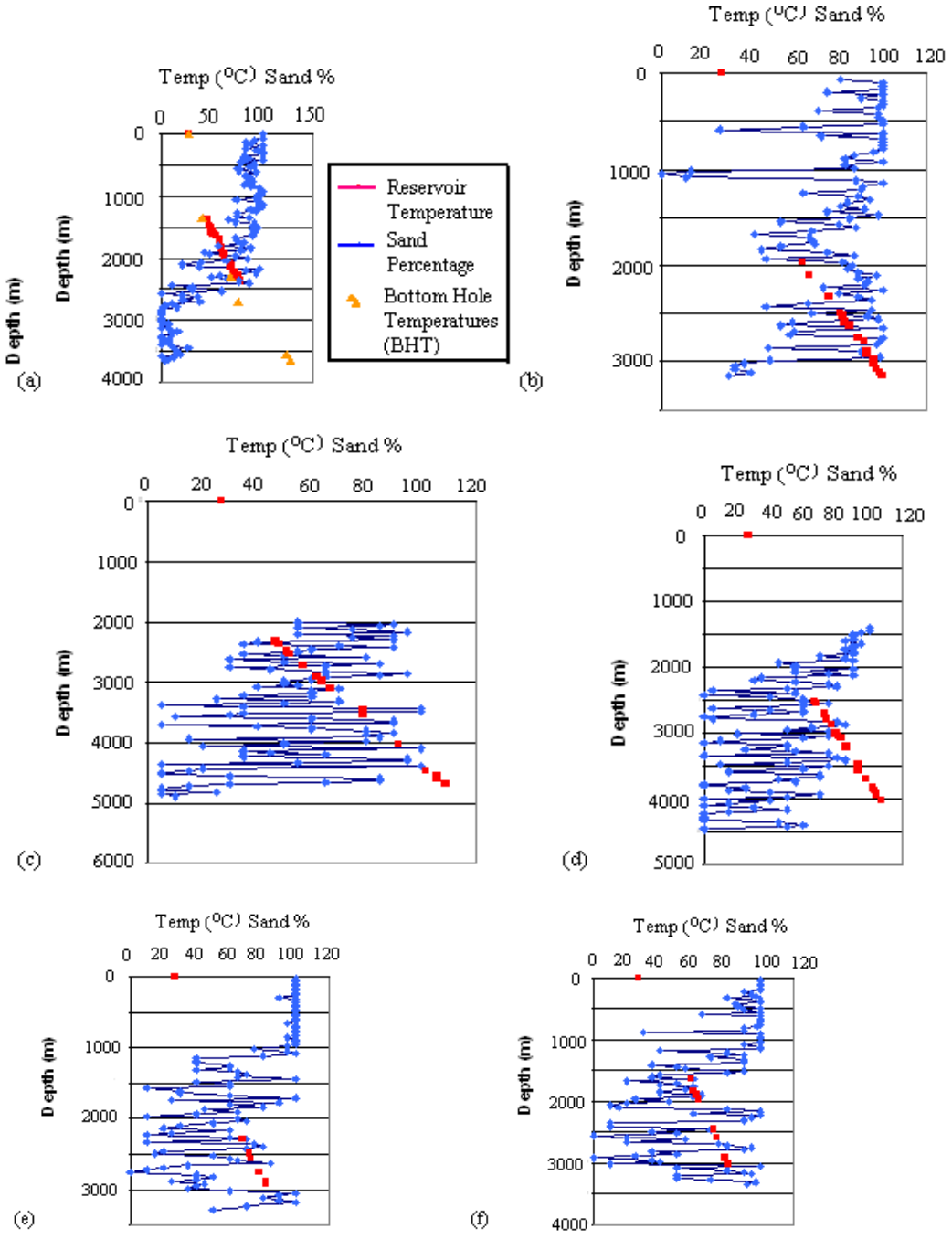

Figure 5.10: Plots of Temperature and Sand Percentage against depth for some wells (a) Akata -1 (Central Swamp) (b) Imo River-1 (Central Swamp) (c) Awoba -1 (Coastal Swamp (d) Odeama Creek -1 (Coastal Swamp) (e) KD-1 (Shallow Offshore (f) KL-1 (Shallow Offshore

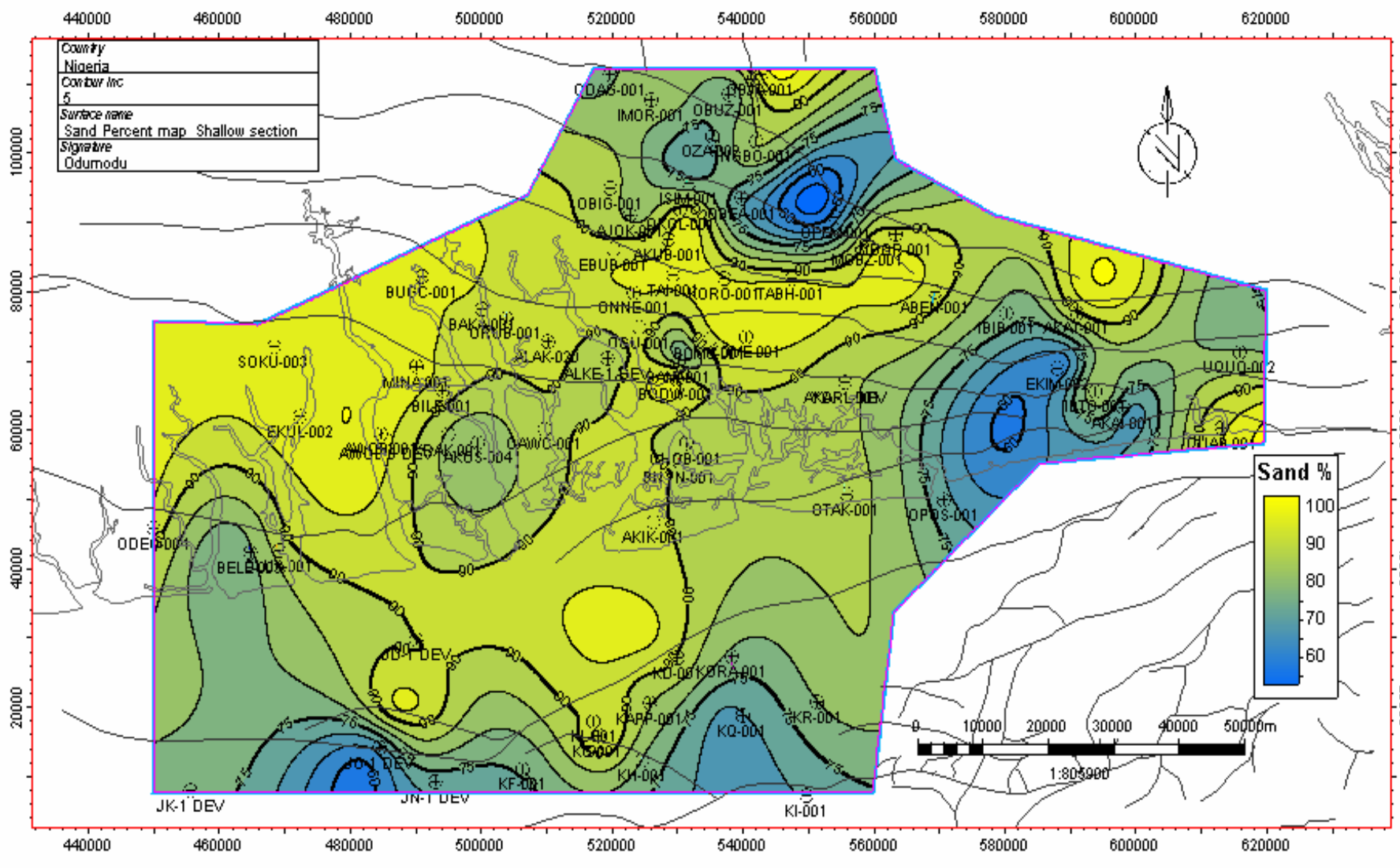

Figure 5.11a: Sand Percentage map for the shallow (Continental section)

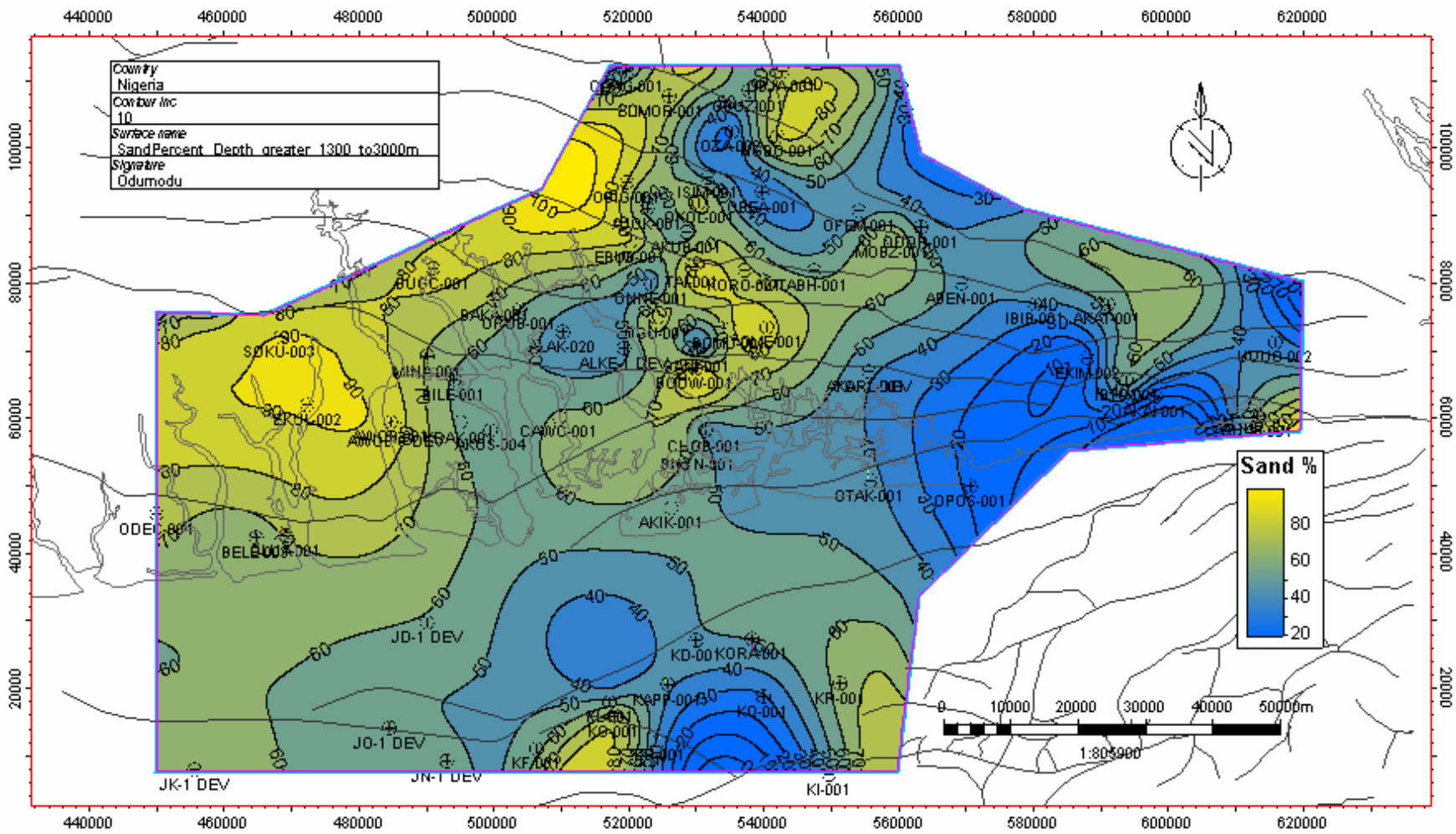

Figure 5.11b: Sand Percentage map for the deeper (Marine / Parallic section)

5.5 Heat Flow variations in the Niger Delta

Heat flow values were computed for seventy (70) wells in the Central Swamp, Coastal Swamp and the Shallow Offshore depobelts by calibrating temperatures predicted using the rifting model with observed temperatures using Petromod 1-D modelling software. The computed heat flow ranges from 29 mWm^{-2} - 55 mWm^{-2}, and an average of 42.5 mWm^{-2} (Fig. 5.12). This represents a heat flow unit (HFU) of 0.69 ï 1.31 and an average of about 1.00 HFU. Higher heat flow values (45 ï 55 mWm^{-2}) were observed in the western parts of the Central Swamp as well as in the eastern parts of Central Swamp, the Coastal Swamp and the Shallow Offshore. Lower heat flow values (< 35 mWm^{-2}) were observed in the observed in the central parts of the Central Swamp, western part of the Coastal Swamp and the Shallow Offshore.

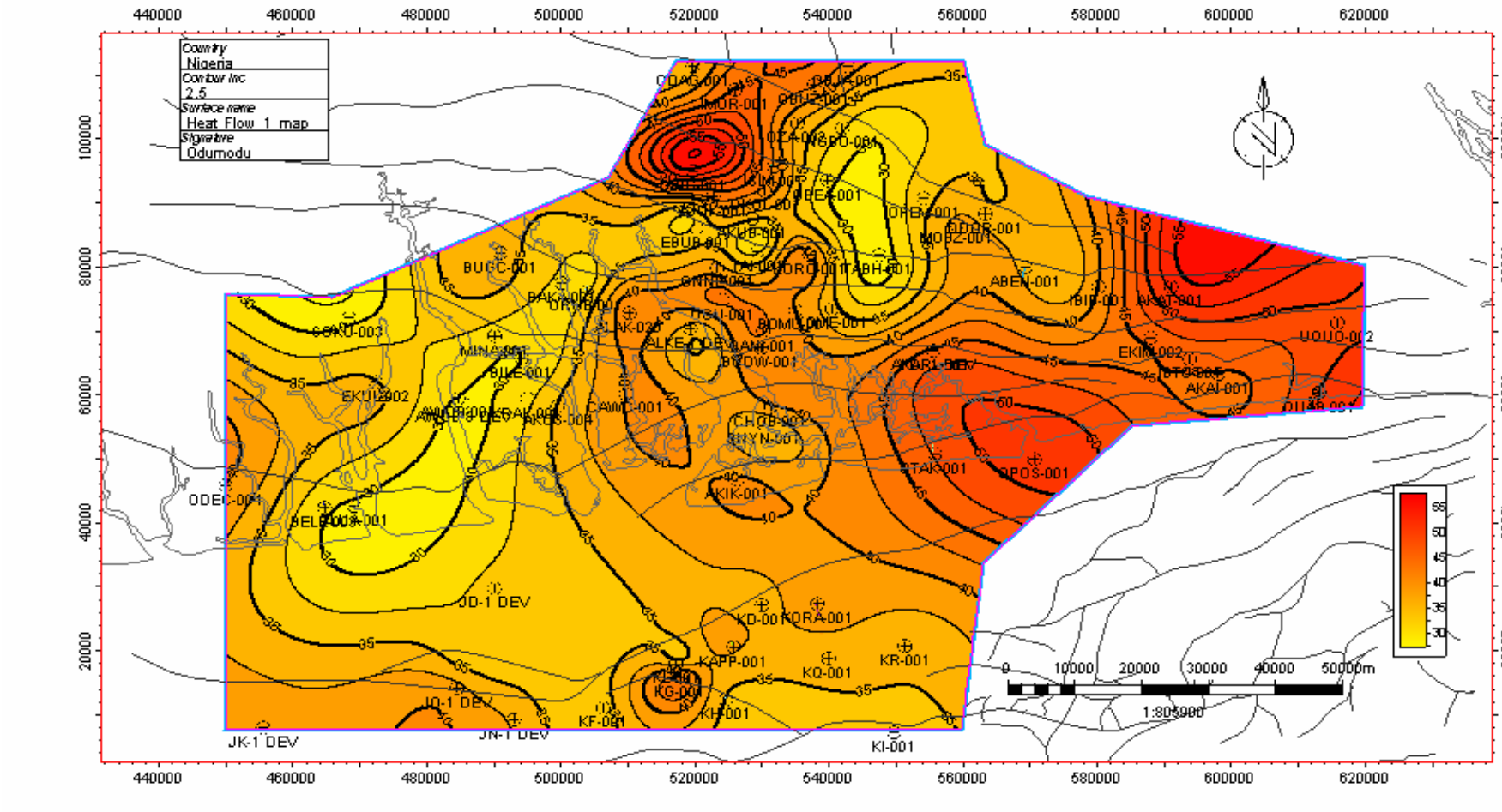

Figure 5.12: Heat Flow Map of parts of the Eastern Niger Delta

5.6 Burial History and Hydrocarbon Maturation Modelling

The wells for which burial history and hydrocarbon maturation modelling include four wells, namely Obigbo ï 1, Opobo-South-4, Akaso-4 and Kappa ï 1. The wells were chosen to represent different depositional, structural and thermal settings Obigbo-1 is located within the Central Swamp depobelt. Opobo-South-4 and Akaso-4 are located in the Coastal Swamp while Kappa-1 is in the Shallow Offshore. The four wells were modelled to reconstruct their hydrocarbon generative histories. Predicted maturation and timing of hydrocarbon generation are based on Easy%R_o of Sweeney and Burnham (1990), while the calculation of kerogen transformation is based on the kinetic dataset of Burnham (1989) for type II/III kerogen. Maturation stages and their corresponding vitrinite reflectance values are illustrated in table 5.8.

Table 5.8: Thermal Maturity stages(Sweeney and Burnham, 1989).

Maturity stage	**Vitrinite Reflectance (R_o %)**
Immature	< 0.6 %
Early Mature	0.6 - 0.7 %
Mid Mature	0.7 - 1.0 %
Late Mature	1.0 - 1.3 %
Main gas generation	1.3 ï 2.2 %

5.6.1 Thermal Modelling of Obigbo – 1 well (Central Swamp)

The input data used for the modelling is given in table 5.9. The well was drilled to a depth of 3734m, in Lower Miocene sediments. The well did not penetrate into the Oligocene, Eocene, and Palaeocene sediments. The thickness of the Oligocene, Eocene and Palaeocene sediments were considered to be the same as encountered at Midim -1 well, which is a nearby well. (Table 4.3).

Maturation was modelled using Petromod 1-D modelling software with vitrinite relectance being calculated using Easy% R_o of Sweeney and Burnham (1990). The predicted vitrinite reflectance values cannot be compared with measured values because no vitrinite reflectance data exists for the well. However, the maturity data were established by calibrating calculated temperature against the measured temperature data for the well. A good fit between calculated and measured temperature data was achieved by using the rifting ï subsidence thermal model, whereby a high heat flow value of 90 mWm^{-2} is applied at 85 Ma, being the break-up phase of the basins initiation.

Burial history diagrams showing isotherms and maturity windows for Obigbo-1 well are shown in figure 5.13. In this study, Upper Miocene, Lower Miocene Oligocene, Eocene and Palaeocene sediments are considered as effective source rocks. The modelling suggests that the Upper Miocene and upper parts of the Lower Miocene (Ro < 0.6%) are immature for oil generation. The modelling also suggests that the basal parts of the Lower Miocene are in the early mature zone (0.60% - 0.70%). The modelling shows that the upper parts of the Oligocene are in the mid-mature zone (0.70 ï 1.0 % Ro) while the middle parts of the Oligocene are in the late mature (1.0% - 1.3%) stage of oil generation. This study also suggests that the Lower Oligocene, the Eocene and the Palaeocene are in the gas generation

phase (Ro = 1.3 ï 2.2). A heat flow of 53 mWm^{-2} is calculated from BHT temperatures with a surface temperature of 27^{o} C.

TABLE 5.9 : MAIN INPUT FOR OBIGBO - 1 WELL (CENTRAL SWAMP)

Layer	Top (m)	Base (m)	Thickness(m)	Eroded (m)	Depo from(Ma)	Depo to (Ma)	Eroded from(Ma)	Eroded to (Ma)	Lithology	PSE	TOC %	Kinetic	H(mgHC/gTOC
Pliocene -Recent	0	591	591		3	0			SAND shaly	Over burden			
U.Miocene (P780/P770)	591	1447	856		9.5	6.5			SAND shaly	Sealrock			
M.Miocene	1447	2559	1112		16	11..6			SHAL Eshaly	Reservoir rock			
L.Miocene	2559	3734	1175		19	15.5			SAND &SHALE	Source rock	1.4	Burnham (1989) II	100
Oligocene	3734	5479	1745		35	26.2			SHALE	Source rock	1.8	Burnham (1989) III	150
Eocene	5479	5635	156		57	35.4			SHAL Esand	Source rock	2.2	Burnham (1989) II	200
Paleocene	5635	5976	341		66	56.5			SHAL Esilt	Source rock	2.4	Burnham (1989) III	250
						65.5							

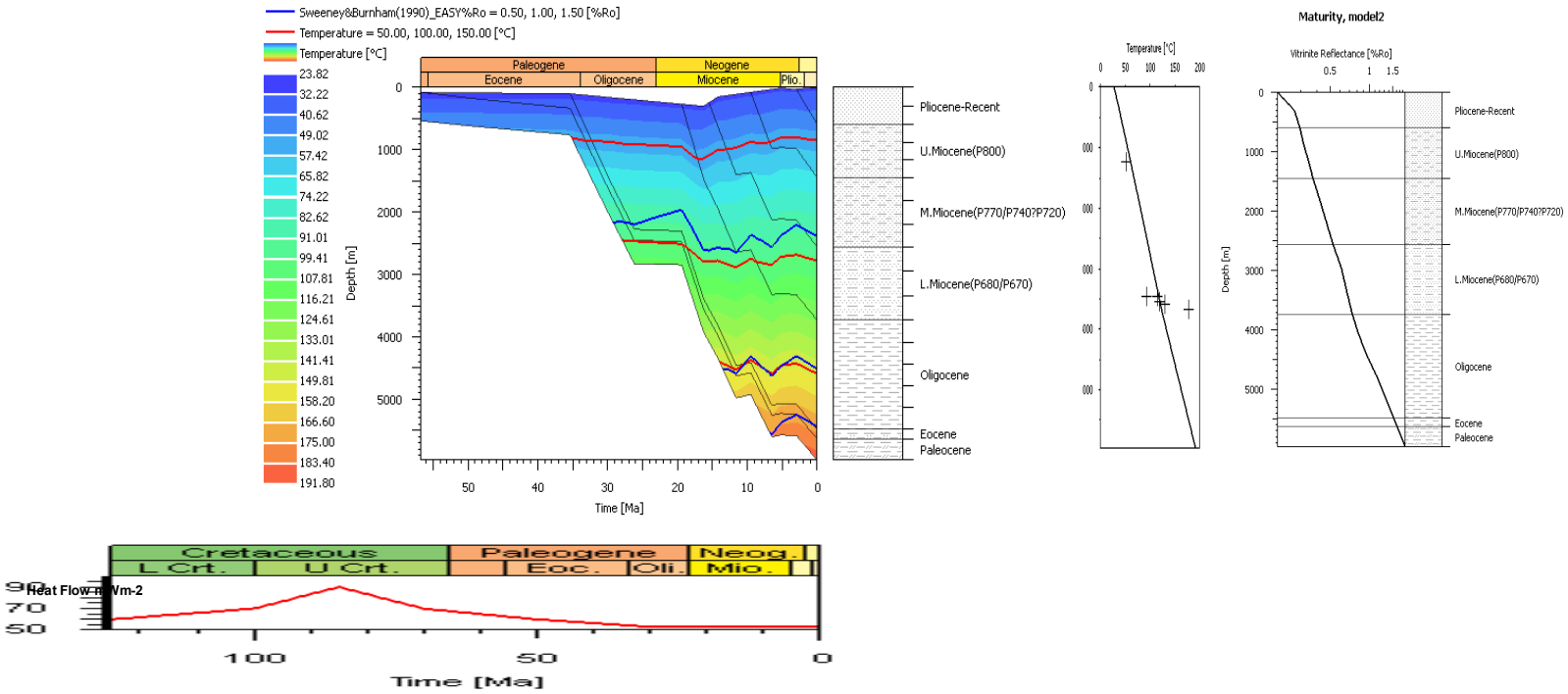

Fig. 5.13: Burial History chart showing isotherms , organic maturity and model calibration with temperature data for Obigbo ï 1 well in the Central Swamp depobelt of the Niger Delta.

5.6.2 Thermal modelling of Akaso – 4 well (Coastal Swamp)

Input data used in the modelling is given in table 5.10. The wells were drilled to a depth of 4306.4m, in Middle Miocene sediments. The well did not penetrate into the Oligocene, Eocene, and Palaeocene sediments. The wells were extrapolated to the base of the Palaeocene, using the thickness of these units as evaluated from seismic sections in the vicinity of the well(Personal communication with Frielingsdorf) (Table 4.4). Maturation was modelled using Petromod 1-D modelling software with vitrinite being calculated using Easy% R_o of Sweeney and Burnham (1990). The predicted vitrinite reflectance values cannot be compared with measured values because no vitrinite reflectance data exists for the well. However, the maturity data were established by calibrating calculated temperature against the measured temperature data for the well. A good fit between calculated and measured temperature data was achieved by using the rifting ï subsidence thermal model, whereby a high heat flow value of 90 mWm^{-2} is applied at 85 Ma, being the break-up phase of the basins initiation.

Burial history diagrams showing isotherms and maturity windows for Akaso-4 are shown in figure 5.14. In this study, the Miocene, Oligocene, Eocene and Palaeocene sediments are considered as effective source rocks. The modelling suggests that the Miocene rocks (Ro < 0.6%) are immature for oil generation. The predicted maturity for the Oligocene, Eocene and Palaeocene rocks ranges from 0.60 % to 1.1 %, which indicates that these source rocks are mature for oil generation. A heat flow of 35 mWm^{-2} is calculated from PRT temperatures with a surface temperature of 27^o C.

TABLE 5.10 : MAIN INPUT FOR AKAS0 - 4 WELL (COASTAL SWAMP)													
Layer	**Top (m)**	**Base (m)**	**Thickness(m)**	**Eroded (m)**	**Depo from(Ma)**	**Depo to (Ma)**	**Eroded from(Ma)**	**Eroded to (Ma)**	**Lithology**	**PSE**	**TOC %**	**Kinetic**	**HI (mgHC/gTOC**
Pliocene -Recent	0	2315	2315		5.6	0			SAND shaly	Over burden			
U.Miocene (P780/P770)	2315	2858	543		9.5	5.6			SAND& SHALE	Sealrock			
M.Miocene	2858	4304	1446		12.1	9.5			SHALE sand	Reservoir rock			
L.Miocene	4304	4719	415		17.7	12.1			SHALE sand	Source rock	1.2	Burnham (1989) II	100
Oligocene	4719	5355	536		35.4	23.3			SHALE	Source rock	1.4	Burnham (1989) III	150
U. Eocene	5255	5955	700		40.4	35.4			SHALE sand	Source rock	1.6	Burnham (1989) II	200
L. Eocene	5955	6655	700		56.7	40.4			SHALE sand	Source rock	2	Burnham (1989) III	250
Paleocene	6655	7355	700		65.5	56.7			SHALE silt	Source rock	2.3	Burnham (1989) II	300
						65.5							

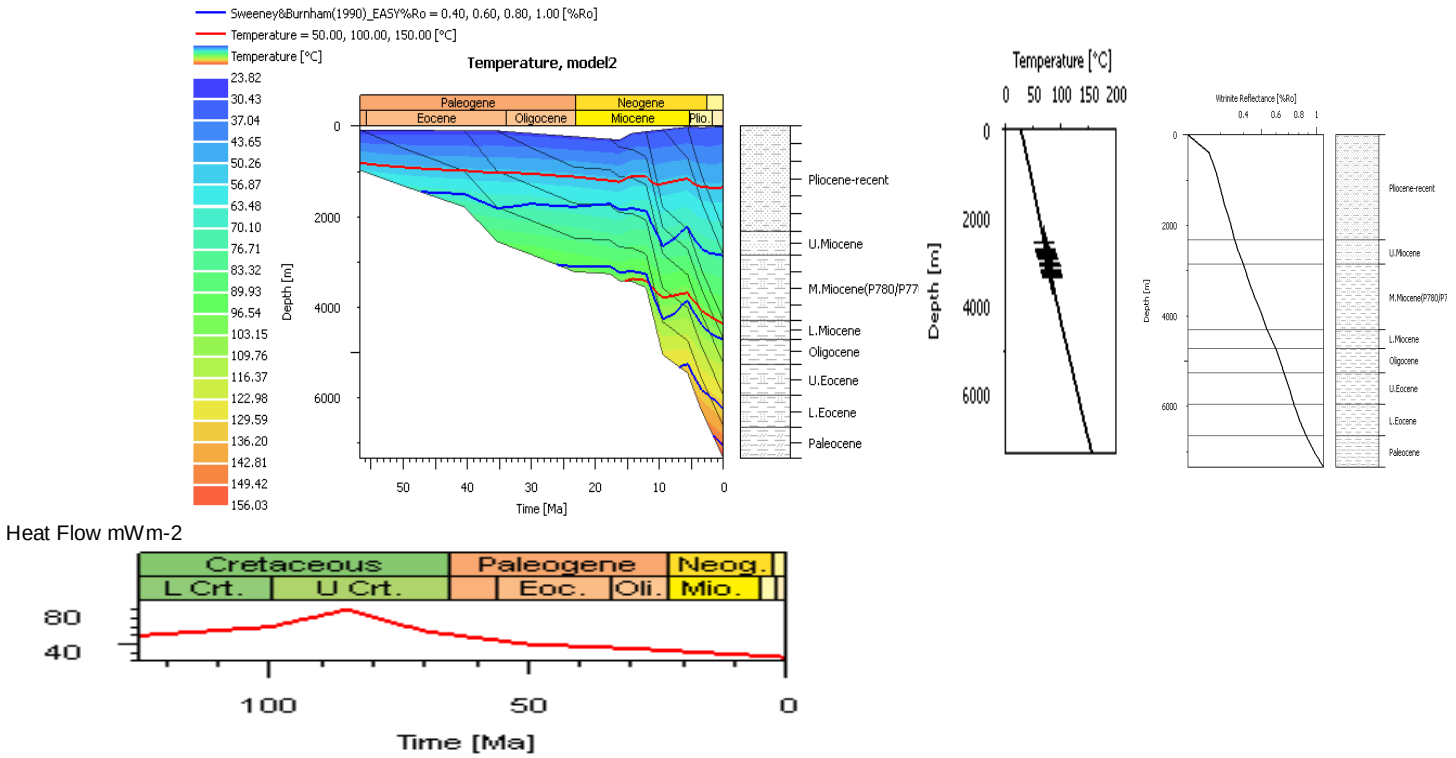

Fig. 5.14: Burial History chart showing isotherms , organic maturity and model calibration with temperature data for Akaso 4 well in the Coastal Swamp depobelt of the Niger Delta.

5.6.3 Thermal Modelling of Opobo South – 4 well

The input data used for the modelling is given in table 5.11. The well was drilled to a depth of 3878.3m, in Lower Miocene sediments. The well did not penetrate into the Oligocene, Eocene, and Palaeocene sediments. The thicknesses of the Oligocene, Eocene and Paleocene sediments were considered to be the same as encountered at Nsit-1 well, which is a nearby well. (Table 4.4). Maturation was modelled using Petromod 1-D modelling software with vitrinite being calculated using Easy% R_o of Sweeney and Burnham (1990). The predicted vitrinite reflectance values cannot be compared with measured values because no vitrinite reflectance data exists for the well. However, the maturity data were established by calibrating calculated temperature against the measured temperature data for the well. A good fit between calculated and measured temperature data was achieved by using the rifting ï subsidence thermal model, whereby a high heat flow value of 90 mWm^{-2} is applied at 85 Ma, being the break-up phase of the basins initiation.

Burial history diagrams showing isotherms and maturity windows for Opobo South - 4 are shown in figure 5.15. In this study, Upper Miocene, Lower Miocene Oligocene, Eocene and Palaeocene sediments are considered as effective source rocks. The modelling suggests that the upper parts of the Upper Miocene (Ro < 0.6%) are immature for oil generation. The modelling also suggests that the basal part of the Upper Miocene is within the early mature zone (0.60% - 0.70%), while the Lower Miocene and the upper part of the Oligocene are in the mid-mature zone (0.70% - 1.0%). The modelling shows that the lower part of the Oligocene, the Eocene and the Palaeocene are in the late mature (1.0% - 1.3%) stage of oil

generation. A heat flow of 51 mWm^{-2} is calculated from PRT temperatures with a surface temperature of 27^{o} C.

TABLE 5.11 : MAIN INPUT FOR OPOBO SOUTH - 4 WELL (COASTAL SWAMP)													
Layer	**Top (m)**	**Base(m)**	**Thickness(m)**	**Eroded (m)**	**Depo from(Ma)**	**Depo to (Ma)**	**Eroded from(Ma)**	**Eroded to (Ma)**	**Lithology**	**PSE**	**TOC %**	**Kinetic**	**HI(mg HC/gTOC**
Pliocene -Recent	0	2139	2139		5	0			SAND shaly	Overburden			
U.Miocene (P800/P784)	2139	3865	1726		11.5	5			SHALE sand	Sealrock			
L.Miocene	3865	4370	505		23.3	11.5			SHALE &SAND	Reservoir rock	1.2	Burnham (1989) II	100
Oligocene (P500)	4370	5309	939		35.4	23.3			SHALE	Source rock	1.6	Burnham (1989) III	150
Eocene (P370/P330)	5309	5429	120		56.7	35.4			SHALE sand	Source rock	2	Burnham (1989) III	250
Paleocene (P200)	5429	5575	146		65.5	56.7			SHALE silt	Source rock	2.4	Burnham (1989) III	300
						65.5							

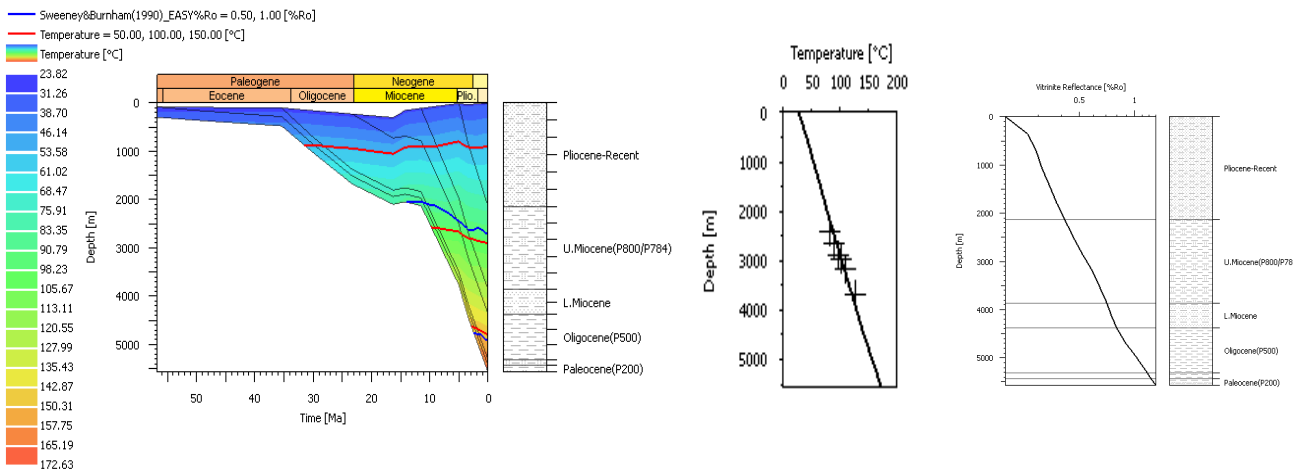

Heat Flow mWm-2

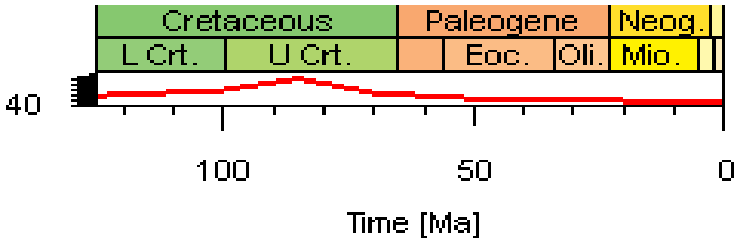

Fig. 5.15: Burial History chart showing isotherms, organic maturity and model calibration with temperature data for Opobo South - 4 well in the Coastal Swamp depobelt of the Niger Delta.

5.6.4 Thermal Modelling of Kappa – 1 well (Shallow Offshore)

Input data used in the modelling is summarized in table 5.12. The well was drilled to a depth of 3622.7m, in Middle Miocene sediments. The well did not penetrate into the Oligocene, Eocene, and Palaeocene sediments. The wells were extrapolated to the base of the Palaeocene, using the thickness of these units as evaluated from a nearby offshore well (Uge ST-1) (Table 4.3). Maturation was modelled using Petromod 1-D modelling software with vitrinite being calculated using Easy% R_o of Sweeney and Burnham (1990). The predicted vitrinite reflectance values cannot be compared with measured values because no vitrinite reflectance data exists for the well. However, the maturity data were established by calibrating calculated temperature against the measured temperature data for the well. A good fit between calculated and measured temperature data was achieved by using the rifting ï subsidence thermal model, whereby a high heat flow value of 90 mWm^{-2} is applied at 85 Ma, being the break-up phase of the basins initiation.

Burial history diagrams showing isotherms, organic maturity and temperature calibration for Kappa -1 well are shown in figure 5.16. In this study, the Upper Miocene, Lower Miocene, Oligocene, Eocene and Palaeocene sediments are considered as effective source rocks. The modelling suggests that the Upper Miocene, the Lower Miocene and the Upper Oligocene are immature (Ro < 0.6%) source rocks. The modelling also suggests that basal part of the Oligocene, the Eocene and the Palaeocene are within the early to mid-mature stages (0.60 % to 1.0 %) of oil generation. A heat flow of 38 mWm^{-2} is calculated from PRT temperatures with a surface temperature of 22^o C.

TABLE 5.12 : MAIN INPUT FOR KAPPA - 1 WELL (SHALLOW OFFSHORE)

Layer	Top (m)	Base (m)	Thick ness(m)	Eroded (m)	Depo from(Ma)	Depo to (Ma)	Eroded from(Ma)	Eroded to (Ma)	Litho logy	PSE	TOC %	Kinetic	HI(mgHC/gTOC
U. Pliocene -Recent	0	567	567		3	0			SAND	Over burden			
L.Pliocene (P880/P870)	567	1027	460		5	3			SAND shaly	Seal rock			
U.Miocene (P860/P840)	1027	3606	2579		6.7	5			SAND & SHALE	Reservoir rock			
L.Miocene	3606	4021	415		23	16.3			SAND &SHALE	Source rock	1.6	Burnham (1989) II	100
Oligocene	4021	4831	810		35	23.3			SHALE	Source rock	1.8	Burnham (1989) III	150
Eocene	4831	6012	1181		57	35.4			SHALE sand	Source rock	2	Burnham (1989) II	250
Paleocene	6012	6533	521		66	56.7			SHALE silt	Source rock	2.3	Burnham (1989) III	350
						65.5							

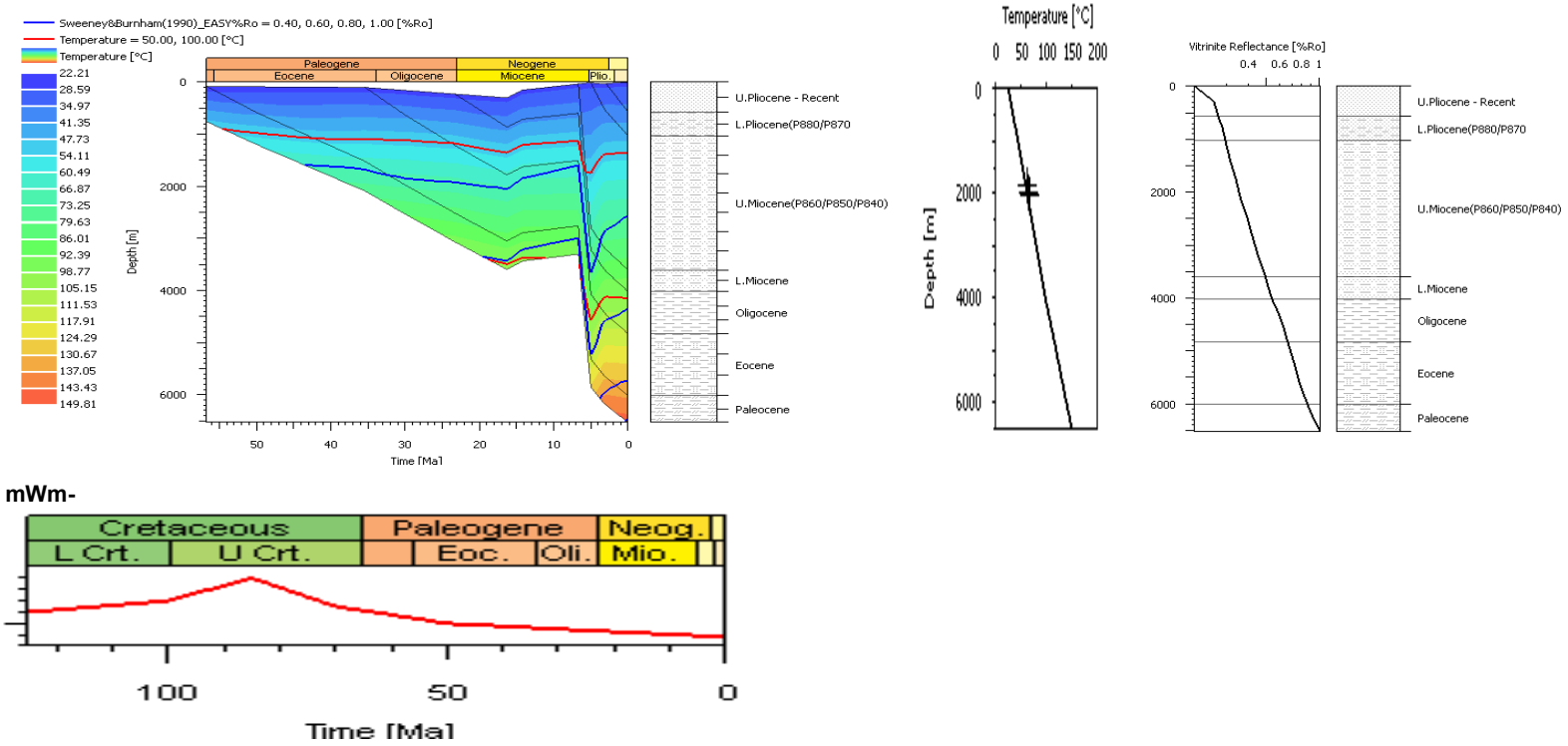

Fig. 5.16: Burial History chart showing isotherms, organic maturity and model calibration with temperature data for Kappa ï 1 well in the Shallow Offshore depobelt of the Niger Delta.

5.7 Maturity and Hydrocarbon Generation

The temperature, maturation and kerogen transformation history derived for the four wells is summarized in figures 5.17, 5.18, 5.19 and 5.20. The calculated curves are plotted for the Paleocene, Eocene, Oligocene and Miocene layers to allow for comparison between different structural positions of these wells. It is noteworthy that important time steps of enhanced maturation and therefore, hydrocarbon generation depends on the structural positions of these wells and in particular on source rock depth.

5.7.1 Paleocene Source Rocks

The temperature, maturation and kerogen transformation history for Paleocene source rock intervals are shown in figure 5.17 a ï d. With the exception of Kappa-1 well, the calculated temperature evolution for the other three wells can be divided into three intervals. This includes; an initial progressive rise in temperature. Similarly, three clear stages of maturity evolution can be observed for the Paleocene source rocks. The observed stages include; an initial progressive maturity rise, an increased maturity rise and a rapid maturity rise (Fig. 5.17 a ï d). At Obig -1 well, the Paleocene source rock interval entered the oil window at 26 Ma and is currently in the gas generation phase (Ro = 1.8%), with a calculated transformation ratio (TR) of around 80%. At Akas ï 4, kerogen transformation into petroleum started at 12 Ma, when the source rocks entered the 100°C isotherm. The present day maturity level for the source rock is about 1.0 % Ro and 100% of the transformation potential has been exploited. At OpoS -4 well, the Paleocene source rock interval entered the oil window at 10 Ma and is currently within the late mature stage (Ro = 1.3 %), with a calculated transformation ratio of around 65%. At Kapp -1 well, two stages of temperature and maturity evolution are apparent for the

Paleocene source rocks. This include; an initial progressive rise in temperature and maturity and a later rapid rise in maturity. Here, the Paleocene source rocks entered the oil window at 19 Ma and is currently in the mid mature stage (Ro = 1.1%). The Paleocene source rocks have a calculated transformation ratio of about 33%.

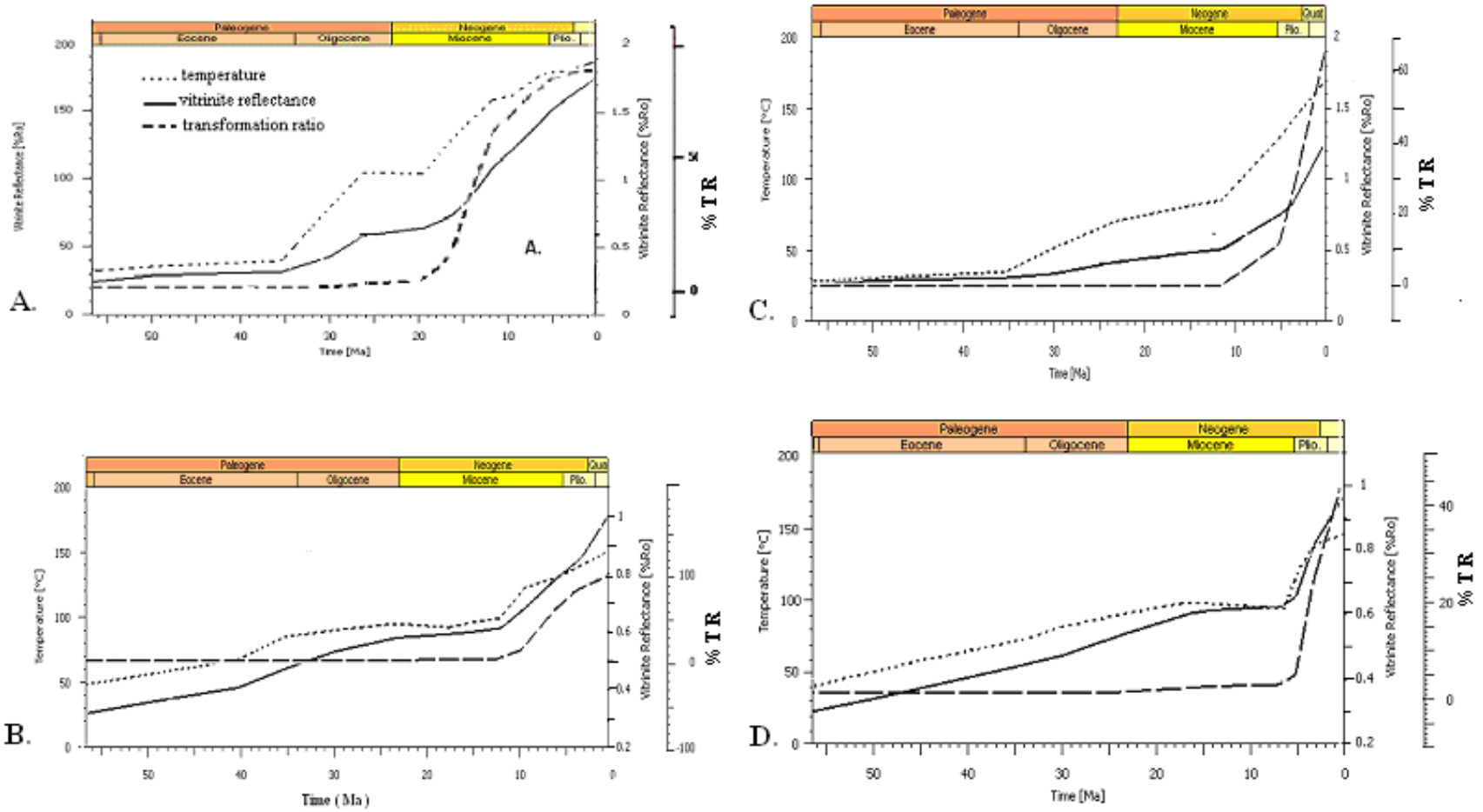

Figure 5.17. Comparison of temperature evolution and maturation as well as kerogen transformation for the Paleocene source rocks. (A) Obig - 1 well (Central Swamp) (B) Akas - 4 well (Coastal Swamp) (C) Opos - 4 well (Coastal Swamp) and (D) Kapp - 1 well (Shallow Offshore)

5.7.2 Eocene Source Rocks

The temperature, maturation and kerogen transformation history for Eocene source rock intervals are given in figures 5.18 a ï d. Three clear stages of temperature and maturity evolution are observed for the Eocene source rocks with the exception of Kappa ï 1 well. At Obig -1 well, the onset of oil generation for the Eocene source rocks took place 21 Ma ago and is currently in the gas generation phase (Ro = 1.6%). At Akas ï 4 well, the kerogen transformation of Eocene source rocks into petroleum started at about 7 Ma, following the renewed subsidence. The present day maturity level for this source rock is about 0.78% and about 25% of the transformation potential has been exploited. At Opobo South ï 4 well, the onset of oil generation for the Eocene source rocks took place 9 Ma ago and the process of generation continues to present day (Ro = 1.1%) and the source rocks have not passed through the oil generation window. At Kappa -1 well, the Eocene source rocks started to generate oil at about 4 Ma and are still generating oil presently with a calculated transformation ratio of about 65%.

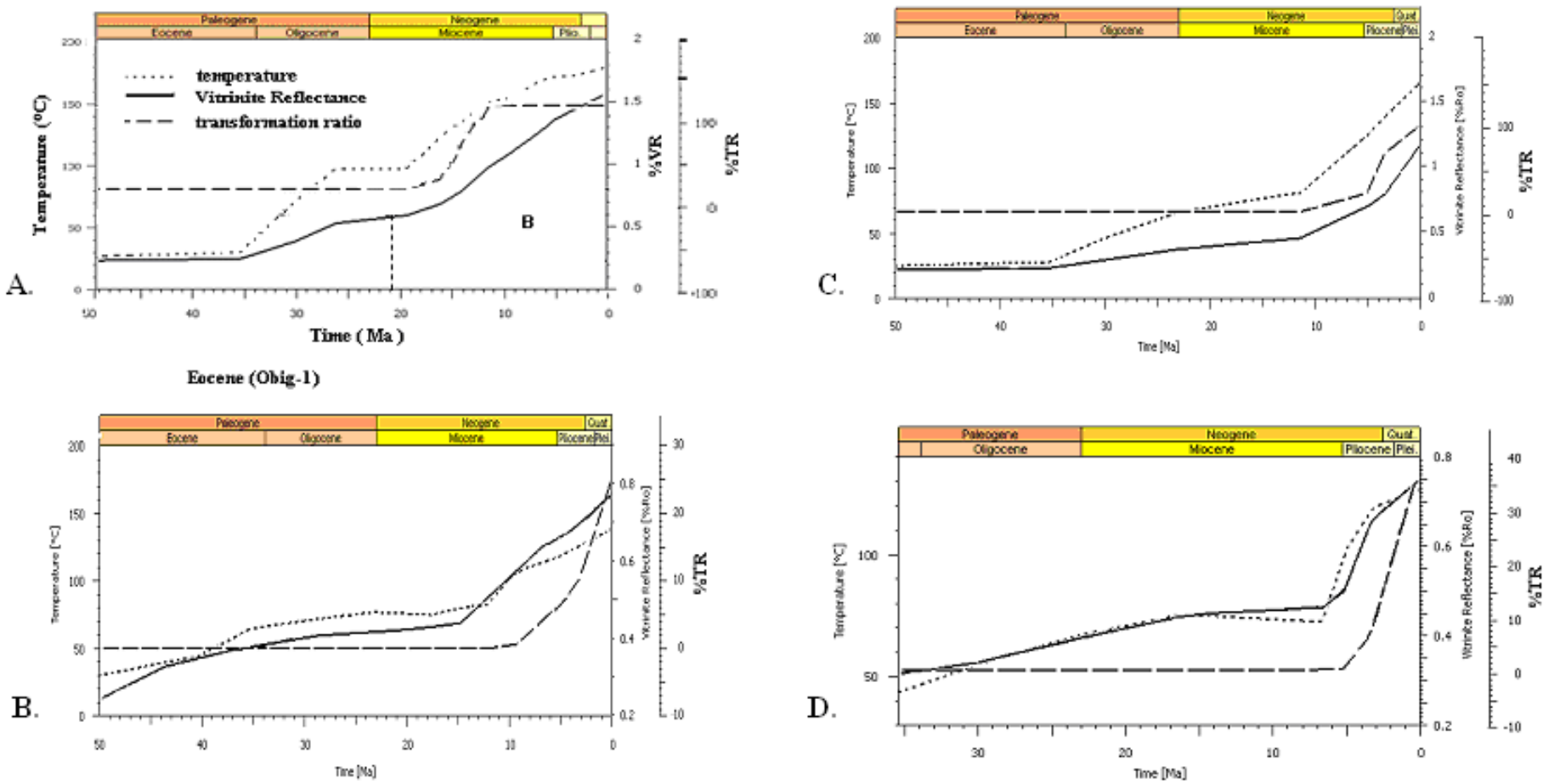

Figure 5.18 . Comparison of temperature evolution and maturation as well as kerogen transformation for the Eocene source rocks. (A) Obig - 1 well (Central Swamp) (B) Akas - 4 well (Coastal Swamp) (C) Opos - 4 well (Coastal Swamp) and (D) Kapp - 1 well (Shallow Offshore)

5.7.3 Oligocene Source Rocks

The temperature, maturation and transformation history of Oligocene source rocks are shown in figures 5.19 a ï d. At Obig ï 1 well, the Oligocene sediments began to generate oil at 12 Ma ago. Oil generation within the Oligocene continued to present with Ro% of about 0.9%. At Akas ï 4, the Oligocene source rocks entered the oil window at about 1.5 Ma and its present day maturity level is about 0.66%. The Oligocene source rock interval has used only 25% of its transformation potential. At OpoS ï 4, well, the Oligocene sediments began to generate oil at 7 Ma, when the sediments entered the 100 ^{o}C isotherm. Oil generation within the Oligocene sediments continued to present with Ro% of about 1.0%. At Kappa-1 well, the basal part of the Oligocene entered the oil window at about 1 Ma with a Ro% of about 1.4%.

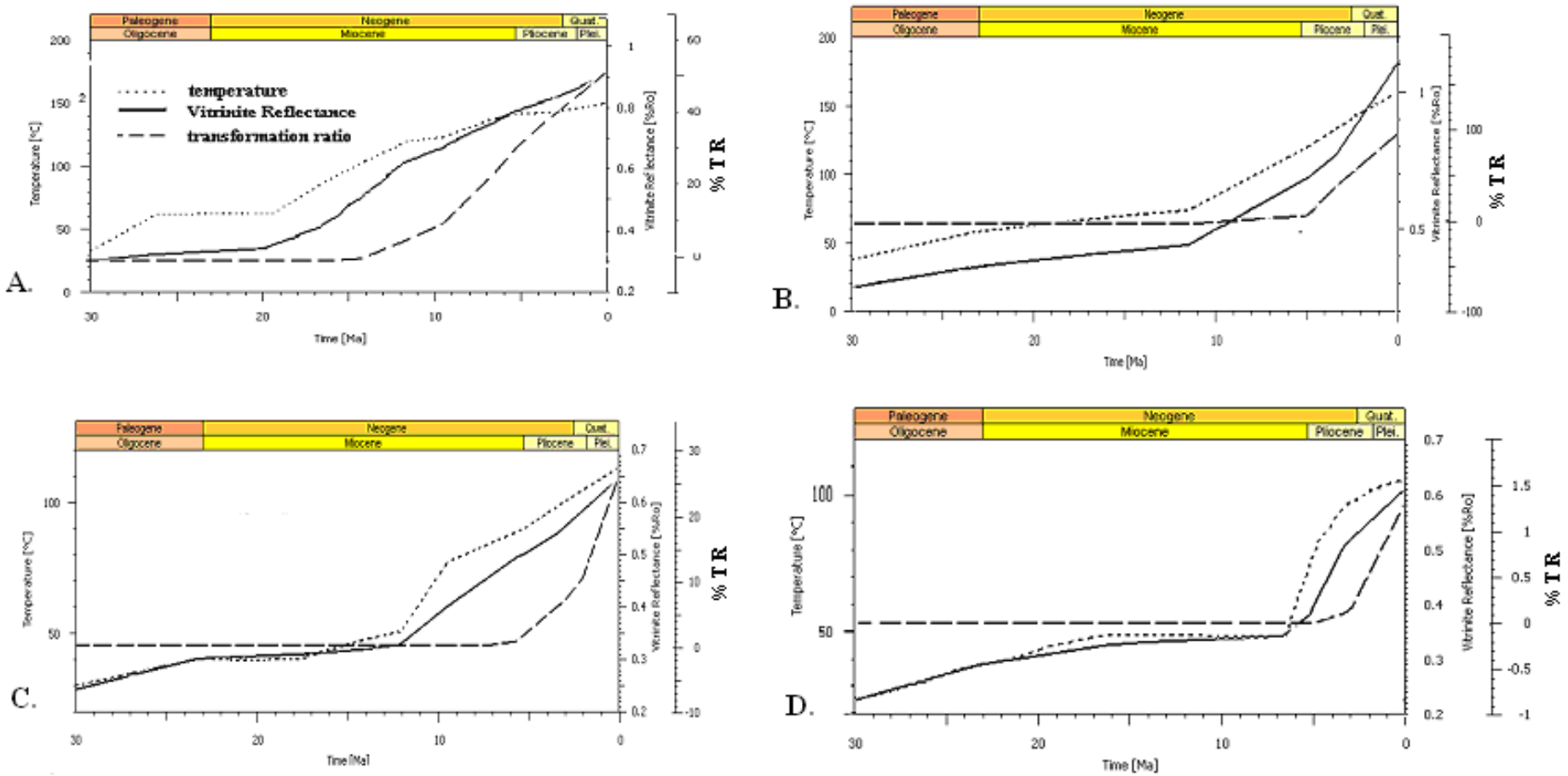

Figure 5.19. Comparison of temperature evolution and maturation as well as kerogen transformation for the Oligocene source rocks. (A) Obig - 1 well (Central Swamp) (B) Akas - 4 well (Coastal Swamp) (C) Opos - 4 well (Coastal Swamp) and (D) Kapp - 1 well (Shallow Offshore)

5.7.4 Lower Miocene Source Rocks

The temperature, maturation and transformation history of Miocene source rocks are shown in figures 5.20 a ï d. At Obig ï 1 well, the Lower Miocene entered the oil window at 3 Ma and its present day maturity level is about 0.75% Ro. At Opobo ï South ï 4, the lower Miocene and the basal part of the Upper Miocene entered the oil window at respectively at 3 and 1.5 Ma and their present maturity levels are 0.75 and 0.65% respectively.

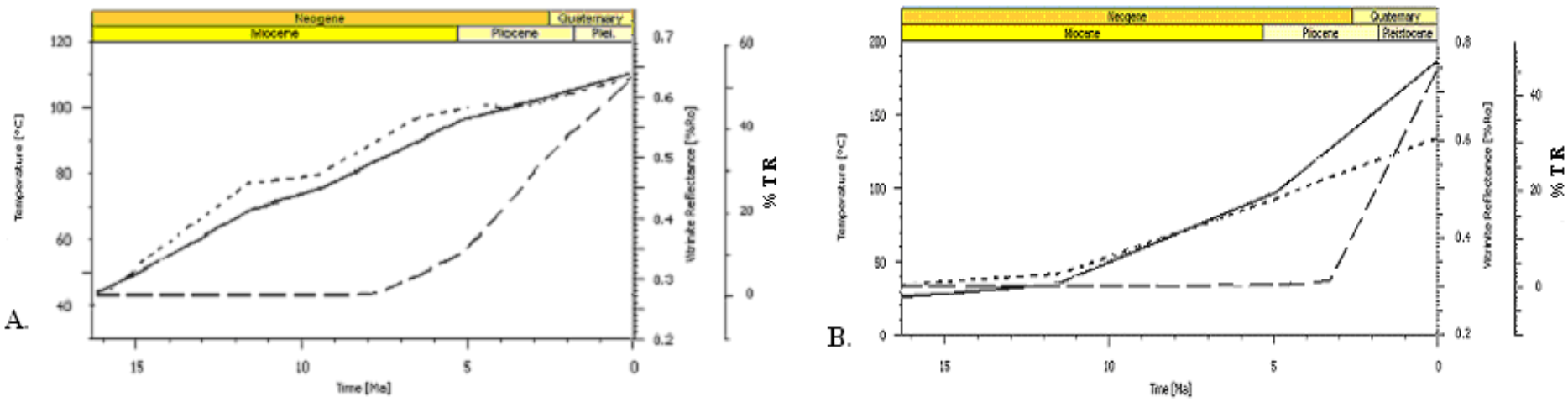

Figure 5.20. Comparison of temperature evolution and maturation as well as kerogen transformation for the Miocene source rocks. (A) Obig - 1 well (Central Swamp) (B) Opos - 4 well (Coastal Swamp)

CHAPTER SIX

6.0 DISCUSSION OF RESULTS AND CONCLUSION

6.1 Geothermal Gradients and Subsurface Temperature Distribution in the Niger Delta

The geothermal gradients pattern in the Eastern Niger Delta consists of a two leg dogleg geothermal gradients and a single leg geothermal gradients. The dogleg pattern is mostly observed in the Central and the Coastal Swamps while the single leg pattern is characterized by the Shallow Offshore. In the dogleg pattern, the upper or shallow thermal gradient belongs to the continental sandstones (Benin Formation), while the lower or deeper thermal gradient belongs to the marine / parallic section.

Generally geothermal gradients in the Niger Delta show a continuous but non linear relationship with depth, increasing with diminishing sand percentages. In the Niger Delta, geothermal gradients vary between 10 ï 24^{o}C/Km in the continental section, and increases to 18 ï 45^{o}C/Km in the deeper (marine / paralic) section. Sand percentages and geothermal gradients maps suggests that as sand percentages decreases eastwards, seawards, and northwards, geothermal gradients increaseôs. Thermal conductivities of the sediments also influence the geothermal pattern in the delta. The thermal conductivities decrease from about 2.3 W/mK in the continental sandstones to 1.56 W/mK in the paralic and continuous shaly sections.

Dogleg geothermal gradient patterns are characterized by a sudden departure of the temperature profile or the thermal gradient from the usual linear increase of the profile with depth. Hunt (1996) referred to this pattern as zones of variable gradient. The break in temperature profile can be likened the leg shape of a dog.

Forest *et al*. (2007), observed some multi-linear, or dogleg geothermal gradient pattern in northern Gulf of Mexico. They suggested that the breaks in the temperature profile are often coincident with the top of overpressure zone or zone of thermal conductivity change. A dogleg feature may correspond to an unconformity associated with a large stratigraphic gap. Dogleg patterns have also been observed in vitrinite reflectance profiles in the Thrace Basin, North-western Turkey. (Huvaz *et al*, 2005. Some variations may occur within the dogleg patterns. It could be in the form of a three-leg pattern or double-dogleg pattern. Single leg geothermal gradient patterns are observed in areas with maximum thickness of the sandy Benin and Agbada Formations.

6.2 Factors Influencing Geothermal Anomalies and Heat Flow Variations in the Eastern Niger Delta

The factors influencing geothermal anomalies and heat flow variations in the Niger Delta include; variations in thermal conductivity, variations in sedimentation rates / sediment thicknesses, variable radiogenic heat production in basement rocks, variations in mantle heat flow, large scale water convection and advective flow of fluids.

(i) Variations in thermal conductivity and heat generation in the sediments.

Heat flow and geothermal anomalies are clearly influenced by lithology. Sands and shale of variable composition constitute the main litho-types in the Niger Delta. The thermal conductivities of these sediments range from 1.56 to 2.30 W/mK. In the study area, thermal conductivities generally decrease with depth. The sand percentage maps (Fig. 5.11a and 5.11b) shows that sand percentages generally decreases eastwards from the western part of the Eastern Coastal Swamp, and also

to the Central Swamp and to the Shallow Offshore. The sand percentage variation is a reflection of the thermal conductivity variation in the sediments. A comparison of the heat flow map with the sand percentage maps has clearly shown that regions of low heat flow correspond with areas of high sand percentage or high thermal conductivity. The reason is because of the fact that sands are better conductors than shale and therefore will show lower heat flow. The sand percentage maps suggest that shale percentage increases as sand percentage decreases. This therefore implies that radiogenic heat production has a significant contribution to the total heat budget in these areas with a high proportion of shales. Clastic sediments such as shale are known to be rich in radiogenic heat producing elements, namely, thorium, uranium, and potassium. These radiogenic elements produce heat that is added to the total heat passing through the sedimentary column.

(ii) Variations in sedimentation rates / sediment thicknesses

An inverse relationship exists between sedimentation rate and seafloor heat flow (i.e., faster sedimentation rate, lower heat flow and vice versa) Nagihara and Jones (2005). The lower heat flow in the western parts of the eastern Coastal Swamp and the Shallow Offshore can be attributed to the Pliocene ï recent high sedimentation rates. The decrease in heat flow resulted from the addition of very thick, newer cold sediments on the surface. These new sediments absorbs heat as it rises through the sedimentary column, decreasing the amount of heat making it to the surface, as they try to equilibrate to the surrounding sediment temperature.

Sedimentation rates are usually calculated by dividing the sediment thickness by the age of the sediment and so they are related. Across the eastern part of the Niger Delta, sediment thicknesses decreases from about 12km in the west to about 3 km in the east corresponding roughly to an eastward increase in heat flow.

(iii) Fluid redistribution by migration of fluids

Fluid migration phenomena are observed worldwide in sedimentary basins (Hunt, 1990) and have been used to explain present day thermal anomalies (Andrew-Speed *et al*.1984, Chapman *et al*.1984, and Majorowicz 1989) The high heat flow in the eastern parts of the Central Swamp, Coastal Swamp and the Shallow Offshore as well as in the western part of the Central Swamp may be attributable to fault controlled fluid migration from deeply buried sediments such as the Akata Formation. A mechanism that may be responsible for high heat flow is the development of overpressure in shale. As sediment experiences compaction, pore water is squeezed out and migrates upward through younger, less compacted sediment or faults. If the flow is focused, along narrow conduits (e.g., faults), temperatures near the flow path become elevated as a result.

Large-scale water convection within the sandy Benin Formation has helped to reduce the heat flow flowing through the sediments especially in the western and central parts of the study area.

(iv) Basement heat flow

The result of magnetic intensity map shows that the magnetisation intensity of the Central Swamp is variable and strong (10 ï 110 nTesla), the Coastal Swamp is moderate (50 ï 90), and the Shallow Offshore is weak (0 ï 50). In the Central Swamp, magnetization highs, (>100 nTesla) occurs around Akata, Ibibio and Ekim fields, as well around Tabangh, Korokoro and Ofemini fields. Magnetization lows (< 50 nTesla) occur around Obigbo, Imo River, Odagwa and Oza fields. In the Shallow Offshore, the magnetization highs (>50 nTesla) occurs around KH-1 and KQ-1 wells, while magnetization lows occur around JD-1, JO-1 and JK-1 wells. Okubo *et al*. (2006) suggested that an aeromagnetic map generally reveals the

subsurface structure of a sedimentary basin. According to them, the magnetic intensity map reveal the general distribution of magnetization near the surface as well as the thickness of the magnetic layer but does not give information on the depth. The magnetic intensity map therefore suggests that the Central Swamp and Coastal Swamp consists of thin Continental Crust except around areas with high magnetic intensity (>100 nTesla). It also suggests that the Shallow Offshore consists of a transitional crust.

According to Nagihara and Jones (2006), basement heat flow consists of two aspects; heat released from the mantle and heat due to radioactive heat production in basement rocks. In a continental margin setting, the extent of lithospheric stretching controls the heat flow experienced during a basins initiation. Generally, mantle heat flow decreases as the lithosphere cools. Radioactive heat production through decay of unstable elements (e.g., Uranium, Thorium and Potassium) from basement rocks also contributes to the total heat flow coming from the basement.

Thus the heat variations across the study area is a reflection of the heat contributions from the basement resulting from both lithospheric stretching and heat contributions from radioactive decay of unstable elements from basement rocks. Thus areas with thicker continental crusts experiences higher heat flow than areas with thinner continental and oceanic crust.

Okubo *et al* (2006) interpreted low magnetization as reflecting fractured or hydro-thermally altered zones caused by up flow of geothermal convection. According to them, in geothermal areas, hydrothermal alteration typically destroys the signature of volcanic rocks either by completely removing the iron or by converting magnetite to haematite, which has low magnetic susceptibility. The

correlation of the magnetic intensity in the area with the heat flow estimates are shown in Profiles 1 (A ï B), Profile 2(C ï D) and Profile 3(E ï F) (Figure 6.1).

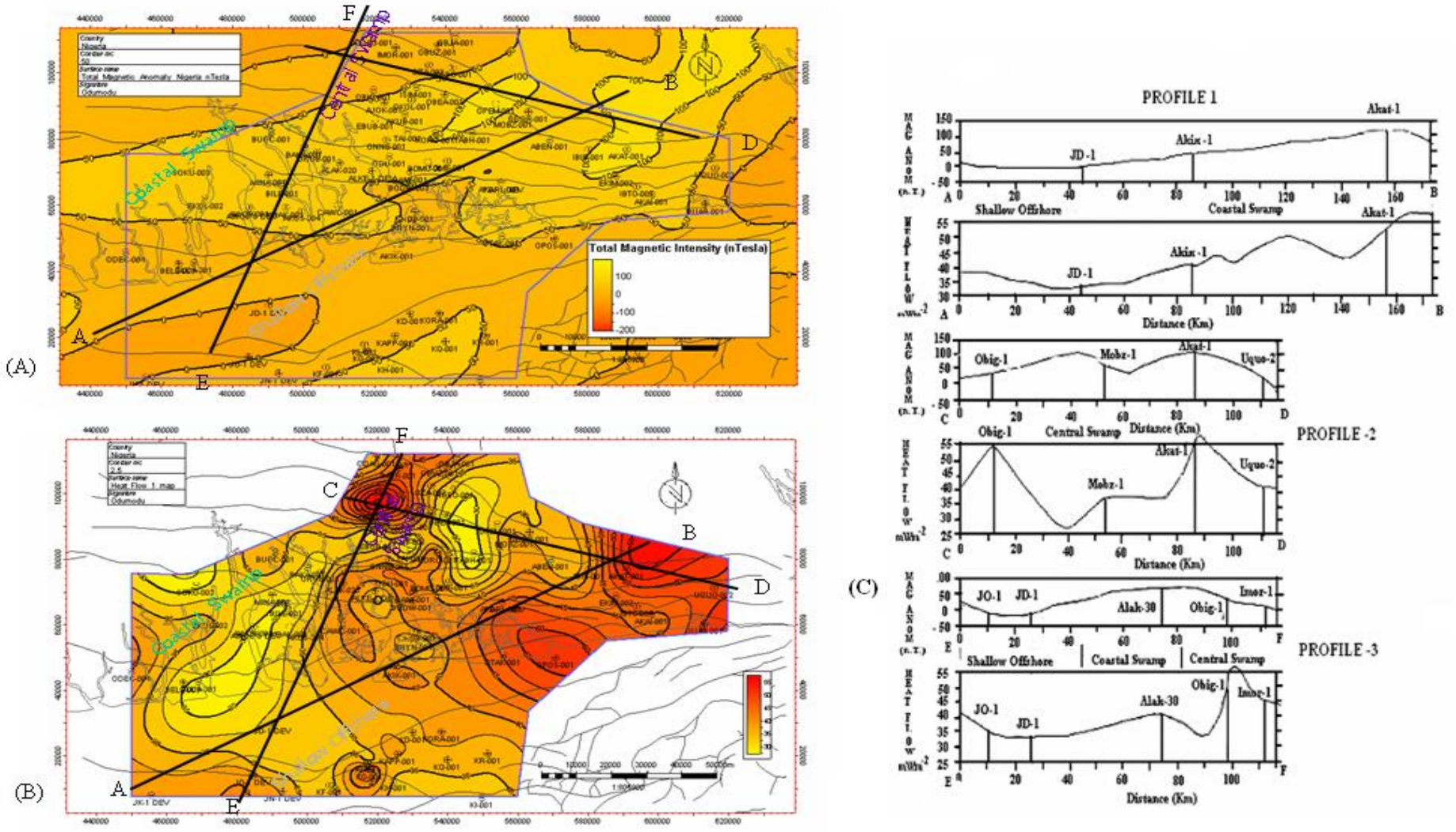

Figure 6.1 Profiles across Total Magnetic Intensity map and Heat Flow map of parts of the Eastern Niger Delta. (a) Magnetic Intensity map (b) Heat Flow map (c) Mag Anomaly and Heat Flow profiles

6.3 Burial History and Hydrocarbon Maturation Modelling

6.3.1 Source rocks

No available source rock samples were used in this study. However source rock analysis of Miocene and upper parts of the Oligocene have been described in some previous studies (Ekweozor and Okoye, Lambert ï Aikhionbare and Ibe, 1984; and Bustin, 1988). Some of these studies attributed the generated petroleum to be solely sourced from the shales of the Akata Formation with no contribution from the Agbada Formation while others suggest variable contributions from both formations and even from the deeper formation. The source rock maturity and hydrocarbon generation modelling results are shown in Figures 5.13 ï 5.20. A summary of the times when possible source rocks attained various levels of maturity in the studied wells is presented in table 6.10.

6.3.1.1 Paleocene source rocks

None of the wells penetrated into the Paleocene. The Paleocene was modelled as a potential source rock, using data from nearby wells especially from the flank. The TOC and Hydrogen index for Paleocene rocks are respectively 2.5% and 350 mgHCg^{-1}TOC respectively. The TOC value indicates a very good source potential while the hydrogen index suggests an oil source potential. The thermal maturity window of the Paleocene varies in different parts of the basin. The thermal maturity windows in these wells indicate that the Paleocene source rocks began to generate oil during the Oligocene and Miocene times. The Paleocene source rocks is inferred to be within; the gas generation window at Obigbo ï 1, late mature window at Opobo South ï 4, mid mature window at Akaso ï 4 and Kappa ï 1. The predicted

generated hydrocarbons are mainly gas and oil. The cumulative generation in the wells range from 0.54 ï 5.05 Mtons of oil and 0.95 ï 2.89 Mtons of gas.

Table 6.10. *Times of different maturity levels attained by the modelled source rocks*

Well name	**Formation or event name**	**Time of Early maturity**	**Time of Middle maturity**	**Time of Late maturity**	**Time of Main gas generation**
Obigbo -1	Palaeocene	26	18	13	9
	Eocene	21	16	11	6
	Oligocene	12	8		
	Lower Miocene	3			
Akaso-4	Palaeocene	12	1		
	Eocene	7			
	Oligocene	1.5			
Opobo South - 4	Paleocene	10	6	3	
	Eocene	9	5	2	
	Oligocene	7	1		
	Lower Miocene	3			
	Upper Miocene	1.5			
Kappa-1	Palaeocene	19	5		
	Eocene	4	3		
	Oligocene	1			

6.3.1.2 Eocene source rocks

None of these wells were drilled in the Eocene source sediments. However Eocene source rocks were assumed as potential source rocks in this study because of the fact that they have been penetrated into in wells located in delta flanks. The Eocene apparently has attained levels of thermal maturity that differ in different time and spaces. Modelled maturity ranged from early maturity to main gas generation. The source rock maturity as indicated by TOC of 1.8 ï 2.3 % is generally fair to good. It has mixed kerogen type II and III. The Eocene source rocks attained proper maturity during the Miocene and Pliocene times. The Eocene source rocks are within; the gas generation window at Obigbo ï 1, late mature window at Opobo South ï 4, middle mature window at Kappa ï 1 and early mature window at Akaso ï 4. The model suggests a cumulative generation of 0.36 ï 1.47 Mtons of oil and 0.24 ï 0.77 Mtons of gas.

6.3.1.3 Oligocene source rocks

In the study area, it is only the upper part of the Oligocene has been penetrated because of the overpressured conditions of the shales at such great depths. Consequently, source rock analysis exists in literature for only the penetrated sections of the formation. It has mixed kerogen type II / III. Analytical results from literature shows the Total organic carbon content (TOC) varies from 1.6 ï 1.7 %, suggesting fair to good source potential whereas the hydrogen index range from 85 ï 150 suggesting a source potential for gas. The Oligocene sediments are currently within; the mid-mature oil window at Obigbo ï 1 and Opobo South ï 4 while it is in

the early mature zone at Akaso ï 4 and Kappa ï 1. The cumulative generation varies from 0.0294 ï 1.05 Mtons of Gas and 0.0130 ï 1.52 Mtons of oil.

6.3.1.4 Miocene source rocks

Some of the wells penetrated into the Upper Miocene, Middle Miocene or the Lower Miocene. Substantial thickness of potential source rocks (shale) exists mainly in the Lower Miocene. The Upper and Middle Miocene serve as a primary reservoir. Source rock analysis for TOC in literature range from 0.80 ï 1.5 % indicating fair to poor source potential while the Hydrogen index of 57 ï 80 suggests a potential for gas. The Lower Miocene source rocks lies within the early ï mature zone at the Obigbo -1 and Opobo South ï 4 wells while it is not yet mature at Akaso ï 4 and Kappa ï 1 wells. The cumulative generation is 0.158 ï 0.196 Mtons for oil and 0.029 ï 0.037 for gas**.** The source rocks at the base of the Upper Miocene is within the early mature zone at the Opobo South ï 4 well while it is not yet near the oil window at the other three well locations.

The present modelling results reveals that higher levels of thermal maturity are attained in areas with high geothermal gradients and heat flow while the cooler areas exhibits lower levels of maturation. The onset of the oil window lies at 2859m at Obigbo ï 1 (Central Swamp), 3240m at Opobo South ï 4(Coastal Swamp), 4732m at Akaso ï 4(Coastal Swamp) and 4344 m at Kappa ï 1 (Shallow Offshore).

6.4 Implications of the Results

Results of this study have again confirmed the usefulness and applicability of reservoir and corrected bottom hole temperatures data for basin analysis studies. The result has also informed us on some new salient features on thermal gradients,

heat flow and hydrocarbon maturation patterns in the Niger Delta. The thermal gradients increase eastwards, seawards and northwards from the Eastern Coastal Swamp. Thermal gradients in the Niger Delta also show a continuous and non linear relationship with depth. These increases in geothermal gradients reflects changes in thermal conductivities, increased shaliness, variation in sedimentation rates / sediments thicknesses, diagenetic differentiation, heat contributions from the basement and fluid redistribution in the sediments. The heat flow trend is a reflection of the geothermal gradients variations in the basin. This study may also give an insight into the regional hydrodynamic systems in the Niger Delta.

Geothermal gradient variations have a significant implication for source rock maturation. A comparison of a map of the study area showing oil and gas fields (Fig. 6.11) with the average geothermal gradient map of the study area (Fig 5.4.) indicate certain trends. Very few oil and gas pools occur in the eastern parts while they are concentrated in the western parts of the study area. Geothermal gradients are higher in the eastern parts of the Coastal Swamp and in the western parts of Central Swamp. Several gas fields that occur within the study area include Obigbo and Afam gas fields in the Central Swamp. Other gas fields occurring within the study area include Alakiri and Soku gas fields. These gas fields usually occur with associated oil and for this fact the Niger Delta is usually described as a gas province associated with an unusual volume of oil. According to Turtle et al (2007), the Niger Delta is ranked as the twelfth position in recoverable gas reserves of all countries of the world and equally occupies an elevated rank in ultimate oil reserves. The large volume of gas in the Niger delta is primarily due to the presence of large quantity of terrestrial plant debris in the clastic sediments and secondly due to thermal maturation status.

Hydrocarbon maturation modelling have shown that potential source rocks in the Niger Delta such as the Paleocene, the Eocene, the Oligocene and the Lower Miocene have attained maturity status to generate hydrocarbons. The results also suggest that vast differences exist in the timing as well as the level of kerogen transformation into petroleum. The results also show that hydrocarbon maturation is greatly influenced by the variations in geothermal gradients.

6.5 Summary, Conclusion and Recommendations

The thermal structure of the Eastern Niger Delta has been investigated so as to understand the thermal gradients pattern using reservoir and corrected bottom-hole temperatures data from about seventy wells. The geothermal gradients show a continuous but non-linear relationship with depth, increasing with diminishing sand percentages. The geothermal gradients vary between 10-24 ^{o}C/km in the continental sandstones, and increases from 18 ï 45 ^{o}C/ km in the marine / paralic sections. Thermal gradients generally increase as sand percentages decreases eastwards and seawards. Thermal conductivities in the Niger Delta generally decrease with depth from 2.3W/mK in the continental sands to 1.56 W/mK in the paralic / continuous shaly sections. Thermal gradients in the Niger Delta are lithologically controlled. Minimum thermal gradients coincide with areas with maximum thickness of the sandy Agbada and Benin formations, while maximum values occur at the delta margins, where the deeper Akata Formation exerts a stronger influence.

Heat flow in the Eastern Niger Delta varies between 29 ï 55 mWm^{-2} (0.69 ï 1.31 HFU), with an average of 42.5 mWm$^{-2.}$ Higher heat flow values occur in the

eastern and northwestern parts of the study area. Lower heat flows characterize the eastern and central parts of the area.

Results of hydrocarbon maturation modelling suggest vast differences as regards to timing and levels of kerogen transformation to petroleum. It shows that the potential source rocks are mature to generate hydrocarbons. The depth to the oil generative window is deeper in the west and shallows to the east and northwest.

It is necessary to suggest that the data set be expanded for a more of comprehensive future studies. It is recommended that continuous temperature logs be ran for some of the wells so as to develop some statistical based correction factors for BHT data in the Niger Delta. It is also suggested that in future, vitrinite reflectance analysis be done for some of the cored source rock samples from these wells studied. The results will be used for geochemical data validation ï i.e. assessing the consistency of predicted vitrinite reflectance data with the measured data.

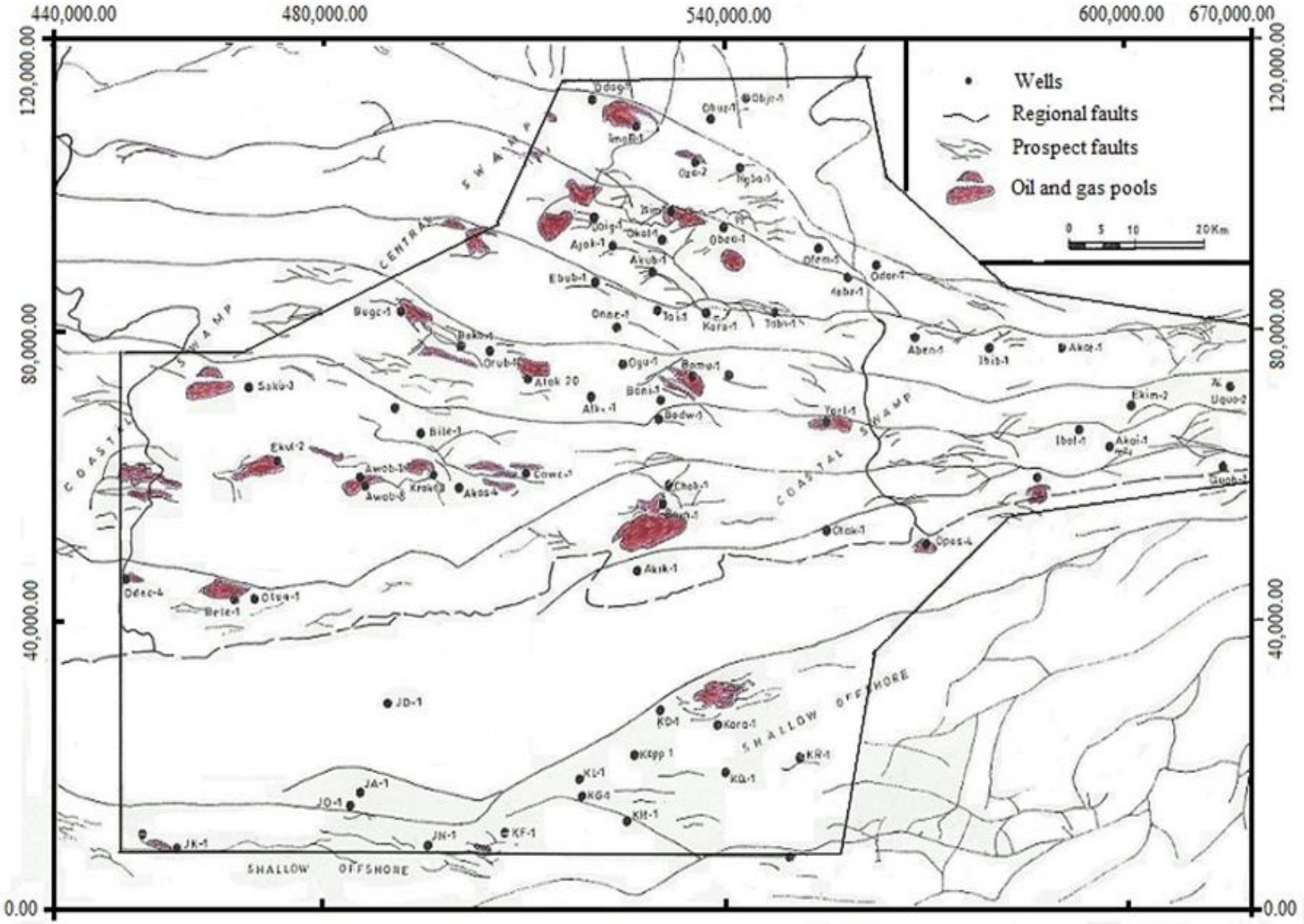

Fig. 6.11: Map of the study Area showing the oil and gas fields

REFERENCES

Akpabio, I.O., Ejedawe J.E., Ebeniro J.O. and. Uko, E.D, 2003. Geothermal gradients in the Niger Delta basin from continuous temperature logs. Global Journal of Pure and Applied Sciences. v. 9 (2), p. 265 ï 272.

Allen, P.A., and Allen, J.R. 1990. Basin Analysis ï Principles and Applications. Blackwell Scientific Publications, London, 449 p.

Anderson, R.N., Cathles L.M. III, and Nelson H.R. Jr., 1991, ñData Cubeò depicting fluid flow history in Gulf area Coast sediments: Oil & Gas Journal, v. 89, November 4, 1991, p. 60 ï 65.

Andrews-Speed, C.P., Oxburgh, E.R. and Cooper, B.A. 1984. Temperatures and depth-dependent heat flow in the western North Sea. American Association of Petroleum Geologists Bulletin,v. 68, p. 1764 ï 1781.

Avbovbo, A.A., 1978, Geothermal gradients in the southern Nigerian basin: Bulletin Canadian Petroleum Geology., v. 26, 2, p. 268 ï 274.

Beardsmore, G.R., and Cull, J.P., 2001, Crustal heat flow: A guide to measurement and modelling: Cambridge, Cambridge University Press, 324p.

Beck, A.E., 1976. An improved method of computing the thermal conductivity of fluid-filled sedimentary rocks. Geophysics, v. 41, 133-144.

Behar, F., Vandenbroucke, M., Tang,Y., Marquis, F. and Espitalie, J. 1997. Thermal cracking of kerogen in open and closed systems: determination of kinetic parameters and stoichiometric coefficients for oil and gas generation. Organic Geochemistry, v. 26, 321 ï 339.

Bodner, D.P. and Sharp J.M. (Jr), 1988. Temperature variations in South Texas subsurface. American Association of Petroleum Geologists Bulletin. v. 72, (1), p. 21 ï 32.

Bradley, J.S.., 1975. Abnormal formation pressure. American Association of Petroleum Geologists Bulletin, v. 59, 957 ï 973.

Brigaud, F., and Vasseur, G., 1989, Mineralogy, porosity and fluid control on thermal conductivity of sedimentary rocks: Geophysical Journal, v. 98, p. 525 ï 542.

Brigaud, F., Chapman, D.S and Le Douaran, S. 1990. Estimating thermal conductivity in sedimentary rocks using lithological data and Geophysical well logs. American Association of Petroleum Geologists Bulletin,v. 74, p. 1459 ï 1477.

Brigaud, F., Vasseur G. and Caillet, G. 1992. Thermal state in the North Viking Graben (North Sea) determined from oil exploration well data. Geophysics, v. 57, 69 ï 88.

Brooks, J. M., Bryant, W.R., Bernard, B.B. and Cameron, N.R. 1999. The nature of gas hydrates on the Nigerian continental slope. Annals of the New York Academy of Sciences.,v. 912, 76 ï 93.

Bullard, E.C., 1947. The time necessary for a borehole to attain temperature equilibrium. Monthly Notes of the Royal Astronomical Society, v. 5, p. 127 ï 130.

Burke, K., 1972, Longshore drift, submarine canyons, and submarine fans in development of Niger Delta: American Association of Petroleum Geologists Bulletin, v. 56, p. 1975 ï 1983.

Burke, K.C., Dessauvagie, T.F.J. and Whiteman, A.J., 1971, the opening of the Gulf of Guinea and the geological history of the Benue depression and the Niger Delta: Nature Physical Science, v. 233, p. 51 ï 55.

Burnham, A.K. 1989. A simple kinetic model for petroleum formation and cracking. Lawrence Livermore National Laboratory report, UCID ï 21665.

Bustin, M., 1988. Sedimentology and characteristics of Dispersed Organic matter in Tertiary Niger Delta. Origin of source rocks in a Deltaic environment. American Association of Petroleum Geologists Bulletin, v. 72, (3), p. 277 ï 298.

Caillet, G., and Batiot, S., 2003. 2 ï D Modelling of hydrocarbon migration along and across faults: an example from Nigeria. Petroleum Geoscience,v. 9, p. 113 ï 124.

Carr, A.D. and Scotchman, I.C. 2003. Thermal history modelling in the southern Faroe - Shetland Basin. Petroleum Geoscience,v. 9, p. 333 ï 345.

Chapman, D.S., Keho, T.H., Bauer, M.S. & Picard, M.D., 1984. Heat flow in the Uinta Basin determined from bottom hole temperature (BHT) data. Geophysics. 49, p. 453 ï 466.

Chen, Z., Osadetz, K.G., Issler, D.R. and Grasby, S.E., 2008. Hydrocarbon migration detected by regional temperature field variations, Beufort ï Mackenzie Basin, Canada. American Association of Petroleum Geologists Bulletin, v. 92 (12), p. 1639 ï 1653)

Chukwueke, C., Thomas, G. and Delfraud. J., 1992. Sedimentary Processes, Eustatism, Subsidence and Heat flow in the Distal parts of the Niger Delta. Bull. Centres Rech. Exploration ï Production. Elf ï Acquitaine. v. 16(1), p. 137 ï 186.

Chulli, B., Bedir, M., and Ben Dhia, H., 2005. Identification of Geothermal and Hydrodynamic Characteristics of the Abiod Reservoir (Eastern Tunisia). Proceedings World Geothermal Congress 2005, Antalya, Turkey, 24 ï 29 April 2005.

Cohen, H.A., and McClay, K., 1996, Sedimentation and Shale tectonics of the north-western Niger Delta front: Marine and Petroleum Geology, v. 13, p. 313 ï 328.

Connan, J., 1974. Time ï temperature relation in oil genesis. American Association of Petroleum Geologists Bulletin. v. 58, p. 2516 ï 2521.

Corredor, F., Shaw, J.H. and Bilotti, F, 2005, Structural styles in the deep-water fold and thrust belts of the Niger Delta: American Association of Petroleum Geologists Bulletin, v. 89, p. 753 ï 780.

Corrigan, J., and Sweat, M, 1995, Heat flow and gravity responses over salt bodies: A comparative model analysis: Geophysics, v. 60, p. 1029 ï 1037.

Corry, D., and Brown, C. 1998, Temperature and Heat flow in the Celtic Sea basins: Petroleum Geoscience, v. 4, p. 317 ï 326.

Deming, D. and Chapman, D.S. 1988. Inversion of bottom hole temperature data: The Pineview field, Utah ï Wyoming thrust belt. Geophtsics,v. 53, p. 707 ï 720.

Doust, H., and Omatsola, E, 1990, Niger Delta, in J.D. Edwards, and P.A. Santogrossi, eds., Divergent/passive margin basins: American Association of Petroleum Geologists Memoir, v. 48, p. 201 ï 238.

Ejedawe, J.E., 1990. Geothermal models of the Níger Delta. S.P.D.C. Expl. Note. 56p.

Ekweozor, C.M. and Daukoru, E.M. 1994. Northern delta depobelt portion of the Akata ï Agbada (!) petroleum system, Niger Delta. In Magoon, L.B. and Dow, W.G. (eds). The petroleum system ï from source to trap. American Association of Petroleum Geologists Memoir, v.460, 599 ï 613

Ekweozor, C. M., Okogun, J.I., Ekong D.E.U and Maxwell, J.M. Preliminary organic geochemical study of samples from the Niger Delta (Nigeria)., Chemical Geology, v.29, p. 29 ï 37.

Ekweozor, C.M. and Okoye, N.V, 1980. Petroleum source- bed evaluation of Tertiary Niger Delta. American Association of Petroleum Geologists Bulletin, v.64, p. 1251-1259.

Espitalie, J., Madec, M., Tissot, B., Mennig, J.J. and Leplat, P, 1977. Source rock characterization method for petroleum exploration: Proceedings of the 9th Annual Offshore Technology Conference, v. 3, p. 439 ï 448.

Evamy, B.D., Haremboure, J., Kamerling, P., Knaap, W.A.,. Molloy, F.A. and Rowlands, P.H., 1978, Hydrocarbon habitat of the Tertiary Niger Delta: American Association of Petroleum Geologists Bulletin, v. 62, p. 1 ï 39.

Farouki, O. T. 1981. Thermal properties of soils. Cold Regions Research and Engineering Laboratory, CRREL Monograph 81ï 1.

Forrest, J., Marcucci, E., & Scott, P., 2007. Geothermal Gradients and Subsurface Temperatures in the Northern Gulf of Mexico. Gulf Coast Association of Geological Societies Transactions, v. 55, p. 233 ï 248.

Forster, A., 2001. Analysis of borehole temperature data in the Northeast German Basin: continuous logs versus bottom-hole temperatures: Petroleum Geoscience, v. 7, p. 241 ï 254.

Frasheri, A., 2005. Geothermal regime and hydrocarbon generation in the Albanides. Petroleum Geoscience, v. 11, p. 347 ï 352.

Frielingsdorf, J, 2009. Unpublished Petroleum Systems Event Chart.

Frost, B.R, 1977. Structure and facies development of the Niger Delta resulting from hydrocarbon maturation. American Association of Petroleum Geologists Bulletin, v. 80, p. 1291.

Haack, R.C., Sundararaman, P., and Dahl, J.,1997. Niger Delta petroleum system, in, Exteneded Abstracts, AAPG / ABGP Hedberg Research Symposium, Petroleum Systems of the South Atlantic Margin, November 16 ï 19, 1997, Rio de Janeiro, Brazil.

Heinio, P., and Davies, R.J., 2006. Degradation of compressional fold belts: Deep-water Niger Delta: AAPG Bulletin, v. 90, p. 753 ï 770.

Hood, A., Gutjahr, C.C.M,. and Leacooks, R.L., 1975. Organic metamorphism and generation of petroleum. American Association of Petroleum Geologists Bulletin., v. 59, p. 986 ï 996.

Horner, D. 1951. Pressure build ï up in wells. In Proceedings of the Third world petroleum congress. The Hague, p. 503 ï 519.

Houbolt, J.J., and Wells, P.R.A, 1980. Estimating Heat Flow in Oil Wells Based on a Relation Between Heat Conductivity and Sound Velocity. Geologie en Mijnbouw, v. 59 (3), p. 215 ï 224.

Http:/www.windows.ucar.edu/tour/link=/earth/water/images/temperature_depth_jpg.

Huang, H.J., 1971. Effective thermal conductivity of porous rocks. Journal of Geophysical Research, v. 76, p. 6420 ï 6427.

Hunt, J.M., 1996, Petroleum Geochemistry and Geology, 2nd Ed., Freeman, San Francisco.

Husson, L., Henry, P. and Le Pichon, X., 2008. Thermal regime of the NW shelf of the Gulf of Mexico, Part A: Thermal and pressure fields. Bull. Soc. Geol. Fr., v. 179 (2), p. 129 ï 137.

Husson, L., Le Pichon, X., Henry, P., Flotte, N., and Rangin, C., 2008. Thermal regime of the NW shelf of the Gulf of Mexico, Part B: Heat flow. Bull. Soc. Geol. Fr., v. 179 (2), p. 139 ï 145.

Hutchison, I., 1985, The effects of sedimentation and compaction on oceanic heat flow: Geophysical Journal of the Royal Astronomical Society, v. 82, p. 439 ï 459.

Huvaz, O., Sarikaya, H., and Nohut, O.M., 2005, Nature of a regional dogleg pattern in maturity profiles from Thrace basin, north-eastern Turkey; A newly discovered

unconformity or a thermal anomaly?, American Association of Petroleum Geologists Bulletin, v. 89, p. 1373 ï 1396.

Illiffe, J.I., Robertson, A.G., Wynn, G.H.F., Pead, S.D.M and Cameron, N. 1999. The importance of fluid pressures and migration to the hydrocarbon prospectivity of the Faeroe ï Shetland White Zone. In Fleet, A.J. and Boldy S.A.R. (eds) Petroleum Geology of Northwest Europe: Proceedings of the 5th conference. Geological Society, London, p. 601 ï 611.

Jarvis, G.T. and Mckenzie, D.P. 1980. Sedimentary Basin formation with finite extension rates. Earth and Planetary science letters, v. 48, p. 42 ï 52.

Klemme, H.D., 1975, Geothermal gradients, heat flow and hydrocarbon recovery, in Petroleum and global tectonics: A.G. Fischer and S. Judson, Ed., Princeton, New Jersey, Princeton Univ. Press. p. 251 ï 304.

Lambert-Aikhionbare, D.O. and Ibe, A.C. 1984. Petroleum Source-Bed Evaluation of Tertiary Niger Delta: Discussion. American Association of Petroleum Geologists Bulletin, v. 68 (3), p. 387 ï 394.

Lawrence, S. R., Munday, S., and Bray, R., 2002, Regional geology and geophysics of the eastern Gulf of Guinea (Niger Delta to Rio Muni): The Leading Edge, v. 21, (11), p. 1112 ï 1117.

Leadholm, R.M., Ho, T.T.Y., and Sahai, S.K., 1985, Heat Flow, Geothermal Gradients and Maturation Modelling on the Norwegian Continental Shelf Using Computer Methods, In Petroleum Geochemistry in Exploration of the Norwegian Continental Shelf: B.M. Thomas et al. eds, Norwegian Petroleum Society. p. 131 ï 143.

Leblanc, Y., Pascoe, L.J., and Jones, F.W., 1981. The temperature stabilization of a borehole. Geophysics, v. 46, p. 1301 ï 1303.

Lopatin, N.V. 1971. Temperature and Geologic Time as factors in coalification. Izvestiya Akademii Nauk, ussr. Seriya Geologicheskaya, v.3, p. 95 ï 106. (in Russian)

Luheshi, M.N., 1983. Estimation of formation temperature from borehole measurements. Geophysical Journal of Royal Astronomical Society. v. 74, p.747 ï 776.

Majorowicz, J.A., 1989. The controversy over the significance of the hydrodynamic effect of heat flow in the Prarries Basin. In Beck A.E., Garven G. and Stegena L. (eds) Hydrological regimes and their subsurface thermal effects. Geophysical Monograph series, v.47, p. 101 ï 105.

Marjorowicz, J.A. & Jessop, A.M. 1981. Regional heat flow patterns in the Western Canadian sedimentary basin. Tectonophysics, v. 74, p. 209 ï 238.

Majorowicz, J.A., Jessop A.M., and Lane, L.S., 2005. Regional heat flow pattern and lithosphric geotherms in the northeastern British Columbia and adjacent territories, Canada. Bulletin Canadian Petroleum Geology, v. 53 (1), p. 51 ï 66.

Matava, T., Rooney, M.A., Chung, H.M., Nwankwo, B.C., and Unomah, G.I. 2003. Migration effects on the composition of hydrocarbon accumulations in the OML 67 ï 70 areas of the Niger Delta. AAPG Bulletin, v. 87 (7), p. 1193 ï 1206.

Mckenna, T. E., Sharp, J. M. & Lynch, F. L. 1996. Thermal conductivity of Wilcox and Frio sandstones in south Texas (Gulf of Mexico Basin). American Association of Petroleum Geologists Bulletin, v. 80, p. 1203ï 1215.

Mckenzie, D.,1978. Some remarks on the development of sedimentary basins formed by extension. Earth and Planetary Science Letters, v. 40, p. 25 ï 32.

Metwalli, F.I. and Pigott, J.D. 2005. Analysis of petroleum system criticals of the Matruh ï Shushan Basin, Western Desert, Egypt. Petroleum Geoscience, v. 11, p. 157 ï 178.

Middleton, M. 1979. A model for bottom hole temperature stabilization: Geophysics, v. 44, p. 1458 ï 1462.

Middleton, M. 1994. Determination of matrix thermal conductivity from dry drill cuttings. American Association of Petroleum Geologists Bulletin, v. 78, p. 1790ï 1799.

Midttomme, K., and Roaldset, E. 1998. The effect of grain size on thermal conductivity of quartz sands and silts. Petroleum Geoscience, v. 4, p. 165 ï 172.

Midttomme, K., Saettem, J. & Roaldset, E. 1997. Thermal conductivity of unconsolidated marine sediments from Vøring Basin, Norwegian Sea. Nordic Petroleum Technology Series, **2**.

Morgan, R., 2004, Structural controls on the positioning of submarine channels on the lower slopes of the Niger Delta, in R.J. Davies, J.A. Cartwright, S.D Stewart, M. Lappin, and J.R. Underhill, eds., 3 D seismic technology: Application to the exploration of sedimentary basins: Geological Society (London) Memoir, v. 29, p. 45 ï 51.

Murat, R.C., 1972. Stratigraphy and Palaeogeography of the Cretaceous and Lower Tertiary in southern Nigeria, In T.F.J. Dessauvagie and A.J. Whiteman, eds.ô African Geology, Ibadan, Nigeria, Ibadan University Press, p. 251 ï 266.

Nagihara, S. and Jones, K.O., 2005. Geothermal heat flow in the northeast margin of the Gulf of Mexico. American Association of Petroleum Geologists Bulletin, v. 89,(6), p. 821 ï 831.

Nagihara, S., and Smith, M.A., 2005, Geothermal gradient and temperature of hydrogen sulphide-bearing reservoirs in the continental shelf off Alabama: AAPG Bulletin, v. 89, p. 1451 ï 1458.

Nagihara, S., and Smith, M.A., 2008, Regional overview of deep sedimentary gradients of the geopressured zone of the Texas ï Louisiana continental shelf: American Association of Petroleum Geologists Bulletin, v. 92 (1), p. 1 ï 14.

Nagihara, S., Sclater, J.G., Beckley, L.M., Behrens, E.W., and. Lawver, L.A., 1992, High heat flow anomalies over salt structures on the Texas continental slope, Gulf of Mexico: Geophysical Research Letters, v. 19, p. 1687 ï 1690.

Norden, B., and Forster, A., 2006, Thermal conductivity and radiogenic heat production of sedimentary and magmatic rocks in the Northeast German Basin: American Association of Petroleum Geologists Bulletin, v. 90 (6), p. 939 ï 962.

North, F.K. 1996. Petroleum Geology, Unwin Hyman, Winchseter, Mass.

Nwachukwu, S.O., 1976, Approximate geothermal gradients in the Niger Delta sedimentary basin: American Association of Petroleum Geologists Bulletin, v. 60, p. 1073 ï 1077.

Nwachukwu, J.I. and Chukwura, I. 1986, Organic matter of Agbada Formation, Niger Delta, Nigeria. American Association of Petroleum Geologists Bulletin, v. 70, p. 48 ï 55.

Nwachukwu, J.I., Oluwole, A.F., Asubiojo, O.I., Filby, R.H., Grimm, C.A., and Fitzgerald, S., 1995. A geochemical evaluation of Niger Delta crude oils, in Oti, M. N., and Postma, G. eds., Geology of Deltas: Rotterdam A.A. Balkema. p. 287 ï 300.

OôBrien, J.I. and Lerche, I., 1984. The influence of salt domes on paleotemperature distributions. Geophysics, v. 49, p. 575 ï 583.

Ogagarue, D.O., 2007. Heat flow estimates in the estern Niger Delta basin, Nigeria. Pacific Journal of Science and Technology, v. 8 (2), p. 261 ï 266.

Okubo, A.T., Nakatsuka, Y. Tanaka, T. And Kagiyama, M.U., 2005. Magnetization structure of the Unzen Graben determined from Aeromagnetic Data. Annals of Disas. Prev. Res. Inst. Kyoto Univ. No 48. unpaginated.

Okubo, A.T., Nakatsuka, Y., Tanaka, T., and Kagiyama, M.U., 2006. Aeromagnetic constraints on the subsurface structure of the Unzen Graben. Earth Planets Space. v. 58, p 23 ï 31.

Olade, M.A., 1975. Evolution of Nigerias Benue Trough (aulacogen): a tectonic model: Geological Magazine, v. 112, p. 115 ï 583.

Onuoha, K.M., 1982. Sediment loading and subsidence in the Niger Delta sedimentary basin. Journal of Mining and Geology, v. 18, p. 138 ï 140.

Onuoha, K.M., 1999. Structural features of Nigerias coastal margin: an assessment based on age data from wells. Journal of African Earth Sciences, v. 29, (2) , p. 485 ï 499.

Onuoha, K.M. and Ekine, A.S., 1999. Subsurface temperature variations and heat flow in the Anambra basin, Nigeria. Journal of African Earth Sciences, v. 28 (3), p. 641 ï 652.

Onuoha, K.M., and Ofoegbu, C.O., 1988. Subsidence and evolution of Nigeriaôs continental margin: implications of data from Afowo ï 1 well. Marine and Petroleum Geology, v. 5, p. 175 ï 181.

Orife, J.M. and Avbovbo, A.A. 1982, Stratigraphic and unconformity traps in the Niger Delta: American Association of Petroleum Geologists, Bulletin ,v. 65,p. 251-265.

Peters, K.E. 1986. Guidelines for evaluating petroleum source rock using programmed pyrolysis. American Association of Petroleum Geologists Bulletin, v. 70, p. 318 ï 329.

Pigott, J.D. 1985. Assessing source-rock maturity in frontier basins. Importance of time, temperature and tectonics. American Association of Petroleum Geologists Bulletin, v. 69, p. 1269 ï 1274.

Pochat, S., Castelltort, S, Vanden Driessche, J., Besnard, K., and Gumiaux, C, 2004. A simple method of determing sand / shale ratios from seismic analysis of growth faults: An example from Upper Oligocene to Lower Miocene Niger Delta deposits: American Association of Petroleum Geologists Bulletin, v. 88, 1357 ï 1367.

Sass, J.H., Lachenbruch, A.H. and Munroe, R.J. 1971. Thermal conductivity on rocks from measurement of fragments and its application to heat flow determinations. Journal of Geophysical Research, v. 76, p. 3391 ï 3401.

Shell Petroleum Development Company of Nigeria Limited (DTW GEO). August 1998. Niger Delta Cenozoic Geological Data Table.

Schwarzer, D. and Littke, R, 2007. Petroleum generation and migration in the (Tight Gasô area of the German Rotliengend natural gas play: a basin modelling study. Petroleum Geoscience, v. 13, p. 37 ï 62.

Sclater, J.G. and Cerlerier, B., 1987, Extensional models for formation of sedimentary basins and continental margins. Norsk Geologisk Tidsskrift, v. 67, p. 253 ï 267.

Sclater, J.G. and Christie, P.A.F. 1980. Continental Stretching: An Explanation of the Post-Mid Cretaceous Subsidence of the Central North Sea Basin. Journal of Geophysical Research, v. 85, p. 33711-33739.

Seiver, R., 1983. Burial history and diagenetic kinetics. American Association of Petroleum Geologists Bulletin, v. 67, p. 684 ï 691.

Shen, P.Y., and Beck, A.E., Stabilization of bottom ï hole temperature with finite circulation time and fluid flow: Geophysical Journal of the Royal Astronomical Society, v. 86, p. 63 ï 90.

Short, K.C., and A.J. Stauble, 1967. Outline of geology of Niger Delta: American Association of Petroleum Geologists Bulletin, v. 51, p. 761 ï 779.

Sleep, N.H. 1971. Thermal effects of the formation of continental margins by continental break ï up. Geophysical Journal of the Royal Astronamical Society, v. 24, p. 325 ï 350.

Somerton, W. 1992. Thermal properties and temperature ï related behaviour of rock / fluid systems. Elseviour, Amsterdam.

Stacher, P., 1995. Present understanding of the Niger Delta hydrocarbon habitat; In Oti, M.N. and Postma, G., eds, Geology of Deltas. Rotterdam, A.A. Balkema. p. 257 ï 267.

Stephens, A. R., Famakinwa, S.B., and Monson, G.D., 1997. Structural evolution of the Eastern Niger Delta and associated petroleum systems of western offshore Bioko Island, Equatorial Guinea. American Association of Petroleum Geologist / Asociacao Brasiliera de Geologos Petroleo Joint Hedberg Research Symposium Meeting Abstracts, Rio de Janeiro, Brasil, extended abstracts, unpaginated.

Sweney, J.J. and Burham, A.K. 1990. Evaluation of a simple model of vitrinite reflectance based on chemical kinetics. American Association of Petroleum geologists Bulletin, v. 74, p. 1559 ï 1570.

Thomas, D., 1995. Exploration gaps exist in Nigerias prolific delta. Oil and Gas Journal, October 30, p. 66 ï 71.

Tissot, B.P. Pelet, R. and Ungerer, P. 1987. Thermal history of sedimentary basins, maturation indices, and kinetics of oil and gas generation. American Association of Petroleum Geologists Bulletin, v. 71, p. 1445 ï 1466.

Tissot, B.P. and Welte, B.P. 1984. Petroleum formation and occurrence. Springer ï Verlag, New York, 699 p.

Turtle, M.L.W, Charpentier, R.R, and Brownfield, M.E. 1999. The Niger Delta Petroleum System: Niger Delta Province, Nigeria, Cameroun, and Equatorial Guinea, Africa. U..S.G.S. Open file Report, p. 50 ï 54.

Udo, O.T., and Ekweozor, C.M., 1988. Comparative source rock evaluation of Opuama Channel Complex and adjacent producing areas of the Niger Delta: Nigerian Association of Petroleum Explorationists Bulletin, v. 3, (2), p.10-27.

Underdown, R and.Redfern, J., 2007. The importance of constraining regional exhumation in basin modelling: a hydrocarbon maturation history of the Ghadames Basin, North Africa. Petroleum Geoscience, v. 13, p. 253 ï 270.

Wang, K., and Davies, E.E., 1992. Thermal effects of marine sedimentation in hydro thermally active areas: Geophysical Journal International, v. 110, p. 70 ï 78.

Waples, D., 1980. Time and Temperature in petroleum formation, application of Lopatins method to petroleum exploration. American Association of Petroleum Geologists Bulletin., v. 64, p. 916 ï 926.

Waples, D.W., and Pacheco, J., and Vera, A., 2004, A method of correcting log ï derived temperatures. Petroleum Geoscience, v. 10, p. 239 ï 245.

Waples, D.W., and Ramly, M., 2001. A statistical method for correcting log ï derived temperatures. Petroleum Geoscience, v. 7 (3), p. 231 ï 240.

Weber, K.J. and Daukoru, E., 1975, Petroleum Geology of the Niger Delta. Ninth World Petroleum Congress Proceedings, v. 2, p. 209 ï 221.

Whiteman, A.J., 1982. Nigeria: Its Petroleum Geology, Resources and Potential: vols. 1 and 2: London, Graham and Trotman, Ltd., 176p. and 238p., respectively.

Zhuoheng, C., Osadetz, K.G., Issler, D.R., and Grasby, S.E., 2008. Hydrocarbon migration detected by regional temperature field variations, Baeufort ï Mackenzie p. 1639 ï 1653.

APPENDICES

APPENDIX 1: BOTTOM HOLE TEMPERATURE (BHT^{o}C) DATA FROM LOG HEADER

S/N	Well Names	Time circulation stopped	Time logger on bottom	Shut in time	BHT(oF)	Depth(FT)	BHT(oC)	Depth(m)	BHT©
						0			
1	**Abak - Enin -1**		30/08/1975	2	140	4520	60	1483	63
		10-9-75/06:00	10-9-75/10:00	4	164	9010	73.33	2956	78
			10/9/1975	6	164	9010	73.33	2956	78
			10/9/1975	9	164	9010	73.33	2956	78
			10/9/1975	13	164	9010	73.33	2956	78
			10/9/1975	16	164	9010	73.33	2956	78
		20/09/75/14:00	20-9-75/20:00	6	184	9438	84.44	3096	90
			22/09/1975	5	168	9408	75.56	3087	80
			22/09/1975	8	168	9408	75.56	3087	80
			22/09/1975	10	168	9408	75.56	3087	80
2	**Ajokpori-1**		19/02/1967		108	4005	42.22	1314	44
			3/3/1967		171	10837	77.22	3555	82
			5/3/1967		173	11235	78.33	3686	83
3	**Akai-1**	18-4-87/20:30	14-4-87/06:20		132	5018	55.56	1646	59
		02/05/87/22:15	3-5-87/10:30		179	8697	81.67	2853	88
		02/05/87/22:15	3-5-87/13:12		179	8697	81.67	2853	88
		5/13/1987	13-5-87/23:30		195	9198	90.56	3018	97
		16-5-87/22:00	19-5-87/09:54		209	9943	98.33	3262	105
5	**Akata-1**		12/4/1953		102	4065	38.89	1334	40
			4/6/1953		150	7000	65.56	2297	70
			2/7/1953		160	8185	71.11	2685	75
			22/07/1953		239	10787	115	3539	124
			7/10/1953		245	11104	118.3	3643	127
			7/10/1953		245	11111	118.3	3645	127
6	**Akikigha-1**	13-09-1987/13:00	13-9-87/18:41	5:41	112	5002	44.44	1641	46
		25-9-87/03:00	25-9-87/20:30	17:30	159	9000	70.56	2953	75
		25-9-87/03:00	25-9-87/15:45	12:45	156	9012	68.89	2957	73
		25-9-87/03:00	25-9-87/10:00	7	154	9001	67.78	2953	72
		25-9-87/03:00	26-9-87/00:15	21:15	163	9008	72.78	2955	78
		5-10-87/17:00	6-10-87/04:00	12	187	10455	86.11	3430	72
		25-9-87/03:00	26-9-87/02:30	11:30	232	14234	111.1	4670	109
		25-9-87/07:45	26-9-87/02:30	6:45	232	14234	111.1	4670	109
		5-10-87/17:00	6-10-87/14:15	21:15	194	10464	90	3433	96
		5-10-87/17:00	6-10-87/09:00	16	191	10468	88.33	3434	94
7	**Akuba-1**		12/2/1967		172	10380	77.78	3406	83
8	**Alakiri-East-1**		11/7/1977	4	107	4004	41.67	1314	44
		19-11-77/11:00	20-11-77/12:30	25:30:00	170	9984	76.67	3276	82
		19-11-77/11:00	20-11-77/16:00	27	174	9983	78.89	3275	84
		19-11-77/23:00	20-11-77/7:15	8:15	163	9984	72.78	3276	78
			4/12/1979	3	190	11822	87.78	3879	94
			4/12/1979	12	190	11822	87.78	3879	94
			10/12/1977	4	192	11975	88.89	3929	95
			13/12/1977	5	196	12190	91.11	3999	97
			13/12/1977	10	196	12190	91.11	3999	97

			12/15/1977	12	218	12190	103.3	3999	111
9	**Alakiri-20**		11/11/1984		174	9174	78.89	3010	84
10	**Awoba-1**		15/09/1965		98	3512	36.67	1152	38
			27/09/1965		184	11978	84.44	3930	90
			28/09/1965		184	11978	84.44	3930	90
11	**Awoba-8**		06/04/2003/08:25		210	12877	98.89	4225	106
			11-5-03/04:00		228	13964	108.9	4581	117
			13-5-03/04:45		228	13964	108.9	4581	117
		28-12-91/01:00	28-12-91/22:03	21:03	241	14997	116.1	4920	125
12	**Bakana-1**		13/04/1971		94	3520	34.44	1155	35
			13/04/1971		109	3520	42.78	1155	45
			22/04/1971		154	9984	67.78	3276	72
			29/04/1971		170	11037	76.67	3621	82
13	**Baniele-1**	22-12-88/07:15	23-12-88/02:15	19	117	6006	47.22	1970	49
					152	8892	66.67	2917	71
		9-1-89/03:00	9-1-89/22:15	19:15	155	8892	68.33	2917	72
					164	8894	73.33	2918	78
		17-1-89/20:45	18-1-89/06:15	9:30	182	11097	83.33	3641	89
					190	11071	87.78	3632	94
		31-1-89/02:45	01-02-89/06:51		220	13075	104.4	4290	112
14	**Belema-1**		20/12/1980	6	110	4534	43.33	1488	45
			10/1/1981	12	170	10966	76.67	3598	81
		10-01-81/12:00	11-01-81/5:00		167	10966	75	3598	80
			12/1/1981	14	165	10976	73.89	3601	79
			4/2/1981		202	13580	94.44	4455	101
			4/2/1981		200	13606	93.33	4464	100
			12/2/1981	11:15	163	10975	72.78	3601	78
			15-12-91/20:23		191	12400	88.33	4068	94
15	**Bille-1**		4/11/1971	2	110	5042	43.33	1654	45
			4/11/1971	6	110	5042	43.33	1654	45
			5/11/1971	11	110	5042	43.33	1654	45
			18/11/1971	4	171	11304	77.22	3709	82
			19/11/1971	15	171	11300	77.22	3707	82
			22/11/1971	29	171	8400	77.22	2756	82
16	**Bodo-WEST-1**								
17	**Bomu-1**		25/2/1958		90	1710	32.22	561	33
			8/3/1958		125	6491	51.67	2130	54
			20/03/1958		137	7569	58.33	2483	61
			23/03/1958		154	8947	67.78	2935	71
			28/03/1958		154	8948	67.78	2936	71
			9/4/1958		182	10262	83.33	3367	89
18	**Bonny-North-1**		6/2/1964		187	7815	86.11	2564	92
			6/2/1964		187	7824	86.11	2567	92
			7/2/1964		185	11883	85	3899	91
			17/02/1964		185	11895	85	3903	91
19	**Buguma Creek-1**		21/03/1960		120	6982	48.89	2291	51
			22/03/1960		150	6970	65.56	2287	70
			22/03/1960		122	6975	50	2288	52

			22/03/1960		120	6976	48.89	2289	50
			5/4/1960		220	10744	104.4	3525	112
			14/04/1960		186	11997	85.56	3936	92
			12/4/1960		196	10025	91.11	3289	97
			18/04/1960		196	12140	91.11	3983	97
			18/04/1960		196	12145	91.11	3985	97
20	**Cawthorne Channel-1**		2/11/1963		156	10050	68.89	3297	73
			2/11/1963		156	10032	68.89	3291	73
			2/12/1963		156	10025	68.89	3289	73
			2/24/1963		196	12428	91.11	4077	97
			2/25/1963		196	12551	91.11	4118	97
			2/27/1963		228	12901	108.9	4233	117
			3/1/1963		228	12908	108.9	4235	117
			3/1/1963		230	12907	110	4235	118
			3/4/1963		225	13140	107.2	4311	115
			18-06-95/07:51		265	11130	129.4	3652	139
			18-06-95/18:08		265	11132	129.4	3652	139
21	**Chobie-1**		3/19/1980	4	110	4504	43.33	1478	45
			4/1/1980	12	184	11001	84.44	3609	90
			4/2/1980	12	190	11000	87.78	3609	94
		01-04-80/12:00	02-04-80/02:00	2	186	11000	85.56	3609	91
			5/2/1980	16	212	12720	100	4173	108
		01-04-80/16:00	2-05-80/02:00	10	201	12720	93.89	4173	101
			4/28/1980		215	13200	101.7	4331	110
		03-05-80/11:30	04-05-80/03:00	3:30	206	12718	96.67	4173	114
22	**Ebubu-1**								
23	**Ekim-2**	04-11-86/17:00	05-11-86/11:00	18	115	4601	46.11	1510	48
		04-11-86/17:00	05-11-86/18:00	25	115	4601	46.11	1510	48
		21-11-86/11:00	22-11-86/19:14	26:14:00	190	9024	87.78	2961	93
		21-11-86/11:30	22-11-86/08:50	21:20	180	9030	82.22	2963	88
		08-12-86/19:15	09-12-86/06:30	11:15	216	10707	102.2	3513	110
		14-12-86/04:30	14-12-86/14:40	10:10	224	11027	106.7	3618	115
		15-12-86/22:00	16-12-86/11:49	13:49	232	11027	111.1	3618	119
24	**Ekulama-2**								
25	**Ibibio-1**		5/11/1959		125	4504	51.67	1478	55
			6/11/1959		140	3650	60	1198	63
			27/11/1959		170	9159	76.67	3005	81
			28/11/1959		171	8500	77.22	2789	82
26	**Ibotio-1**		17/06/195		100	516	37.78	169.3	39
			26/06/1955		129	3520	53.89	1155	57
			28/06/1955		131	4355	55	1429	58
			12/7/1955		163	7559	72.78	2480	79
			23/07/1955		188	9060	86.67	2972	93
27	**Imo River-1**								
28	**Isimiri-1**		17/03/1964		153	3061	67.22	1004	71
			31/03/1964		155	10030	68.33	3291	72

			16/04/1964		192	11889	88.89	3901	95
29	**Korokoro-2**		11/8/1962		112	4019	44.44	1319	46
			29/08/1962		160	10950	71.11	3593	75
30	**Krakama-2**		24/03/1962		102	2495	38.89	818.6	40
			2/5/1962		146	8503	63.33	2790	67
			15/02/1972		158	8144	70	2672	74
			23/09/1958		178	11076	81.11	3634	86
			19/03/1972		166	11576	74.44	3798	79
31	**Minama-1**		19/01/1967		144	11250	62.22	3691	66
32	**Mobazi-1**		28/12/1960		104	3830	40	1257	41
33	**Ngboko-1**				152	9047	66.67	2968	71
					158	9495	70	3115	74
34	**Obeaja-1**		30/01/1976	12	172	7738	77.78	2539	83
35	**Obeakpu-1**		14/10/1975	2	120	3762	48.89	1234	51
			25/10/1975	19	152	8100	66.67	2657	71
			25/10/1975	19.5	152	8100	66.67	2657	71
			25/10/1975	11	152	8268	66.67	2713	71
		24-10-75/21:00	25-10-75:04:00	7	152	8284	66.67	2718	71
				15	152	8276	66.67	2715	71
				19.5	153	8285	67.22	2718	71
36	**Obigbo-1**		11/8/1958	2	120	3762	48.89	1234	51
			11/8/1958		214	10280	101.1	3373	108
			11/8/1958		224	10543	106.7	3459	114
			11/10/1974		230	10782	110	3537	118
37	**Obuzor-1**		12/9/1971		110	2993	43.33	982	45
			20/09/1971		179	8525	81.67	2797	88
38	**Odagwa-1**			3	100	3014	37.78	988.8	39
		1-10-77/8:30	18-10-77/03:30		145	7519	62.78	2467	67
		17-10-77/08:30	17-10-77/02:40	7:10	140	7518	60	2467	63
		17-10-77/08:30	17-10-1977/06:20		140	7521	60	2468	63
		04-11-77/07:00	04-11-77/14:00	7:00	140	7521	60	2468	63
		04-11-77/07:00	04-11-77/14:00	7:00	178	9490	81.11	3114	86
		04-11-77/07:00	04-11-77/23:30	13:30	181	9498	82.78	3116	89
					182	9490	83.33	3114	89
39	**Odeama-Creek-4**		17/03/1981	22:30	172	10912	77.78	3580	83
			19/03/1981	6:00	177	11388	80.56	3736	86
		19-3-81/06:00	20-3-81/08:15	14:15	178	11388	81.11	3736	86
			3/4/1981	19:30	200	13143	93.33	4312	100
			7/4/1981	16:00	204	13773	95.56	4519	113
			7/4/1981	16:00	206	13775	96.67	4519	113
		6-4-81/16:00	7-4-81/17:30		210	13725	98.89	4503	116
40	**Odoro-Ikot-1**		10/8/1971	8	130	4785	54.44	1570	57
			10/8/1971	12:00	130	4785	54.44	1570	57
			10/8/1971	38	130	4785	54.44	1570	57
			25/08/1971	4	152	8401	66.67	2756	71
			25/08/1971	5	152	8501	66.67	2789	71
			25/08/1971	5	152	8507	66.67	2791	71

41	**Ofemini-1**								
42	**Ogu-1**		12/2/1965	3	163	8481	72.78	2782	78
			12/2/1965	6	163	9982	72.78	3275	78
			2/4/1973	6	184	11101	84.44	3642	90
			20/04/1973	10	216	12323	102.2	4043	110
			28/04/1973		242	12834	116.7	4211	125
43	**Okiori-1**		8/10/1975	3	100	4050	37.78	1329	39
			15/10/1975	10	148	9509	64.44	3120	68
			15/10/1975	14	148	9509	64.44	3120	68
			15/10/1975	18	148	9509	64.44	3120	68
			23/10/1975	10	160	11496	71.11	3772	75
			23/10/1975	12	160	11496	71.11	3772	75
			23/10/1975	16	160	11496	71.11	3772	75
44	**Okoloma-1**								
45	**Okoroba-1**	10-12-90/02:30	10-12-90/09:01	6:31	93	4426	33.89	1452	35
46	**Olua-1**	2-2-79/11:45	2/1/1979		105	3492	40.56	1146	42
		19/01/1979/17:00	20/01/1979/04:30	11:30	160	10211	71.11	3350	75
			20/01/1979	16	166	10212	74.44	3350	79
			20/01/1979	24	168	10213	75.56	3351	81
		02/01/1979/11:45	02/01/1979/19:15	7:30	192	12368	88.89	4058	95
		02/01/1979/11:45	02/01/1979/21:30	9:45	196	12367	91.11	4057	97
			2/1/1979	12	200	12367	93.33	4057	99
		2-2-79/11.45	2-2-79/10:30		202	12368	94.44	4058	101
47	**Onne-1**		22/03/1965		98	3505	36.67	1150	38
			2/3/1965		154	10370	67.78	3402	72
			3/4/1965		154	10370	67.78	3402	72
			3/4/1965		154	10380	67.78	3406	72
			4/3/1965		154	10384	67.78	3407	72
			5-10-92/19:20		174	9692	78.89	3180	84
48	**Opobo-South-4**		4/8/1974		197	9517	91.67	3122	99
			28/08/1974		183	9953	83.89	3265	90
			15/09/1974		200	11821	93.33	3878	100
49	**Orubiri-4**		6/2/1972	3.5	102	4040	38.89	1325	40
			14/02/1972	3	160	9401	71.11	3084	75
			15/02/1972	24	160	9400	71.11	3084	75
			16/02/1972	13	160	9402	71.11	3085	75
50	**Otakikpo-1**								
51	**Oza-2**		11/5/1962		92	1004	33.33	329.4	34
			19/05/1962		116	7000	46.67	2297	49
			24/05/1962		140	8999	60	2952	63
			4/6/1962		190	10997	87.78	3608	94
52	**Qua-Ibo-1**		26/01/1960		122	5179	50	1699	53
			4/2/1960		165	8473	73.89	2780	79
			9/2/1960		200	9496	93.33	3115	100
53	**Soku-3**		3/1/1963		104	2523	40	827.8	41
			14/01/1963		142	10074	61.11	3305	64
			25/01/1963		167	12377	75	4061	80
54	**Tabangh-1**		6/10/1962		100	3522	37.78	1156	39

			24/10/1962		150	9995	65.56	3279	70
			12/11/1962		170	11623	76.67	3813	82
	Tai-2		22/11/1963	6	160	9600	71.11	3150	75
			6/12/1973	6	170	11339	76.67	3720	82
56	**Uquo-2**		10/5/1971		124	4012	51.11	1316	53
			16/05/1971		150	7185	65.56	2357	70
			17/05/1971		150	7181	65.56	2356	70
			17/05/1971		150	7189	65.56	2359	70
			18/05/1971	15	149	7139	65	2342	69
			24/05/1971	12	180	8906	82.22	2922	88
			26/05/1971	12	180	8915	82.22	2925	88
			26/05/1971	8	180	8885	82.22	2915	88
			26/05/1971		180	8895	82.22	2918	88
57	**Yomene-1**		2/4/1962		90	2018	32.22	662.1	33
			15/04/1962		161	9480	71.67	3110	76
			15/04/1962		161	9484	71.67	3112	76
58	**Yorla-1**		4/11/1970		105	4514	40.56	1481	43
			25/11/1970		188	10500	86.67	3445	93
			18/11/1970	12	190	11900	87.78	3904	94
			18/11/1970	18	190	11888	87.78	3900	94
59	**KH-1**		8/1/1967		107	4035	41.67	1324	44
			21/01/1967		189	10976	87.22	3601	93
			22/01/1967		189	10973	87.22	3600	93
			28/01/1967		189	10976	87.22	3601	93
60	**KL-1**		28/01/1967		110	3021	43.33	991.1	45
			6/2/1967		188	10224	86.67	3354	91
61	**Koronama1**		18/03/1983		188	10575	86.67	3469	91
62	**KR-1**		31/05/1971	3	101	3015	38.33	989.2	39
			9/6/1971	25	164	8989	73.33	2949	78
63	**KG-1**		26/11/1966		107	4008	41.67	1315	44
			11/12/1966		191	10870	88.33	3566	94
64	**KF-1**		27/02/1971		109	3498	42.78	1148	45
			27/02/1971		109	3506	42.78	1150	45
			11/3/1971		180	10485	82.22	3440	88
			11/3/1971		180	10495	82.22	3443	88
			11/3/1971		180	10497	82.22	3444	88
			12/3/1971		180	10497	82.22	3444	88
65	**JO-1**		31/01/1971		118	4040	47.78	1325	50
			16/02/1971	10	182	9954	83.33	3266	89
66	**JD-1**		1/7/1966		110	3470	43.33	1138	45
			14/07/1966		160	10986	71.11	3604	75
67	**JA-1**		30/01/1965		102	3498	38.89	1148	40
			15-16/02/1965		180	10998	82.22	3608	88
			17/02/1965		180	10999	82.22	3609	88
68	**JK-1**		28/03/1967		110	3013	43.33	988.5	45
			4/4/1967		182	9083	83.33	2980	89
69	**JN-1**		29/10/1971		115	4016	46.11	1318	48
			8/11/1971		194	10972	90	3600	96

APPENDIX II

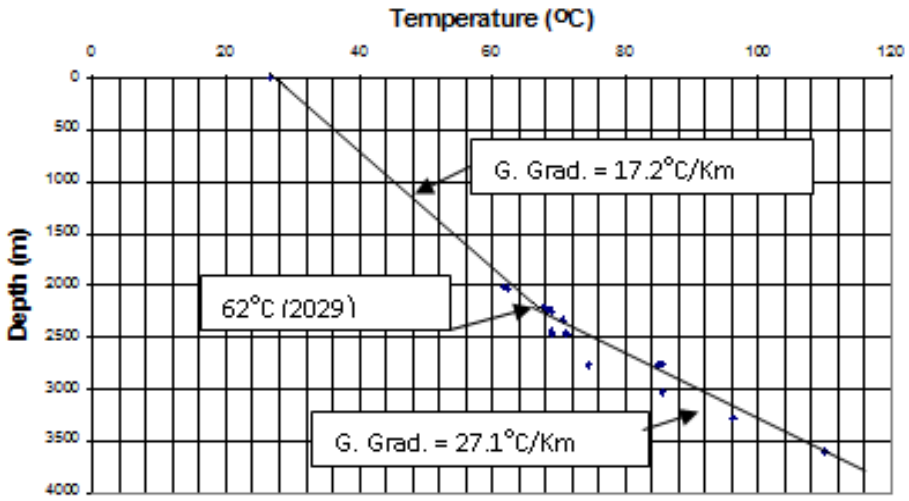

Figure 1: Temperature - Depth plot of the Bodo- West field

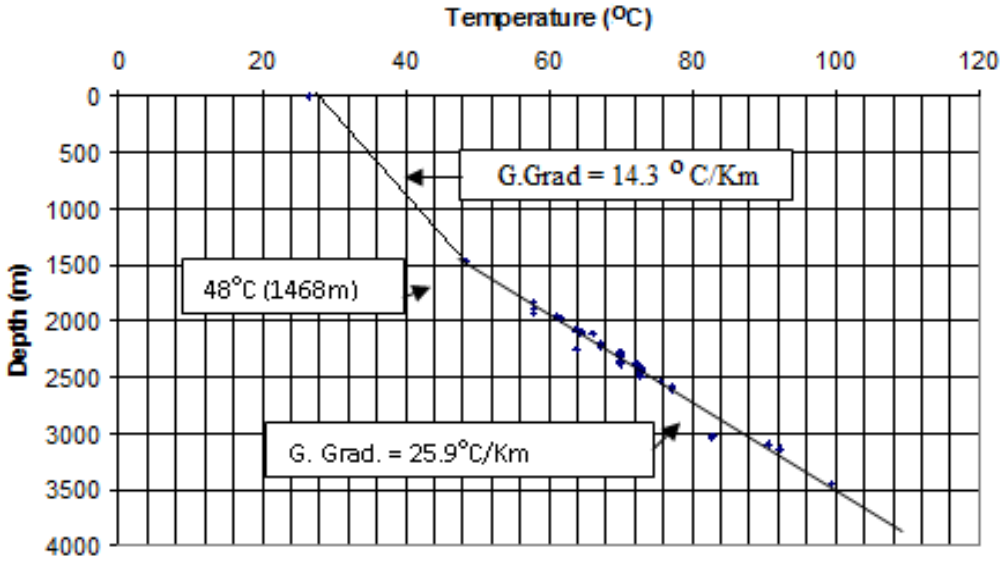

Figure 2: Temperature-Depth plot for Bornu field

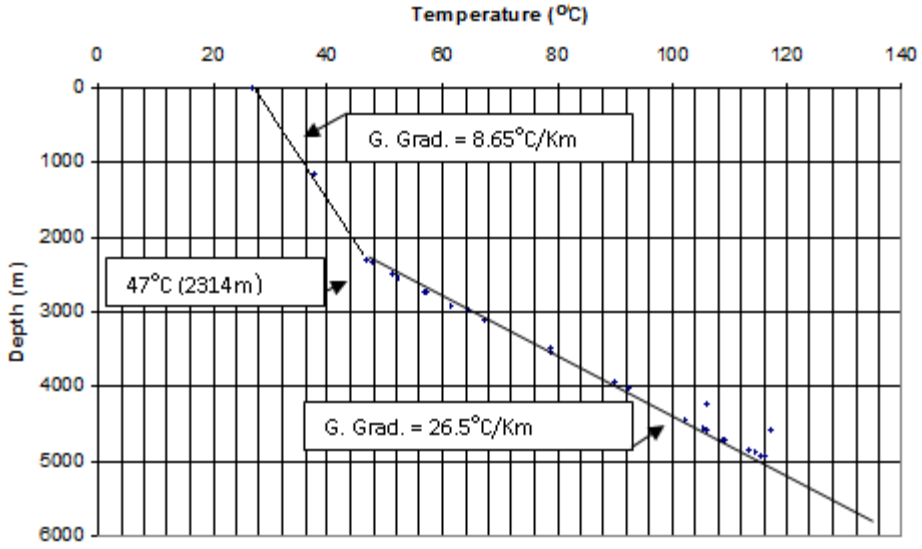

Figure 3: Temperature - Depth plot of the Awoba field

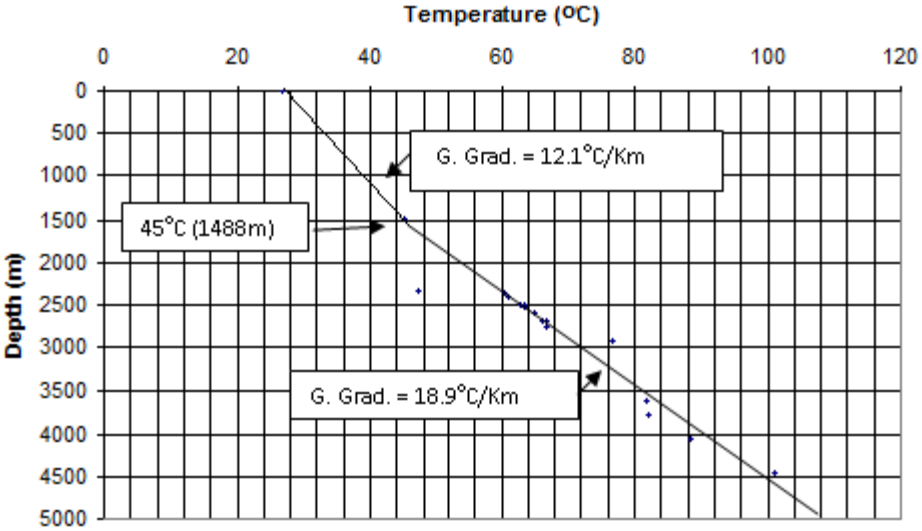

Figure 4: Temperature - Depth plot of the Belema field

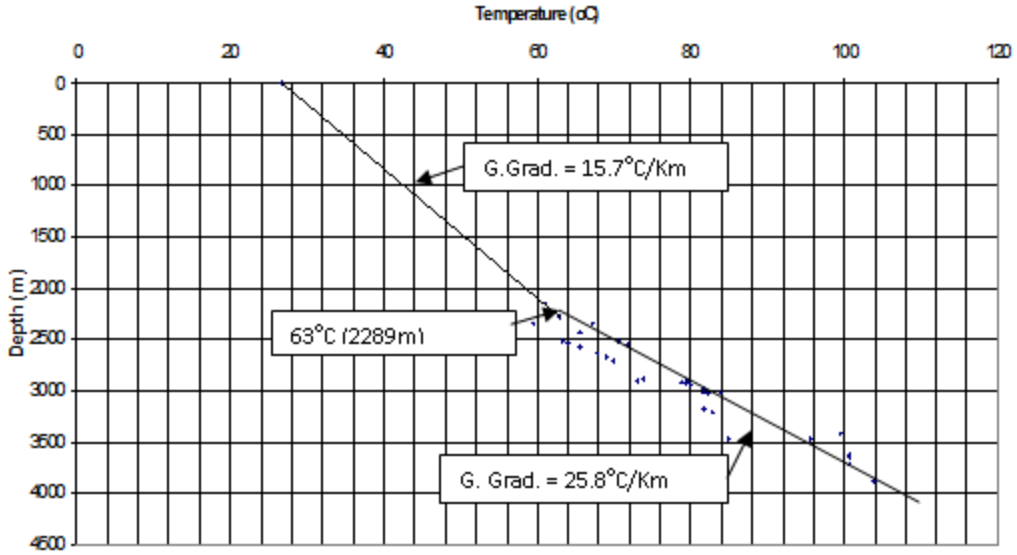

Figure 5: Temperature - Depth plot for Alakiri field

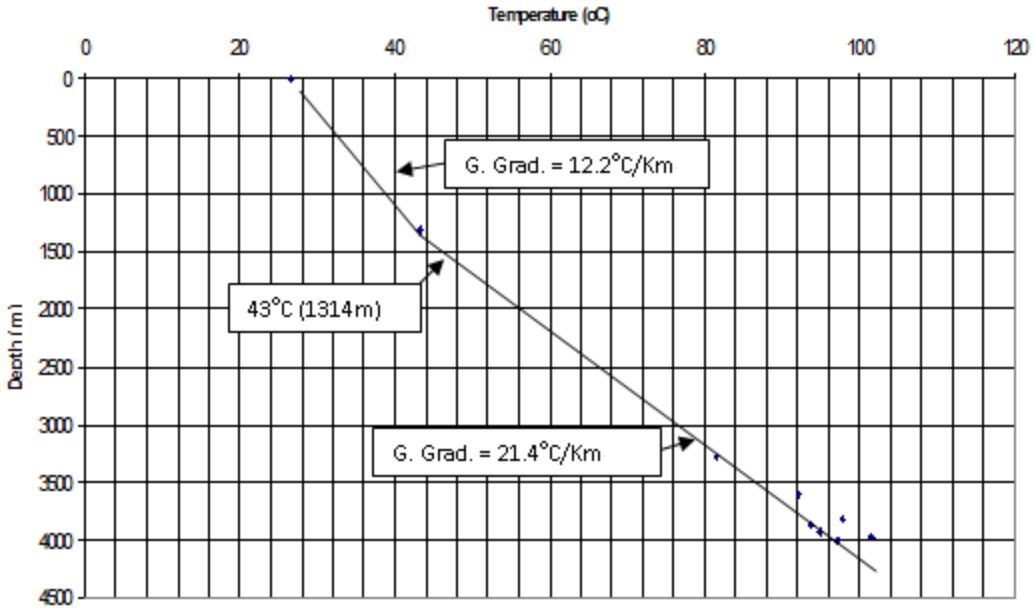

Figure 6: Temperature - Depth plot for Alakiri - East field

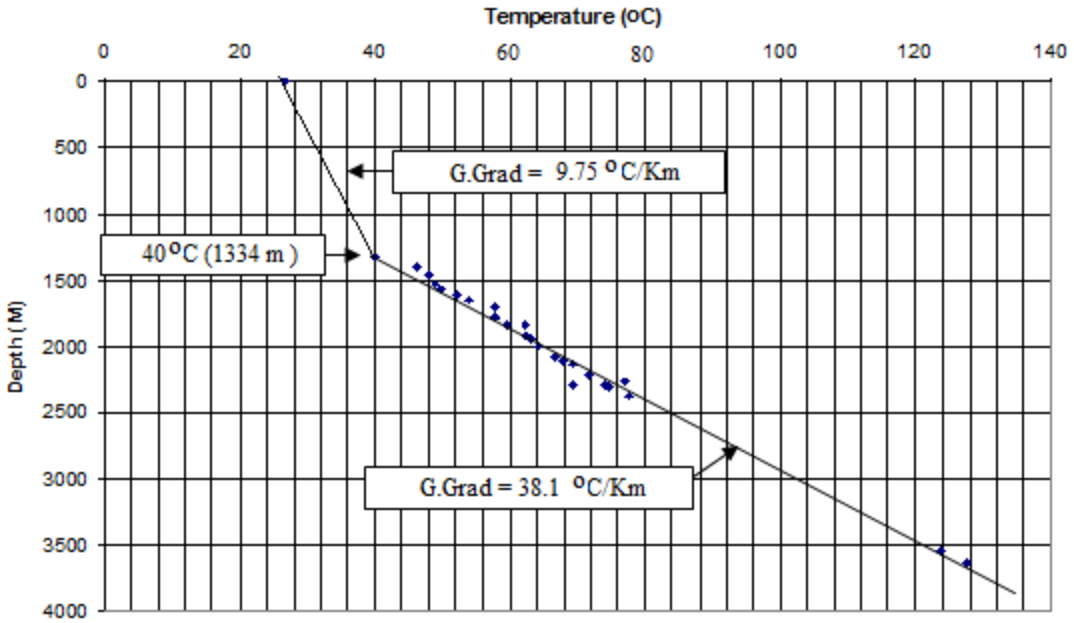

Figure 7: Temperature - Depth plot for Akata field

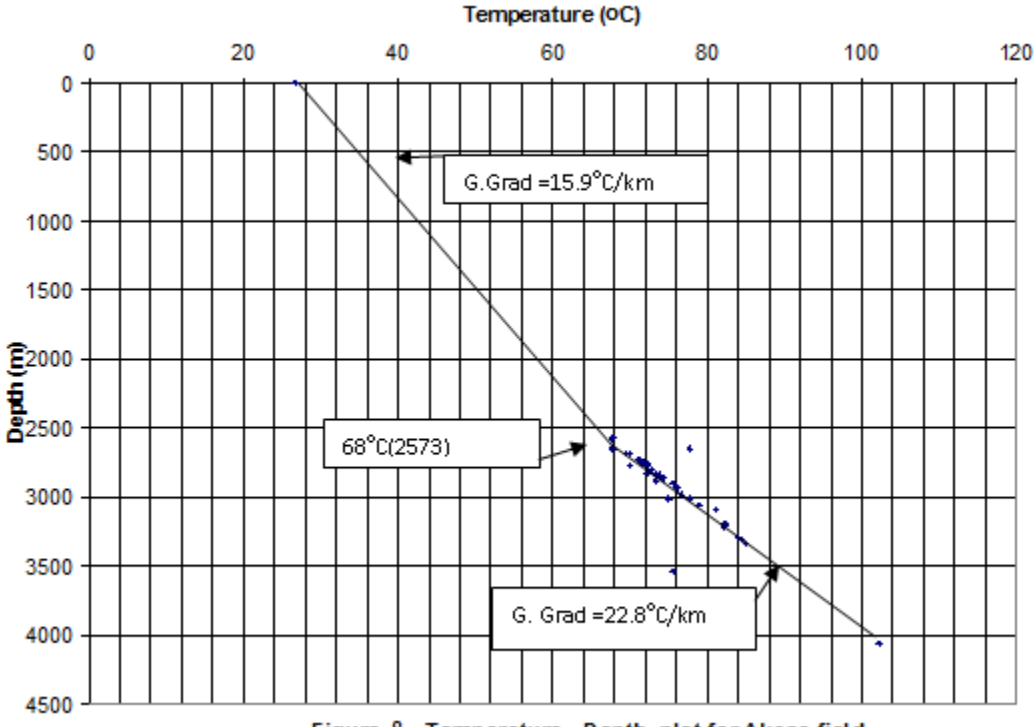

Figure 8 Temperature - Depth plot for Akaso field

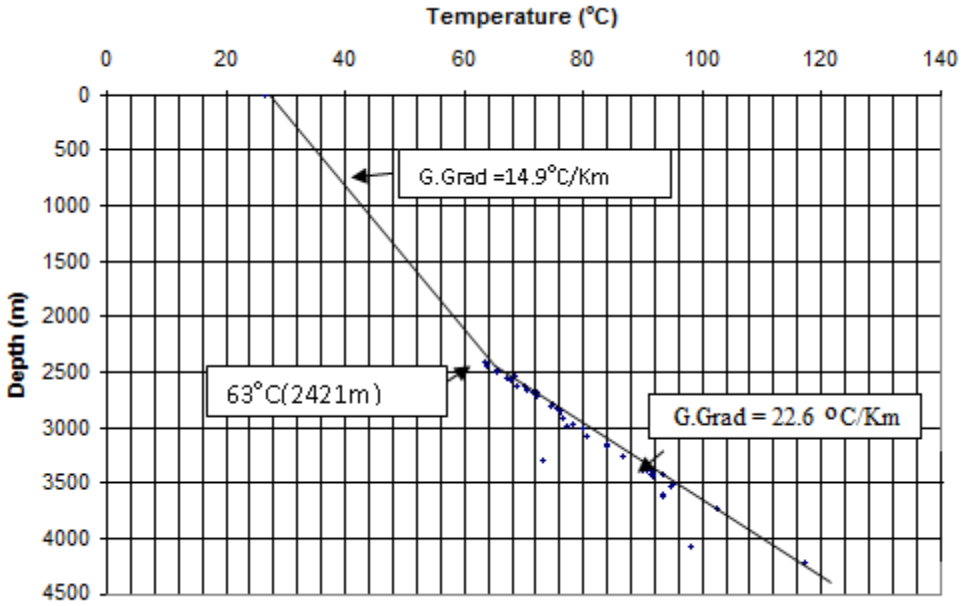

Figure 9: Temperature - Depth plot for Cawthorne Channel - 1

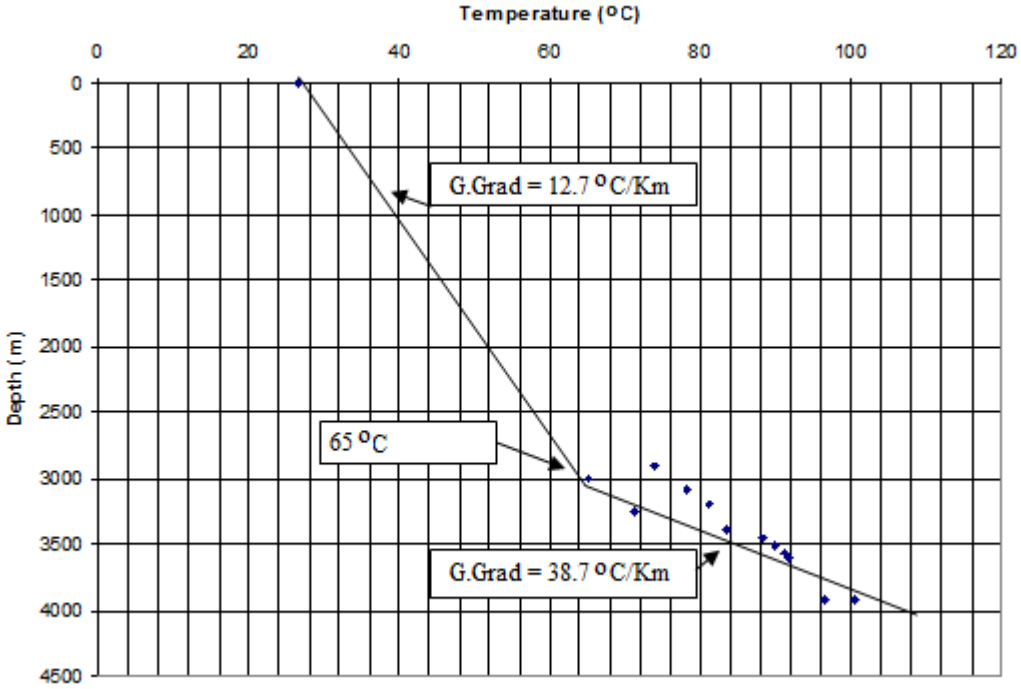

Figure 10: Temperature - Depth plot for Buguma - Creek field

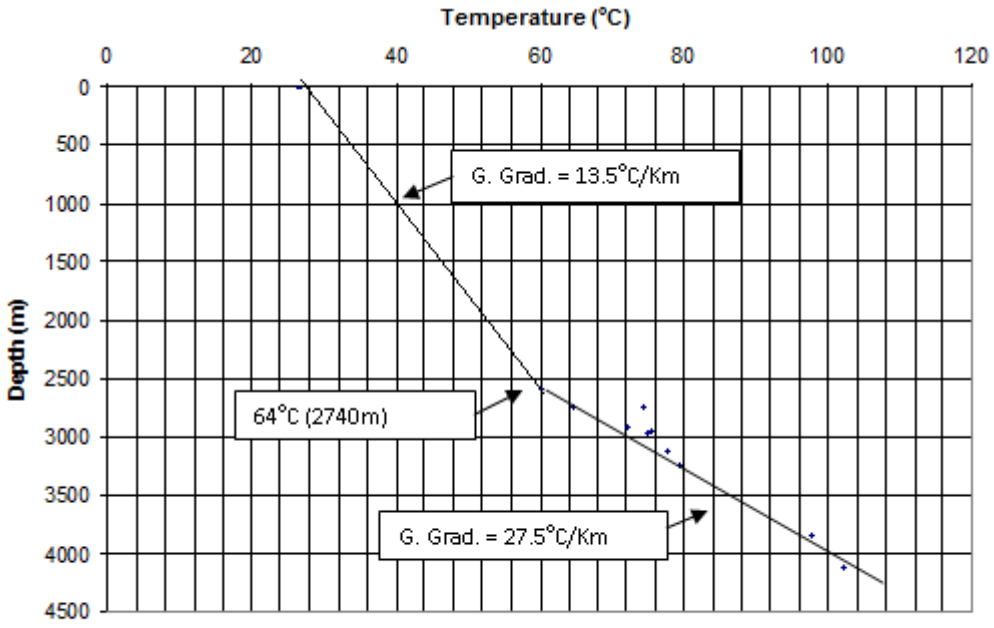

Figure 11: Temperature - Depth plot of the Ekulama field

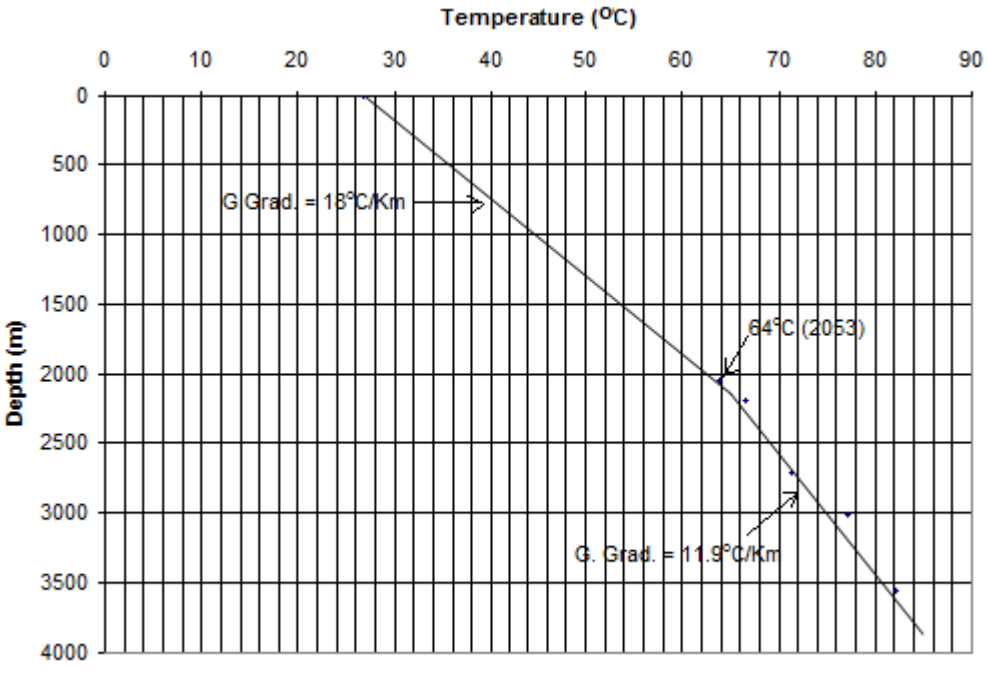

Figure 12 : Temperature - Depth plot for Bonny-North field

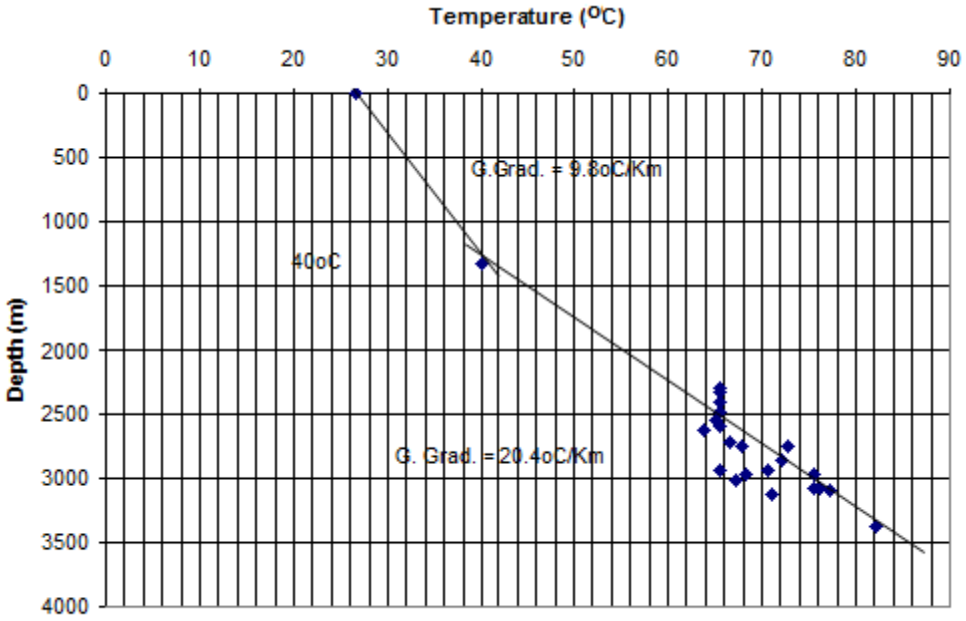

Figure 13: Temperature - Depth plot for the Orubiri field

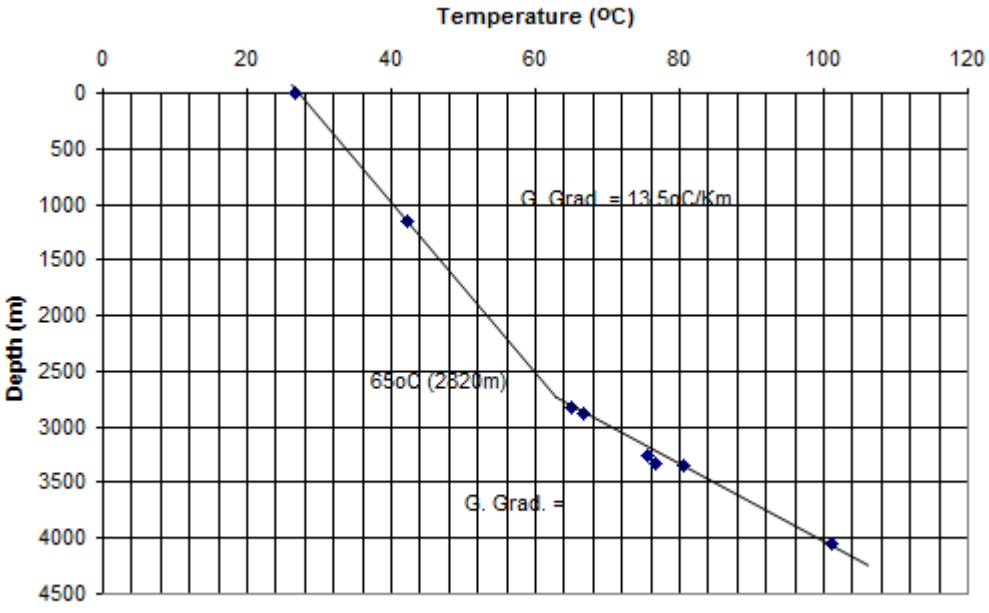

Figure 14: Temperature - Depth plot for the Olua field

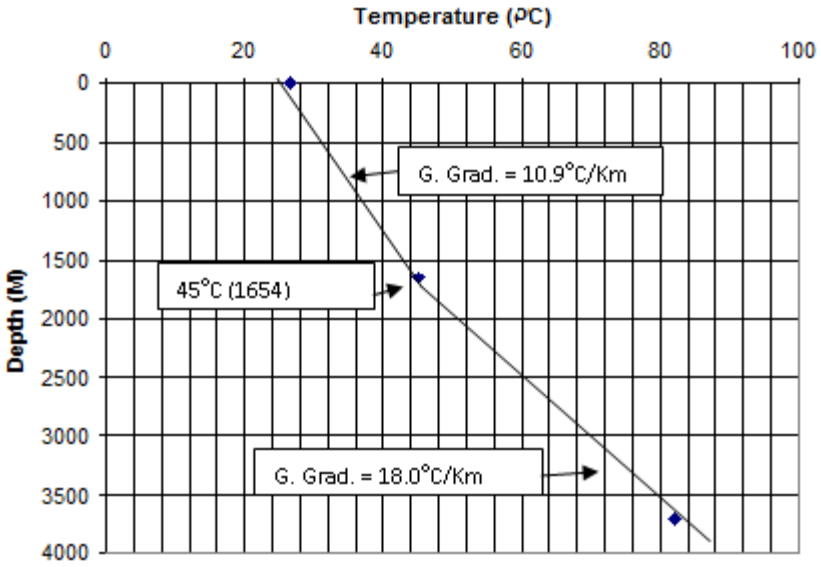

Figure 15: Temperature - Depth plot for Bille-1

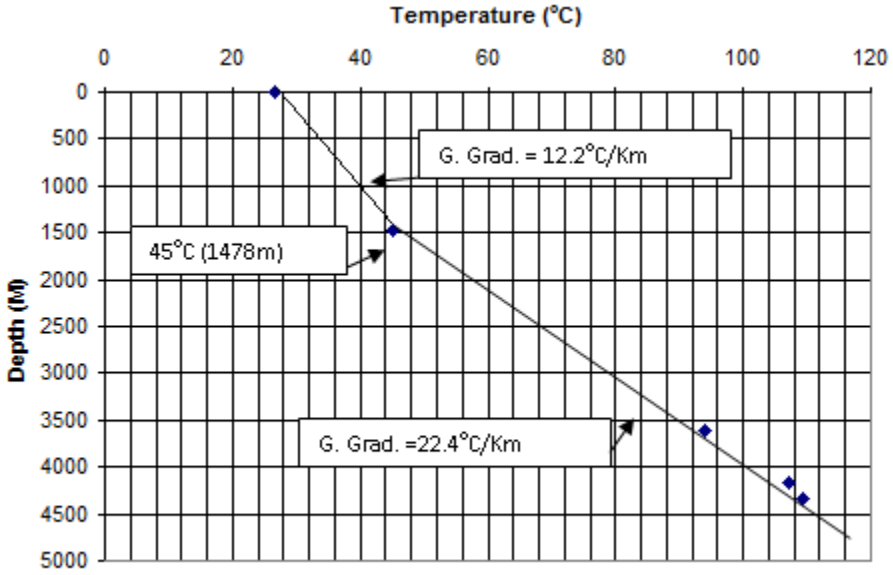

Figure 16: Temperature - Depth plot for Chobie-1

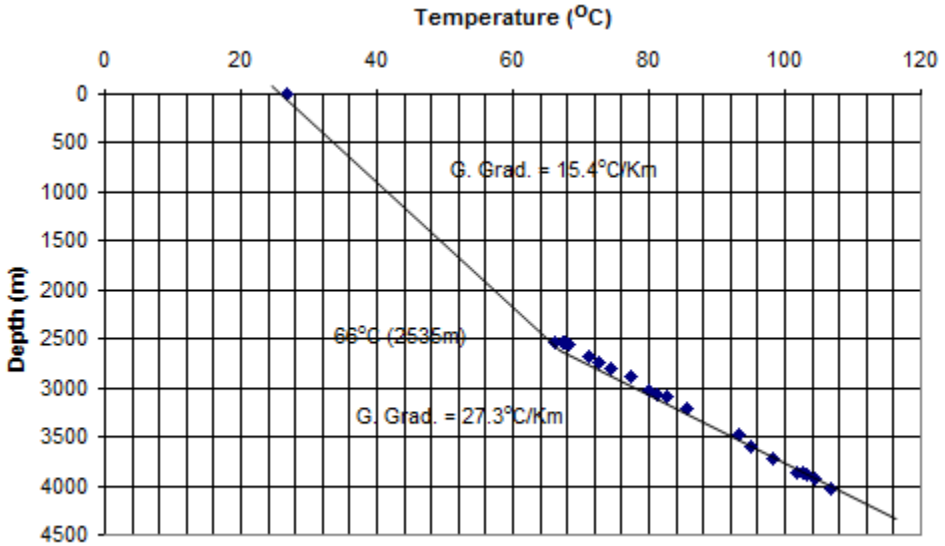

Figure 17: Temperature - Depth plot for Odeama Creek field

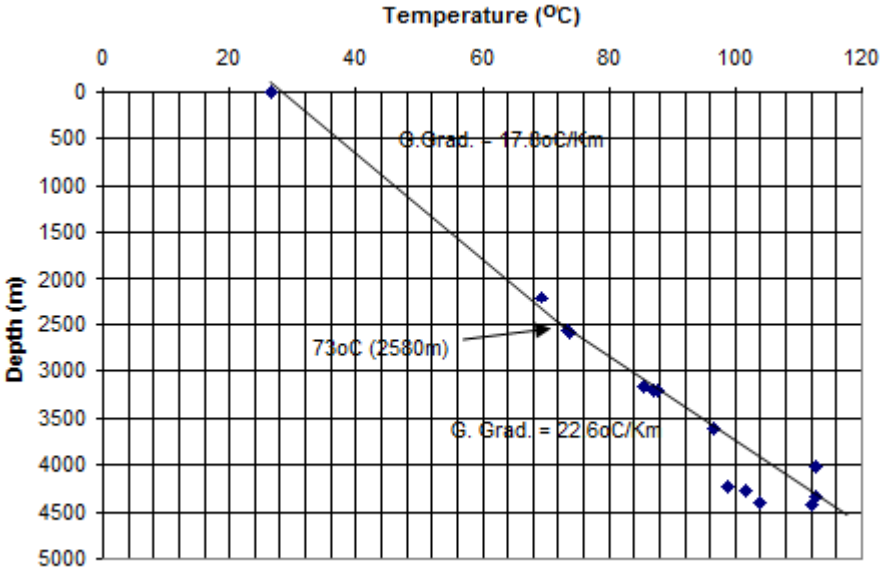

Figure 18: Temperature - Depth plot for Krakama field.

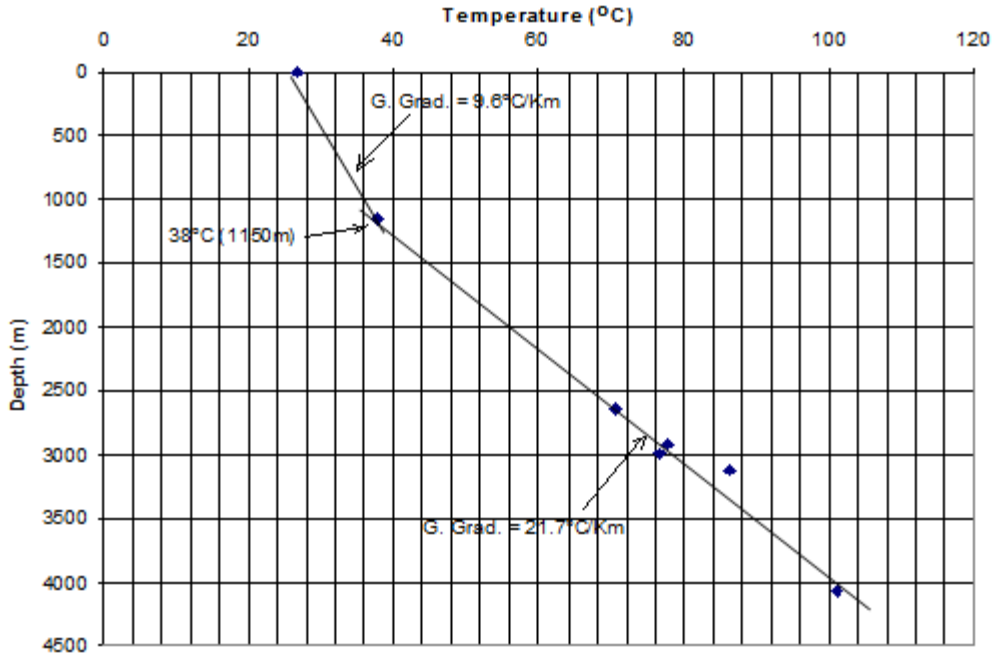

Figure 19: Temperature - Depth plot for the Onne field

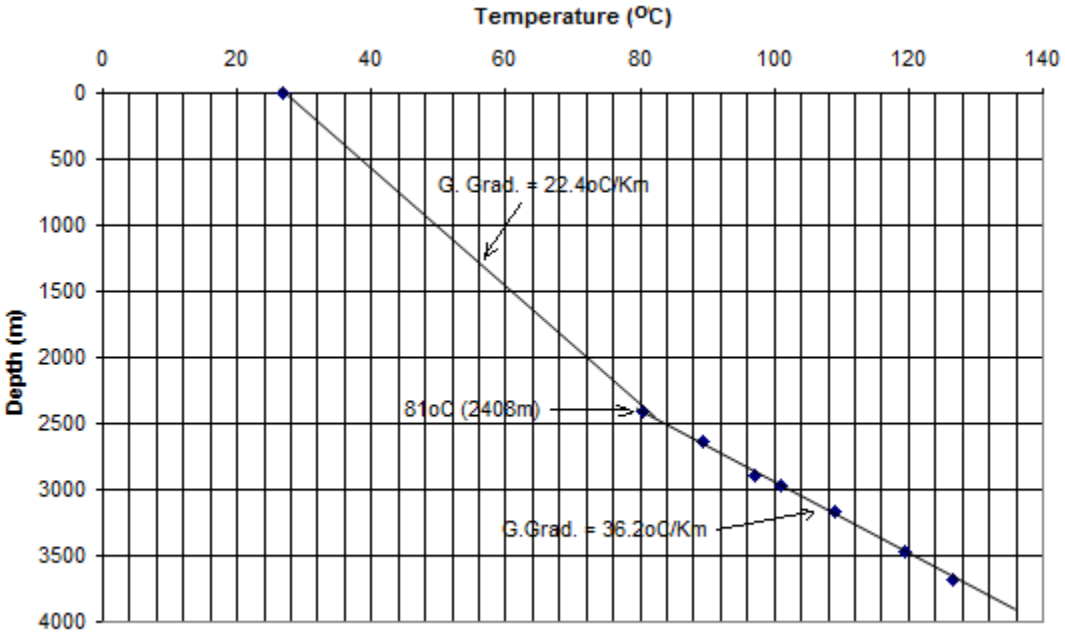

Figure 20: Temperature - Depth plot for Opobo - South field

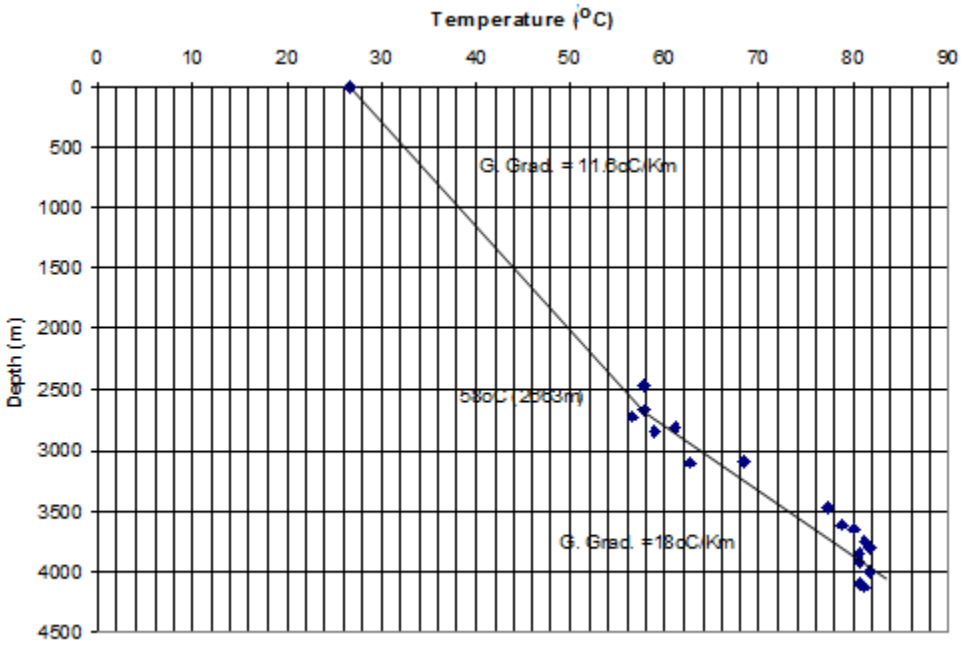

Figure 21: Temperature - Depth plot for Soku field

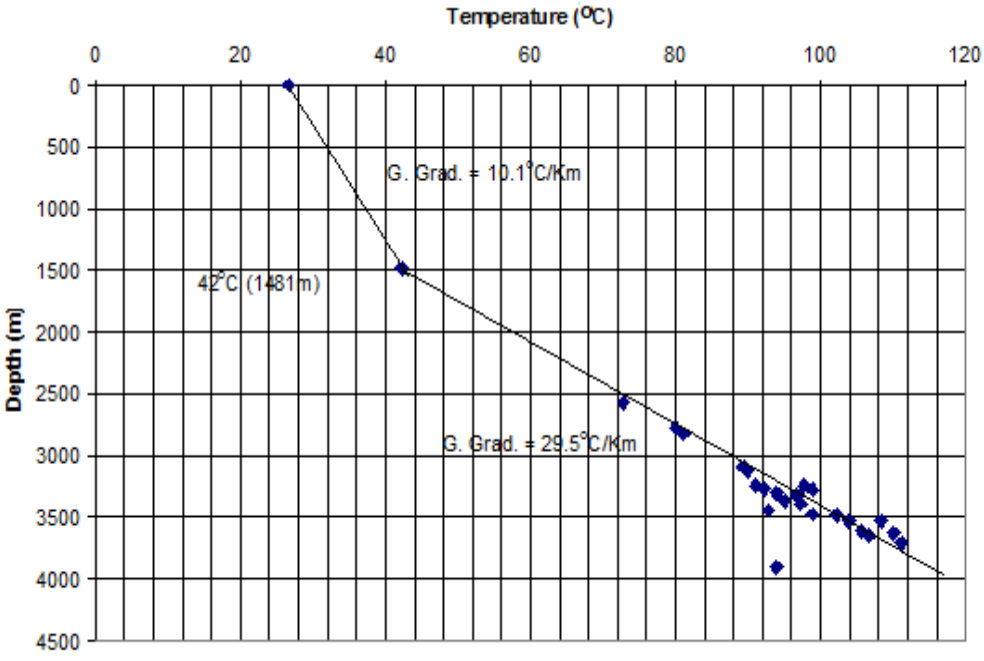

Figure 22: Temperature-Depth plot for Yorla field

APPENDIX III

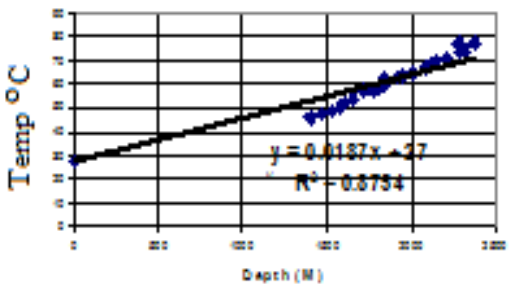

Fig. 1: Average Temperature / Depth plot for Akata - 1

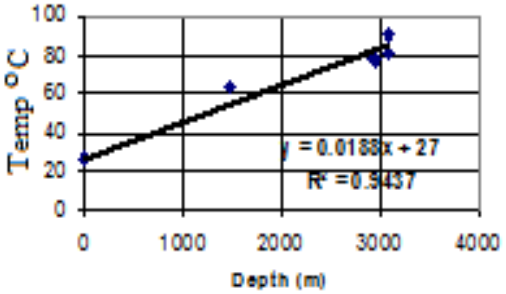

Fig. 2: Average Temperature / Depth plot for Abak Enin - 1

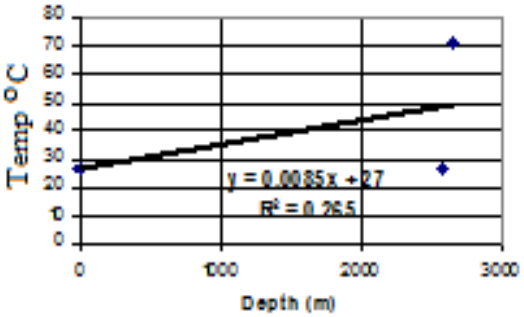

Fig. 3: Average Temperature / Depth plot for Akuba 1

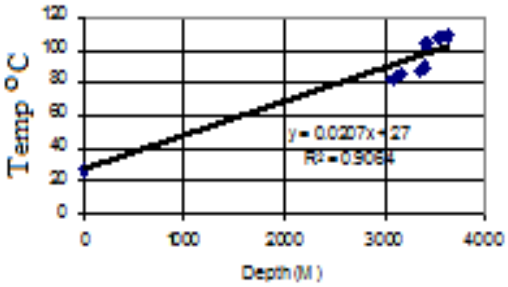

Fig. 4: Average Temperature / Depth plot for Ajokpori-1

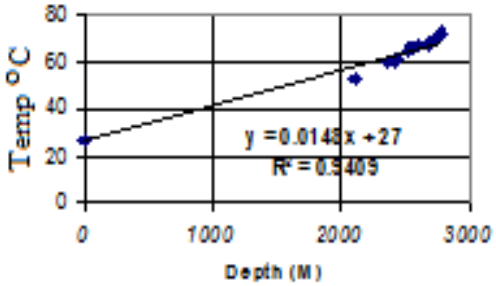

Fig. 5: Average Temperature Depth plot for Ebubu - 1

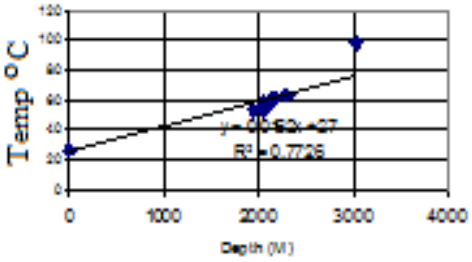

Fig. 6: Average Temperature/Depth plot for Isimiri-1

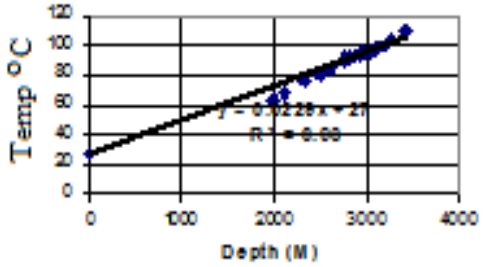

Fig. 7: Average Temperature Depth plot for Imo River-1

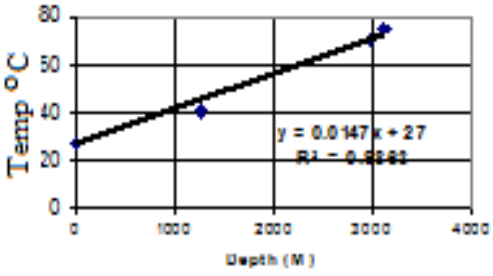

Fig. 8: Average Temperature/Depth plot for Mobazi-1

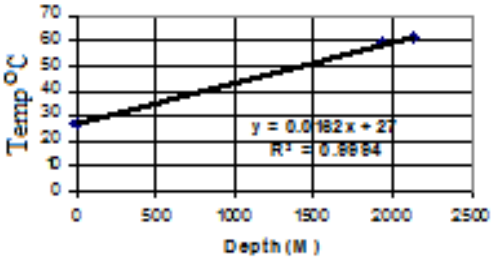

Fig. 9: Average Temperature/Depth plot for Ngboko-1

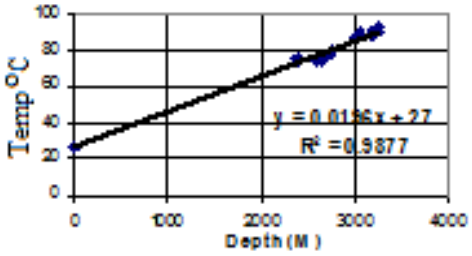

Fig. 10: Average Temperature/Depth plot for Koroko ro-1

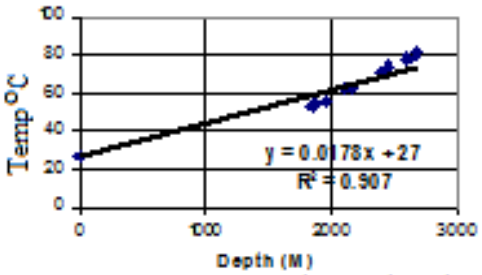

Fig. 11: Average Temperature/Depth plot for Ibiblo-1

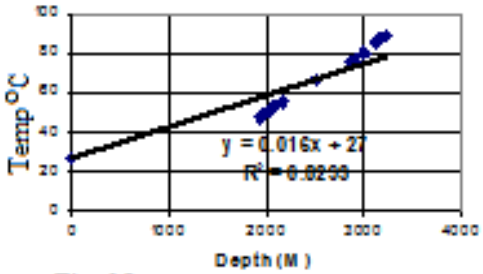

Fig. 12: Average Temperature/Depth plot for Obeakpu-1

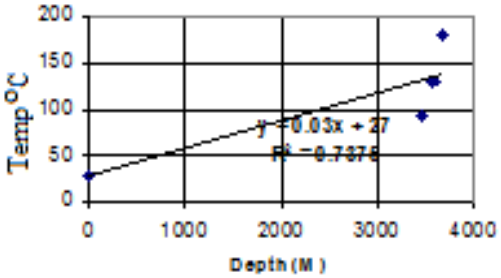

Fig. 13: Average Temperature/Depth plot for Obigbo-1

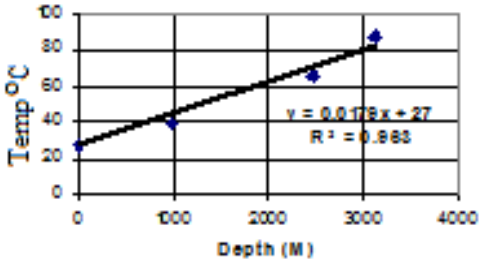

Fig. 14: Average Temperature/Depth plot for Odagwa-1

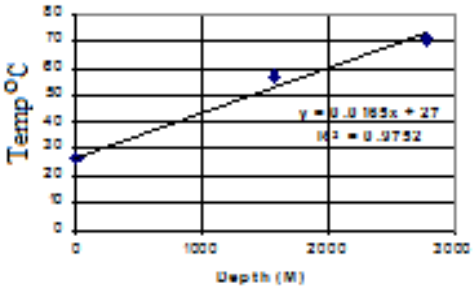

Fig. 15: Average Temperature/Depth plot for Odoro Ikpe-1

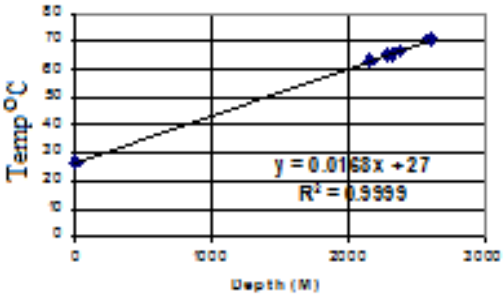

Fig. 16: Average Temperature/Depth plot for Otamini-1

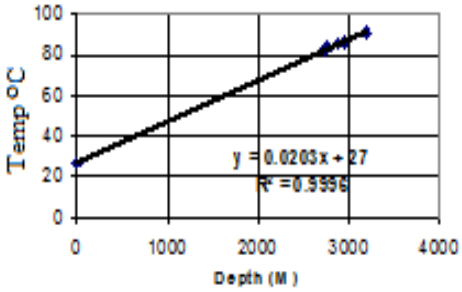

Fig. 17: Average Temperature/Depth plot for Okoloma -1

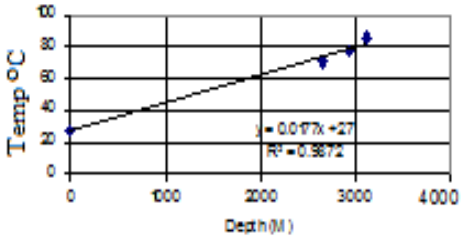

Fig. 18: Average Temperature Depth plot for Onne -1

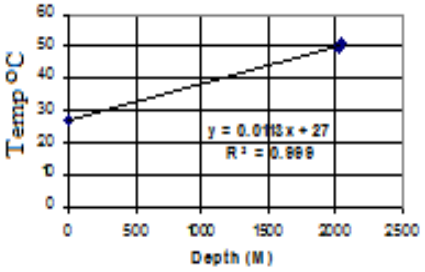

Fig. 19: Average Temperature/Depth plot for Oza-2

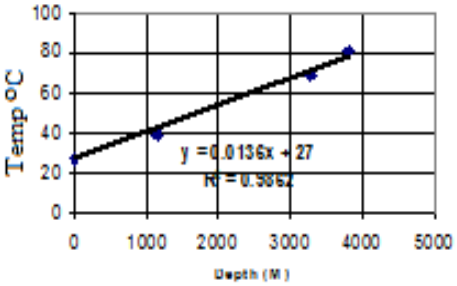

Fig. 20: Average Temperature/depth plot for Tabangh -1

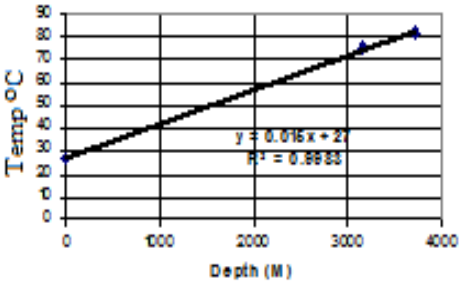

Fig. 21: Average Temperature/Depth plot for Tai-1 well

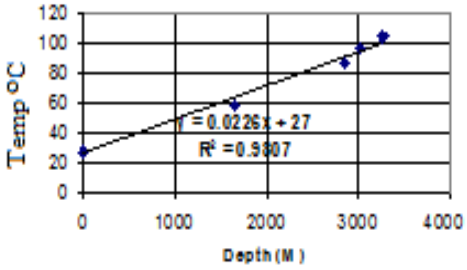

Fig. 22: Average Temperature/Depth plot for Akal -' well

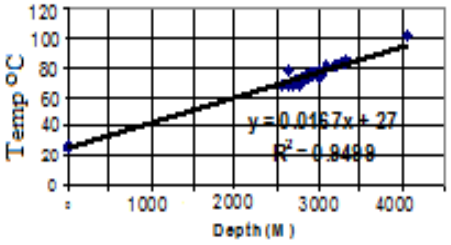

Fig. 23: Average Temperature/Depth plot for Akaso - 4

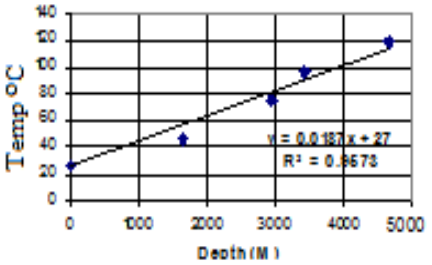

Fig. 24: Average Temperature/Depth plot for Akikigha-1

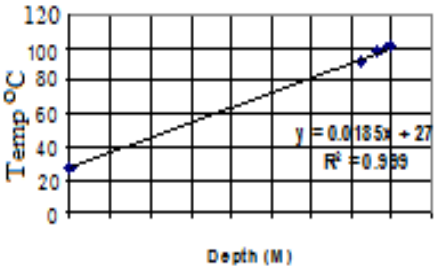

Fig. 25: Average Temperature/Depth plot forAlakiri - East -1

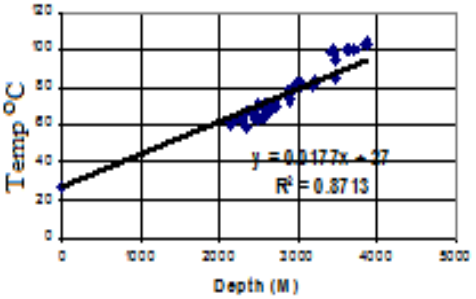

Fig. 26: Average Temperature/Depth plot for Alakiri - 20

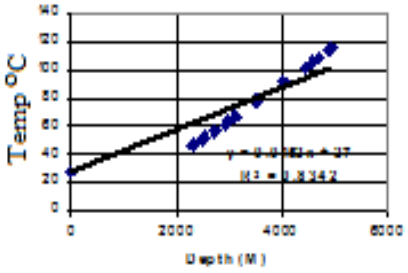

Fig. 27: Average Temperature Depth plot for Awoba - 1

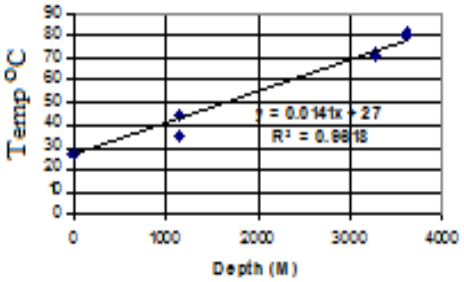

Fig. 28: Average Temperature/Depth plot for Bakana-1 well

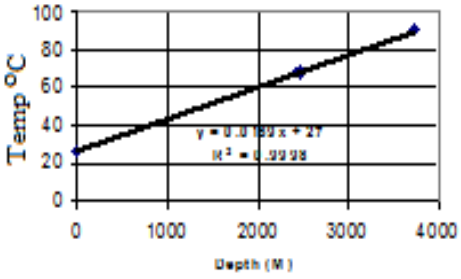

Fig. 29: Average Temperature/Depth plot for Ekeraile -1

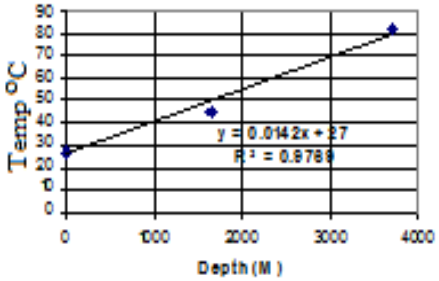

Fig.30: Average Temperature/Depth plot for Bille-1well

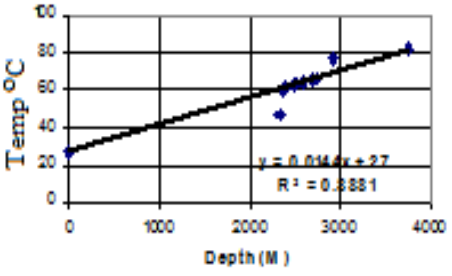

Fig. 31: Average Temperature/Depth plot for Belema-1

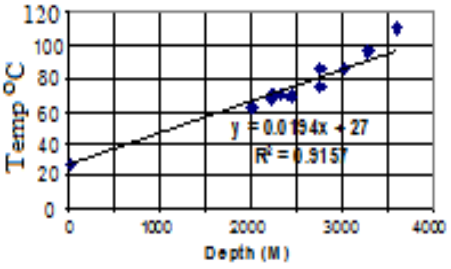

Fig. 32: Average Temperature/Depth plot for Bodo West -1

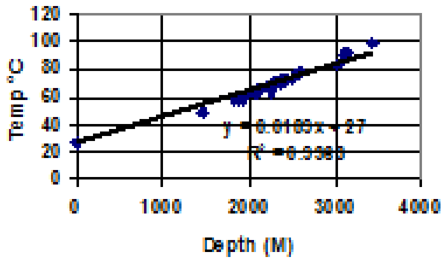

Fig. 33: Average Temperature/Depth plot for Bomu - 1

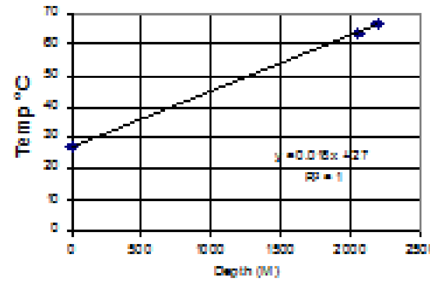

Fig. 34: Average Temperature/Depth plot for Bonny North - 1

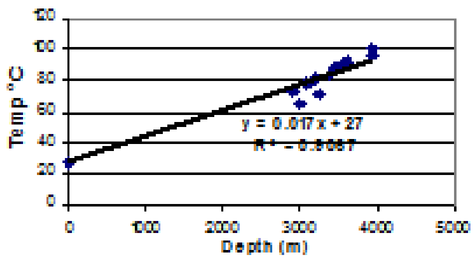

Fig. 35: Average Temperature/Depth plot for Buguma Creek -1

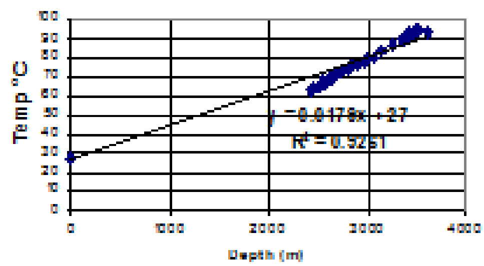

Fig. 36: Average Temperature Depth plot for Cawthorne Channel -1

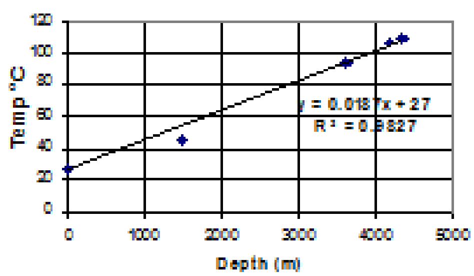

Fig. 37: Average Temperature Depth plot for Chobie -1

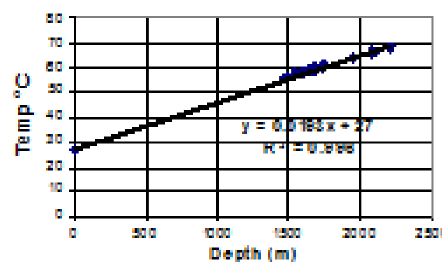

Fig. 38: Average Temperature Depth plot for Ekim -2 well

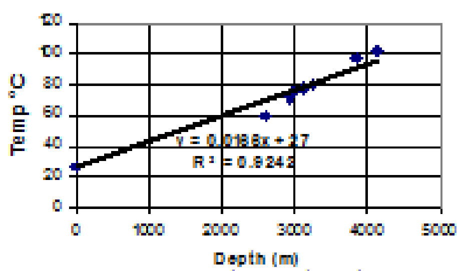

Fig. 39: Average Temperature Depth plot for Ekulama -2 well

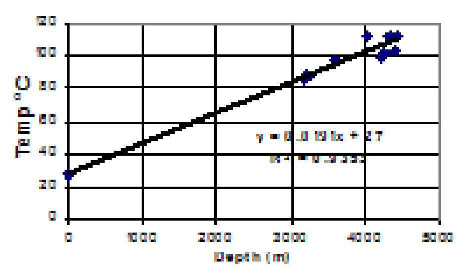

Fig. 40: Average Temperature Depth plot for Krakama - 13

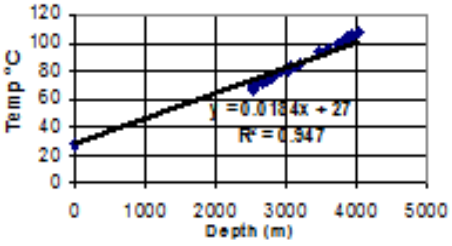

Fig. 41: Average Temperature Depth plot for Odeama Creek -1well

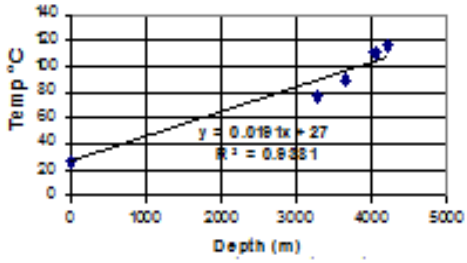

Fig. 42: Average Temperature Depth plot for Ogu - 1 well

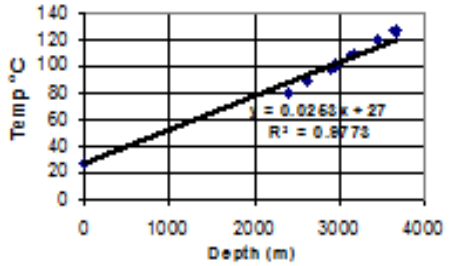

Fig. 43: Average Temperature Depth plot for Opobo South well

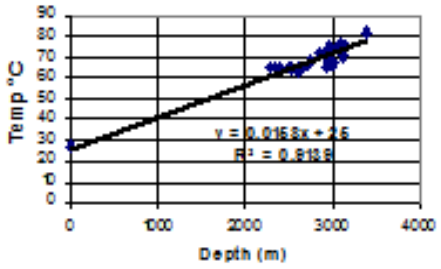

Fig. 44: Average Temperature Depth plot for Orubiri - 1well

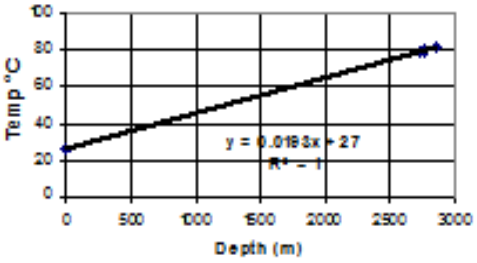

Fig. 45: Average Temperature Depth plot for Otakikpo -1well

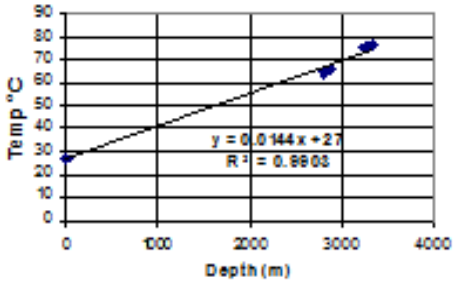

Fig. 46:

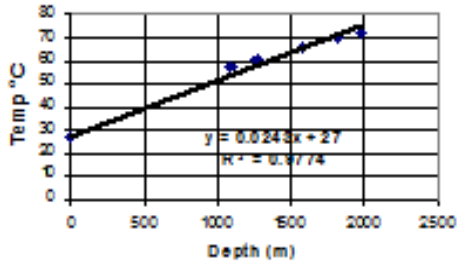

Fig. 47: Average Temperature Depth plot for Gua Ibo North -1 well

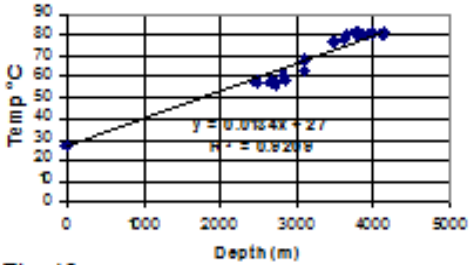

Fig. 48: Average Temperature Depth plot for Soku -3 well

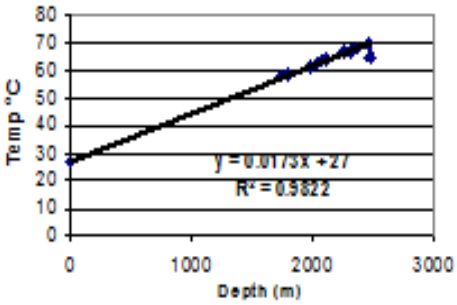

Fig. 49: Average Temperature Depth plot for Uquo - 2

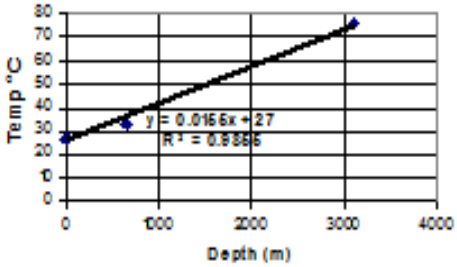

Fig. 50: Average Temperature Depth plot for Yomene -1well

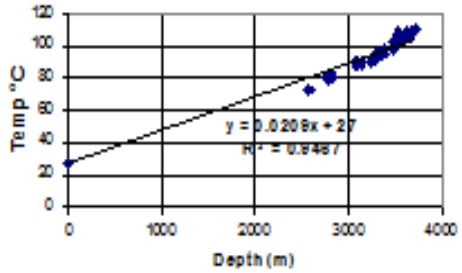

Fig. 51: Average Temperature Depth plot for Yoria-1well

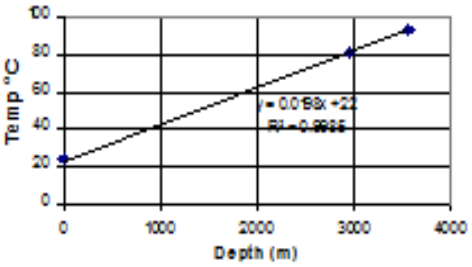

Fig. 52: Average Temperature Depth plot for Koronama -1 well

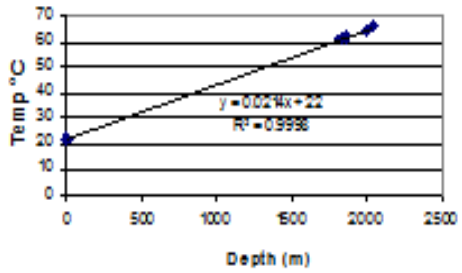

Fig. 53: Average Temperature Depth plot for Kappa - 1 well

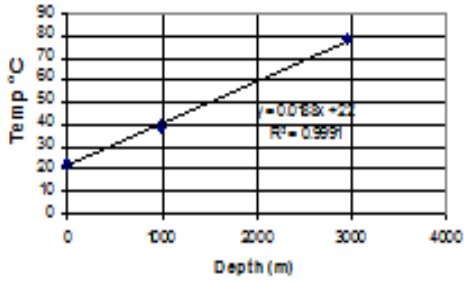

Fig. 54: Average Temperature Depth plot for KR-1 well

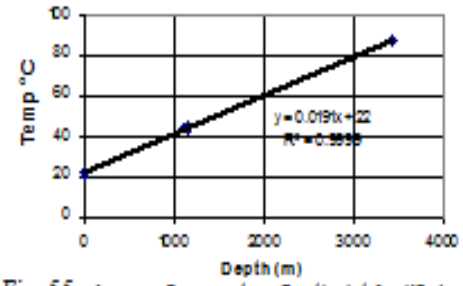

Fig. 55 Average Temperature Depth plot for KF-1 well

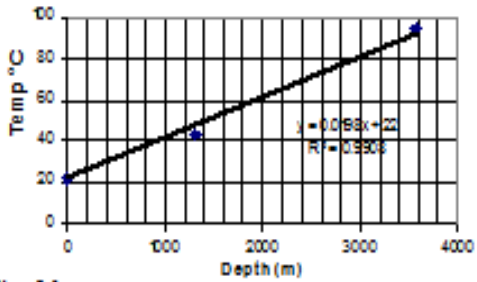

Fig. 56: Average Temperature Depth plot for KG-1 well

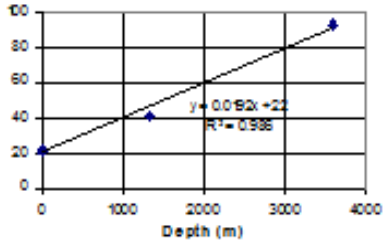

Fig. 57: Average Temperature Depth plot for KH-1 well

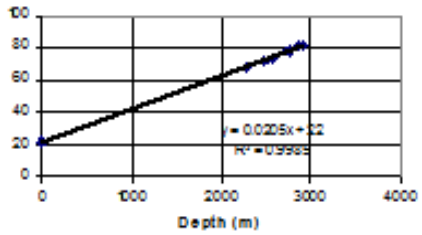

Fig. 58: Average Temperature Depth plot for KD-1 well

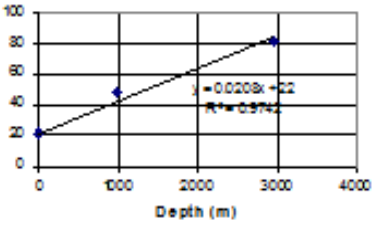

Fig. 59: Average Temperature Depth plot for KQ-1well

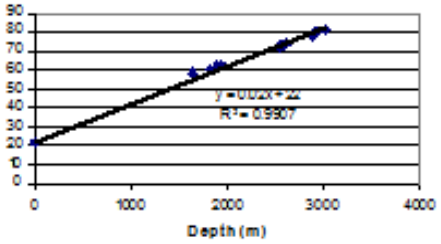

Fig. 60: Average Temperature Depth plot for KL-1well

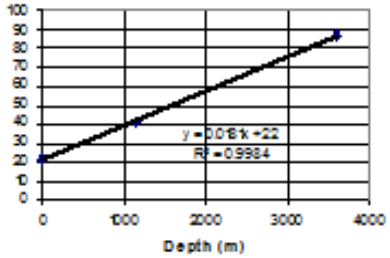

Fig. 61: Average Temperature Depth plot for JA-1well

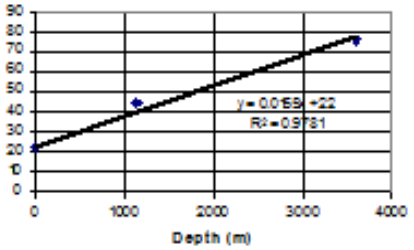

Fig. 62: Average Temperature Depth plot for JD-1 well

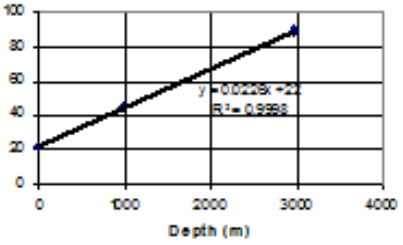

Fig. 63: Average Temperature Depth plot for JK-1 well

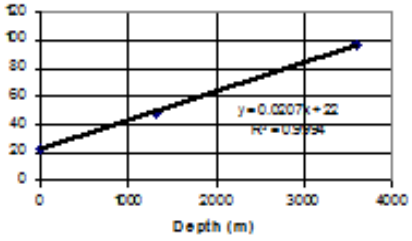

Fig. 64: Average Temperature Depth plot for JN-1 well

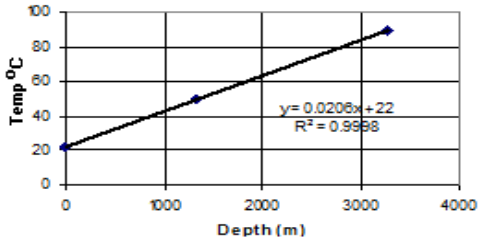

Fig. 65: Average Temperature Depth plot for JO-1 well